सरदार वल्लभभाई राष्ट्रीय प्रौद्योगिकी संस्थान, सुरत
Sardar Vallabhbhai National Institute of Technology, Surat

TECHNICAL PROJECT REPORT

IMPACT OF CLIMATE CHANGE ON WATER RESOURCES OF SABARMATI BASIN

Submitted to

MINISTRY OF JAL SHAKTI,
DEPARTMENT OF WATER RESOURCES,
RIVER DEVELOPMENT & GANGA REJUVENATION
GOVERNMENT OF INDIA.

PRINCIPAL INVESTIGATOR
PARTNERING INSTITUTE
Dr. P. L. PATEL
DEPARTMENT OF CIVIL ENGINEERING
SVNIT-SURAT

DEPARTMENT OF CIVIL ENGINEERING
SARDAR VALLABHBHAI NATIONAL INSTITUTE OF TECHNOLOGY (SVNIT)
SURAT-395007, GUJARAT, INDIA

This is Draft Report and yet to be accepted by Competent Authority

CERTIFICATE

Subject: "Impact of Climate Change on Water Resources of Sabarmati basin"

This is to certify that current research project, **"Impact of climate change on Water Resources of Sabarmati basin"** includes the findings as per the terms of reference (ToR) conveyed vide administrative approval letter no. 16/22/2016-R&D/3044-3058 dated November 07, 2016.

The current study has investigated the trend analysis of climate variables, like temperature and precipitation indices, for baseline and future periods, hydrological modelling using SWAT and HEC-HMS for the catchment of Dharoi reservoir; assessing the hydrologic response of the Dharoi catchment for change in climatic variables of future periods; and impact of change of climatic variables on Gross irrigation requirements of command area of Dharoi reservoir.

The report includes objectives and scope of work; literature review, description of Sabarmati basin and data sources; trend analysis of climatic variables like temperature and precipitation indices; hydrological model and hydrological response of the basin for future climatic variables, Impact on irrigation demand of climate changes.

The results reported in the current report are based on data provided by downscaling team of IIT Bombay and observed data from other data providing agencies. Due acknowledgement has been given to the funding and data providing agencies and those who have supported in completion of project.

प्रेमलाल पटेल

Dr. P. L. Patel
Professor & PI, Partnering Institute,
SVNIT Surat.

EXECUTIVE SUMMARY

The current project "Impact of climate change on water resources of Sabarmati basin'" was investigated by analysing the trends of climatic variables like rainfall and temperature indices for baseline (1951-2019) and future (near-2020-2040), mid -2041-2070) and far future -2071-2100) periods; calibration and validation of hydrological model (SWAT) for baseline Period (1995-2019) for prediction of inflows into Dharoi reservoir of Upper Sabarmati basin; hydrological response of the Upper Sabarmati basin for future periods and impact on irrigation demands under changing climatic conditions in the command area of Dharoi reservoir.

The results of the trend analyses indicated that minimum temperature (T_{min}) and average temperature (T_{av}) have shown significantly increasing trend, at 5% significance level, over the basin, particularly post 1985 period. This alarming increase in temperature in the basin may have adverse impact on crop yield and human health due to heat stress.

The results of trend analyses of precipitation indices indicated that Annual Precipitation (PRCPTOT), Rainy days (RD), Light rainfall (LRF), Medium rainfall (MRF) have shown increasing trend for the base line and future periods. This indicates that Sabarmati basin is shifting towards wet regime in future.

The calibrated hydrological model performed satisfactorily for past data (2015-2019) as per the criteria suggested by Moriasi et al. (2007). The calibrated and validated hydrological model, in turn, has been used for prediction of response of Upper Sabarmati basin for inflows into Dharoi reservoir in future. From the flow duration curves derived from hydrological model output, for downscaled data of ensembled GCMs for both RCP4.5 and RCP8.5, indicated that high dependable flows (low discharges) are likely to increase while the low dependable flows (floods) are likely to decrease in future. This condition could be favourable to the water users as reservoir is likely to get more water for the usage in the future.

The Gross irrigation requirements in few months are likely to increase (decrease), particularly for January and October months (September, November and December) months with reference to the base line period. Due to change in the gross irrigation requirement (GIR) for future periods, and increase in the inflows into the Dharoi reservoir, suitable muti-objective optimization techniques need to be implemented for changing climatic conditions in near, mid and far future.

प्रेमलाल पटेल

Dr. P. L. Patel
Professor & PI, Partnering Institute,
SVNIT Surat.

...

ACKNOWLEDGEMENT

The Project team thankfully acknowledge the support provided by the Sardar Vallabhbhai National Institute of Technology for permitting the team to take up the project and help towards carrying out the relevant procurement and computational work. We are thankful to the Directorate, Indian National Committee on Climate Change (INCCC), Ministry of Jal Shakti, Department of Water Resources, River Development & Ganga Rejuvenation, Government of India (GoI) for funding the research project entitled **"Impact of Climate Change on Water Resources of Sabarmati Basin"** as partnering institute of the project to SVNIT Surat. We express our heartfelt gratitude to Indian National Committee on Climate Change (INCCC) for their timely evaluation and suggestions in the meeting. Special thanks to Dr. R P Pandey, Scientist 'G', National Institute of Hydrology, Member Secretary, INCCC and his team for nice suggestions and quick administrative support.

We are thankful to India Meteorological Department (IMD), Pune for rainfall and temperature data, Central Water Commission (CWC) for hydrological and meteorological data and Dharoi dam office Satlasana under the jurisdiction of Narmada and Water Resources, Water Supply and Kalpsar Department, Government of Gujarat, for providing inflows and reservoir data. Thanks are also to National Remote Sensing Centre (NRSC) Hyderabad and National Bureau of Soil Survey & Land Use Planning (NBBS&LUP) Nagpur for providing the essential data required for current study. We express special thanks to Indian Institute of Technology, Bombay for providing statistically downscaled precipitation and temperature data of GCMs.

Our special thanks to Ms. Alka Sharma, Senior Research Fellow (SRF) who worked as Project staff in the Project. Her significant contribution in shaping the project is highly appreciated.

We are thankful to Mr. Gaurav Ninama, Asst. Engineer; Mr. Nihal Singh Chaudhary, Executive Engineer; Mr. Harpal Raol, Asst. Engineer for the assistance provided during the data collection of Dharoi command area. We acknowledge the support rendered by Ms. Trushti Sanghvi, Post-graduate student; Mr. Kalpesh Baldaniya, Research scholar; Mr. Lalit Kumar Gehlot, Research Scholar; Dr. Priyank J Sharma, Asst. Professor at IIT, Indore; and Ms. Meenal Dave, Technical staff for their contribution to the project.

We show deep sense of gratitude to all those who helped us directly or indirectly in completion of this project.

प्रेमलाल पटेल

Dr. P.L. Patel
Professor,
Department of Civil Engineering, SVNIT, Surat

CONTENTS

LIST OF FIGURES

LIST OF TABLES

1 INTRODUCTION

1.1 PROJECT SUMMARY

Adequate water availability is needed for development of human society. The increase in population along with climate variability is expected to impact water availability, which in turn poses the challenge to the water security (Vorosmarty et al., 2000). Vorosmarty et al. (2010) reported in their study that nearly 80% of global population is expected to expose with high level of threat to water security. Agricultural regions are especially vulnerable to freshwater insecurity as agriculture water use accounts for about 70% of total water which is withdrawn from surface and ground water resources (Wisser et al., 2008). Furthermore, irrigation is the most important water use sector accounting for about 70% of global freshwater withdrawals and 90% of consumptive water use (Siebert et al., 2010). Optimization of existing water resource projects proves to be better alternative in managing present as well as future demands. Therefore, impact studies on the availability of water resources are necessary for designing suitable adaptation techniques to avoid future adverse consequences and also for optimal allocation of water to meet the demand and supply gap.

Our earth is now about 1.1°C warmer than it was in the late 1800s (https://www.un.org/en/climatechange). It is predicted that over the last century, increase in average global temperature of 0.74°C is noticed as compared to pre-industrial era due to increasing greenhouse gases emissions (NMSA 2001). Increasing concentration of carbon dioxide (CO2) and global industrialization (Abbasnia and Huseyin 2016) is mainly responsible for the emissions of these greenhouse gases, and thus climate change (AR6). The Intergovernmental Panel on Climate Change (IPCC) Sixth Assessment Report (AR6) estimated that in the coming decades climate changes will increase globally and the average global temperature will probably reach or exceeds 1.5°C, resulting shorter cold seasons, long warm seasons, and increasing heat waves, which is threat to human health and agriculture (AR6).

Climate is one of the important components in the earth system which refers to average condition of climatic variables like temperature, atmospheric pressure, precipitable water, and humidity that directly or indirectly affects the hydrologic variables like evaporation, runoff, and precipitation, etc. Keeping in view the changing climatic conditions across the globe, understanding the regional hydrology by evaluating the extent and magnitude of climate change, interlinking of climatic and hydrologic variables are highly required. Most frequently used climatic variables are precipitation and temperature in the climate sciences and hydrology

to understand the impact of climate change and variability (IPCC 2007) as it reflects the picture of the environmental condition of the region, which affects the agricultural productivity as well (Kumar and Gautam, 2014). Among the various climatic variables, temperature has most significant effect on almost all hydrologic variables. Usually, with increase (decrease) in temperature the relative humidity decreases (increases). Evapotranspiration is also affected by weather parameters and crop growth dynamics (Sonali and Kumar 2013). Thus, understanding the spatial and temporal patterns of surface temperature is of prime importance for application in the fields of agriculture, environmental engineering, climatology, hydrology, and forestry both at global and local scales (Anandhi et al., 2009; Tabari et al., 2011). Thus, global warming is forcing the changes in precipitation patterns, either resulting in frequent and severe precipitation, or evoking drought events. The climate change manifested uncertainty and irregularity in precipitation occurrence and distribution which results in concurrence of floods and drought conditions (Seneviratne et al., 2012) in many regions across the globe. The likely changes in the future precipitation and temperature trends would have significant impact on the regional hydrologic processes across the globe. Heavy floods are expected over Asian regions in the future, especially over India, China, and Bangladesh (IPCC, 2012).

The climate change (CC) influences the rainfall variability, humidity, peak flow, flow routing time, and runoff volume, and thus, impact the hydrological regimes and spatio-temporal water availability (Kundzewicz et al., 2008; Ghosh et al., 2012; Sinha et al., 2020). For instance, the increase in surface temperatures would accelerate the evapotranspiration rates, thereby, altering the regional hydrological cycle which would intensify the frequency and magnitudes of hydrological extremes (i.e., floods and droughts) (Huntington, 2006; Lucas-Borja et al., 2020). Whereas the Land Use Land Cover Change (LULCC) can cause modifications in the rainfall pathways to generate surface runoff through alterations in key water balance components such as evaporation, interception, infiltration, base flow, and groundwater recharge (Wei et al., 2013; Tan et al., 2015; Mekonnen et al., 2018).

India is a predominantly an agrarian nation wherein 70% of its water availability for irrigation is primarily dependent on the summer monsoon rainfall (June to September). Thus, climate change induced disturbances in the frequency, magnitude and occurrence of precipitation would pose a threat to water and food security and that could adversely affect the socio-economic fabric of the country. It is studied that the developing country like India whose economy is agriculture-based will face more seasonal variation in temperature and more warming in the winters than summers (Chen 2007; McCarthy 2001). Significant impact on water resources

management, agriculture production and economy of the country (Saha and Mooley 1979) due to changing pattern, and variability of South-west monsoon. Such worsening situation needs to be addressed properly by assessing the historic as well as future changes in climatic variables using different RCP's. Therefore, investigating historic and future climate changes in water availability at local scales can be taken to get an idea of potential hazards and develop appropriate strategies.

Impacts of historic climate variability and projected future climate change on hydrologic processes and water resources may have large spatial and temporal variations. For instance, soil moisture, runoff, and evapotranspiration can vary greatly within the watershed affecting the dynamics associated with the streamflow generation. So far, efforts to understand climate change impacts on water resources have largely been devoted to national scale. Regional scale impact studies may provide better understanding of the impacts associated with climate change and their socioeconomic implications. Here, we propose to evaluate impacts of climate variability and climate change in the Sabarmati River basin using the downscaled climate projections from multiple models and the physically based hydrologic modelling system.

1.2 MOTIVATION OF THE STUDY

The present study deals with Sabarmati River basin (SRB) which is one of the major west flowing River basin of India. The Sabarmati basin is largely dependent on agriculture and exhibits arid climate type (91%), water scarce basin, and densely populated (WRIS). The SRB lies in the central North part of the Gujarat state where rapid growth of commercialised agriculture and industrialization are taking place (Ballabh and Singh 1997). The SRB is located in the region where groundwater withdrawal for irrigation is quite high that could even worsen under the climate warming. The average annual flow in the SRB is 3.81 km^3 out of which 1.93 km^3 is usable (Kumar et al., 2005). The western India including the SRB has experienced significant changes in precipitation and air temperature during the last 50 years (Rodell et al., 2009). With the growing urbanisation, the rural people are facing the health issues and low agriculture productivity. Ahmedabad is one of the major cities of SRB in which more than 1300 lives were lost due to heat waves in 2010 (Knowlton et al., 2014) and the city has reported significant increase trend in minimum and maximum temperature (Pingale et al., 2014). Thus, for sustainable water resources management in the SRB, detailed study about the future and historical climate extremes, and its spatiotemporal variability is required for adopting suitable strategy to cope up the water demand of agriculture and domestic/industrial usage for future.

1.3 HISTORICAL BACKGROUND OF STUDY

The Prime Minister of India unveiled the National Action Plan for climate change on 30-06-2008 wherein eight mission including the National Water Mission (NWM) were launched. One of the agendas of the NWM was to predict the future climate change and its possible impact on water resources of India basins. The Prime Minister had also shown concern over the depleting water resources in the country and its vulnerability under changing climatic conditions during India Water Week on April 10, 2012. Under NWM, 20 river basins in the country were identified for the detailed study on impact of climate changes on Water Resources of respective basins. The Sabarmati River basin was one the 20 basins selected for the study. The information on future climate scenarios may help in adapting to the climate changes and mitigation of its adverse impacts like flood and droughts.

The Project proposals was submitted on 'Impact of Climate Change on Water Resources of Sabarmati Basin' by the IIT Gandhinagar as Lead Institute and SVNIT Surat as partnering Institute. The Ministry of water Resources, R&D (now Ministry of Jal Shakti) had accorded the administrative approval vide letter no. 16/22/2016-R&D/3044-3058 dated November 07, 2016. The financial approval was received vide 28/6/2016-R&D-186-201, dated Feb.09, 2018. Subsequently, the project was started during March 2018 after getting the sanctioned amount deposited in the Institute account for first installment.

1.4 PROJECT OBJECTIVES

a) Assess the climatic variability (precipitation and temperature) over the Sabarmati basin for historical time period.
b) Prediction of inflows into Dharoi reservoir using calibrated SWAT and HEC-HMS models.
c) Extract the climatic variables for Sabarmati basin from downscaled data for India, and assess the water availability for future (near, mid and far future) in Sabarmati basin using calibrated SWAT model.
d) Evaluate the Impact on Irrigation demand and develop the reservoir operation module for existing condition and those to be adopted for future.

1.5 SCOPE OF STUDY: SVNIT SURAT

a) Data collection from various sources for soil type, land use land cover, streamflow, meteorological inputs (precipitation, maximum and minimum temperature, wind, solar radiation), and groundwater levels.
b) Assessing the trends in climatic variables for base line time period.

c) Hydrologic modelling using HEC-HMS and SWAT, including its calibration and validation in prediction of inflows into Dharoi reservoir.
d) Implications of projected hydrologic change due to possible climate changes.
e) Assess the Impact on Irrigation demand in the Command area of Dharoi reservoir and suggest the possible measures for operation of reservoir.

1.6 OUTLINE OF THE REPORT

Proposed report entitled "Impact of climate change on water resources of Sabarmati basin" consists of seven chapters. The summary of these chapters are included in the succeeding paragraphs.

Chapter 1: A brief introduction about the problem and the model used is explained.
Chapter 2: Includes literature review based on objectives.
Chapter 3: The study area and data sources required for the analysis of present study are presented.
Chapter 4: Investigation of trend detection of climatic variables are presented for Sabarmati River basin.
Chapter 5: Results and analysis of hydrological modelling using HEC-HMS and SWAT are presented.
Chapter 6: Results and analysis of impact on irrigation demand are presented.
Chapter 7: Conclusions and adaptive measures of the present work are presented.

2 LITERATURE REVIEWS

2.1 GENERAL

The recent studies on hydroclimatic variability, hydrological modelling using SWAT and HEC HMS, and muiti-objective reservoir optimization are included which are inline the theme of the project.

2.1.1 Hydroclimatic variability

Goswami et al. (2006) and **Rajeevan et al. (2008)** used absolute threshold approach on the basis of the event classified as heavy rainfall (≥100 mm/day), moderate rainfall (≥5 and <100 mm/day) and very heavy rainfall (≥150 mm/day) and pointed out increasing (decreasing) trend in extreme rainfall (moderate rainfall) for Indian region.

Sonali and Nagesh (2013) performed temporal as well spatial trend analysis of temperature in India for the period 1901-2003 using non-parametric methods and reported significant increasing trend in maximum and minimum temperature after 1970.

Shastri et al. (2015) identified 42 urban regions across India and compared their extreme rainfall characteristics with those of surrounding rural areas. Impacts of urbanization on extreme rainfall in central and western regions of India are reported. Overall, the study identifies the climatological zones in India, where increased urbanization affects regional rainfall pattern and extremes, with a detailed case study of Mumbai. They insisted the need of further experimental investigation to identify the affect of urbanization in climatological processes at various regions in India.

Mazdiyasni et al. (2017) analysed the impact of increasing global temperature and cause of floods, drought and heat waves in India using IMD temperature data for the period of 1960 and 2009. Mean temperatures across India have risen by more than 0.5°C over this period with statistically significant increases in heat wave. The study concluded that Moderate increase in mean temperature, may cause great increase in heat-related mortality.

Ye et al. (2018) used twenty-eight extreme indices derived from station-based precipitation and temperature data to explore the relation between dry and wet years, and warm and cold years in terrestrial ecoregions globally. They found that extreme warm years have increased with high occurrence of warm nights.

Sharma et al. (2018) used twelve extreme precipitation indices and five extreme temperature indices to understand the spatial and temporal variability of precipitation in Upper Tapi basin in India. The study reported an increase (decrease) in rainfall intensity (annual total precipitation and rainy days) across the region. It is also observed that 1-day and 5-day annual maximum rainfalls shows mixed trends in the basin with the increase (decrease) in dry spells (wet spells). The increasing (decreasing) trend in hottest and coldest days (coldest night) is also reported in the basin.

Diaz et al. (2020) studied temperature and precipitation extremes (2020) for the period of 1980-2016 on Brazil climate change. They considered total eight extreme temperature and precipitation indices and reported significant warming pattern for both cold and hot extreme indices and increase (decreased) in consecutive wet days (consecutive dry days) with time in the region. They also reported that minimum and maximum temperatures, under RCP4.5 and RCP8.5 are likely to increase, for the period 2046-2100.

Kumar et al. (2020) quantified climate change signals using long term trend of extremes precipitation and temperature across India. They indicated R95p and R90p exhibits significant increasing trend. Increasing (decreasing) trend of warm days (cold days) were also reported. They used CanESM2 climate model (RCP8.5) to understand the projected change and found the increasing (decreasing) trend in warm days (cold days) in some of locations while increasing (decreasing) trend in warm nights (cold nights) in other locations.

Vijay et al. (2021) reported climate change signals by using precipitation and temperature indices for Kerala state and found decreasing (increasing) trend of extreme precipitation (temperature) indices. The decreasing trend of rainy days (2.8 days/decade) and increasing trend of temperature (1.3°C/decade) were also reported in the study.

Gehlot et al. (2020) studied the spatial and temporal variability of precipitation by using twelve precipitation indices across the Tapi basin. They reported mixed trend of total annual rainfall across the basin with decreasing (increasing) trend of rainy days (rainfall intensity). An increase (decrease) in extreme rainfall, hottest and coldest days (rainy days, coldest night) are observed across the Tapi basin over the period 1944 to 2013 indicating the shifting of basin to drier climatic regime.

2.1.2 Hydrological modelling

This section deals with the past studies and their inferences used in the present study for hydrologic modelling using SWAT and HEC-HMS models.

2.1.2.1 Event-based hydrologic modelling

Saleh et al. (2011) investigated the various runoff loss method (Green & Ampt, Initial and constant loss rate and Deficit and Constant loss) with different objective functions (percent error in peaks and volumes) to simulate the runoff using HEC-HMS. They concluded that Initial and constant loss rate method simulated observed data closely and provided good statistical performance with both objective functions.

Majidi and Shahedi (2012) estimated surface runoff on the basis of hydrologic response, i.e., precipitation and quantified discharge at the outlet. They used HEC-HMS 3.4 and simulated five rain storm events in Abnama catchment located in the South of Iran. Green-Ampt, SCS Unit hydrograph and Muskingum routing methods were used to calculate the hydrologic process of infiltration, rainfall excess and flow routing respectively. The model was further calibrated using optimization approaches. Model validation was carried out by taking the most sensitive parameters, i.e., lag time; and good result was reported showing less difference in the simulated and observed peak flows.

Abushandi and Merkel (2013) used HEC-HMS and IHECRAS models to simulate single stream flow event in Wadi Dhuliel arid catchment. HEC-HMS was coupled with HEC-GEOHMS as an extension in the ARC View 3.3 while IHECRAS supports Java version. Input of HEC-HMS model included soil type, land use/land cover, and slope. The lumped model IHECRAS was also applied on hourly rainfall and temperature data. Both the models were calibrated and validated, and results demonstrated that HEC-HMS provided better performance with Nash Sutcliffe efficiency of 0.88.

Choudhari et al. (2014) simulated rainfall runoff process in Balijore Nala watershed, Odisha, India. For the computation of runoff volume, peak runoff, base flow and flow routing, SCS curve number, SCS unit hydrograph, Exponential recession and Muskingum routing methods were applied respectively. The 24 rain storm events from 2010-2013 were taken, out of which 12 events were used for calibration and rest of the 12 events were used for validation. The model performed well and gave the root mean square error for observed runoff depth and peak

discharge of 2.30 mm and 0.28m^3/sec. They also concluded that model can perform well in ungauged watersheds also.

De Silva et al. (2014) successfully applied HEC-HMS for event-based simulation and continuous simulation in Kelani River basin, Sri Lanka. Green-Ampt method and six layer soil moisture accounting method were used for getting the infiltration loss, in event based modelling and continuous modelling respectively. For simulation of direct runoff, Clark unit hydrograph was used while recession base flow method was used for simulating the base flow. The result demonstrated that average value of Nash Sutcliffe was 0.91 for event-based simulation and 0.8 for continuous simulation. They also concluded that HEC-HMS can also be applied in disaster mitigation, flood control, and water management in medium sized river basin in Tropical countries.

Mokhtari et al. (2016) performed modelling in Wadi Cheliff-Ghrib by using HEC-HMS. Calibration schemes include selection of the event and finding the optimized parameter which were further used in validation. The study recommended that HEC-HMS model can be used for flood simulation, low flow forecast, flood predetermination, sizing of structures, changes in the land use due to urbanization, deforestation and real time modelling. They discussed that in spite of very complex behaviour of the rivers which requires good knowledge of flows and field, HEC-HMS yields reliable result.

2.1.2.2 Continuous hydrologic modelling

Bennett and Peters (2004) gave explanation regarding the computational steps and equations used in the SMA loss method in HEC-HMS model to simulate the processes. Satisfactory results of model are reported in Tifton, Georgia, and Riesel, Texas watersheds .

Fleming and Neary (2004) performed sensitivity analysis in HEC-HMS model and concluded that maximum infiltration rate, the maximum soil depth, and tension zone depth, are the sensitive parameters. All the groundwater parameters except parameter groundwater 1 percolation rate were varied during the model calibration. Seasonal parametrization approach was evaluated. An annual, a semi-annual, and seasonal models were developed. Both the semi-annual and seasonal models performed better than the annual model for these months. Manual calibration helped to determine a practical range of parameter values, while automated calibration was used to refine the search for the optimum parameter value.

Meselhe et al. (2004) showed that distributed model (MIKE-SHE) performed slightly better in predicting the runoff volume, overall runoff discharge, and peak magnitude, while the lumped model (HEC-HMS) had a better time to peak prediction. The distributed model results were more sensitive to temporal resolution of rainfall.

Merz et al. (2009) simulated the water balance dynamics of 269 catchments in Austria using a semi distributed conceptual model with 11 parameters based on a daily time step using semi-distributed conceptual rainfall-runoff model based on HBV model. The simulation results suggested that Nash-Sutcliffe model efficiencies increase over the scale range of 10 and 10,000 km^2. The performance of the model in terms of scatter plot indicated that model performance decreases with catchment scale, particularly the volume errors. This implies that the model simulates the long-term water balance more reliably as one goes up in scale. Most calibrated parameters do not change with catchment scale, but there is a trend with catchment area of the upper and lower envelopes for some parameters. The study also examined time scale effects, and results showed that calibration efficiencies decrease, and verification efficiencies increase with the number of years available for calibration. *The study also suggested that a calibration period of 5 years captures most of the temporal hydrological variability, hence, this would be the minimum period for achieving a reasonable predictive model performance.*

Abbaspour et al. (2009) created hydrologic model using the Soil and Water Assessment Tool (SWAT) model and calibrated for period from 1980 to 2002 using daily river discharges and annual wheat yield data at a subbasin level in Iran. Future climate scenarios for periods of 2010–2040 and 2070–2100 were generated from the Canadian Global Coupled Model (CGCM 3.1). The hydrologic model was then applied to these periods to analyse the effect of future climate on precipitation, blue water, green water, and yield of wheat across the country. It was found that for future scenarios wet regions of the country will receive more rainfall while dry regions will receive less. Analysis of daily rainfall intensities indicated more frequent and larger-intensity floods in the wet regions and more prolonged droughts in the dry regions.

Du et al. (2013) quantified the hydrological processes in a rapid urbanization region and used SWAT model in Qinhuai River basin which is most urbanized region in China. They developed varied parameterization strategy establishing regression equations with selected SWAT parameters as dependent variables and catchment impermeable area as independent variable. The performance of the newly developed varied parameterization approach was compared with the conventional fixed parameterization approach in simulating the hydrological processes

under LULC changes. The results showed that the model simulation with varied parameterization approach has a large improvement over the conventional fixed parameterization approach in terms of both long-term water balance and flood events simulations. The proposed modelling approach could provide an essential reference for the study of assessing the impact of LULC changes on hydrology in other regions.

Razmkhah (2016) compared different loss methods i.e., Green and Ampt (GA), Initial Constant (IC), Deficit Constant (DC) and Soil Moisture Accounting (SMA) for event-based rainfall runoff simulation in HECHMS 3.5. The SMA method provided good Nash Sutcliffe efficiency and minimum peak weighted root mean square error (PWRMSE) during calibration and validation in simulating the stream flow. They reported the second best method as SCS method with good Nash Sutcliffe efficiency and PWRMSE for event based simulation.

Haque et al. (2017) simulated rainfall-runoff in HEC-HMS using soil moisture accounting method as a loss method and found that tension storage is the most sensitive parameter for simulating the stream flows during the calibration periods. The surface storage, maximum infiltration and soil percolation have no influence on the model performance. The GW2 storage was found to be the least sensitive parameter.

Deng at al. (2019) studied Tongtianhe and Ganjiang basins (China) and reported that the model parameters that may vary temporally due to human activities, and climate variability and changes. They proposed a framework for quantifying hydrological model parameters as functions of time-variant catchment properties, aiming to improve the capability of capturing hydrograph and the explore the ability of hydrological models under changing environment.

Sahana and Timbadiya (2020) studied the variation in water balance components of the semiarid Upper Girna basin (UGB), Maharashtra, India, and flow quantiles of a dam downstream of the UGB under changing climate using the semi-distributed hydrologic model Soil and Water Assessment Tool (SWAT). They found that water balance components of UGB, as simulated by the calibrated SWAT model for the historical observed period (1981–2010), have water yield and evapotranspiration contributions of 17% and 56%, respectively, out of total 100% precipitation input to the system. The present work provides significant insights for resource managers and policy makers for efficient water resources planning and management.

Ma et al. (2020) proposed hydrological modelling framework based on Soil and Water Assessment Tool (SWAT) to investigate the variability of model parameters in three different experiments and assess the impacts of climate and/or land-use change on these parameters in the upstream of the Lancang River Basin, China. In Experiment 1 (E1), most parameters show clear temporal trends under changing climate and land use, implying that model parameters are strongly influenced by their combined effects. Experiments 2 (E2) and 3 (E3) investigate the separate impacts of land-use change and climate change, respectively. Due to the almost invisible changes in land use in E2, there is no change detected in the model parameters. Temporal trends are found in most parameters in E3 and over half of them show consistent trends with E1, which indicates that climate change has greater impacts on model parameter variability. The simulated extreme streamflow and sediment fluxes vary substantially with time-variant parameters, implying that the variations in model parameters do matter for hydrological prediction.

2.1.3 Multi-objective reservoir optimization

Heidari et al. (1971) proposed discrete differential dynamic programming approach for optimization of water resources system. The main objective was to rectify the limitations of traditional dynamic programming - memory requirements and computer time requirements. A trial trajectory having set of initial and final conditions for Bellman' recursive equation is used. A Discrete Time Four Reservoir Operation (DFRO) system solved by Larson (1968) is solved by Discrete Differential Dynamic Programming (DDDP) to understand its approach in developing operating policy for reservoir system.

Jain et al. (1998) presented the reservoir Operation studies of Sabarmati System, India. The operation of system consisted of four reservoirs and threes diversion structures was studied. The function of the system was to provide a municipal and industrial water supply, irrigation and flood control. The operational procedure for flood regulation of Dharoi reservoir was developed. Since, the primary damage centre was located well away from the Dam, it was essential to estimate the effect of releases from Dharoi Reservoir. A computer algorithm was developed to assist the operator at the dam site in determining the safe releases.

Wardlaw and Sharif (1999) formulated several alternatives of genetic algorithm and implemented them for different reservoir systems. The models differed by alternating representation, selection, crossover and mutation. Four - reservoirs, finite-horizon and deterministic reservoir problems were undertaken. The results showed that four reservoir problem comprises real value coding, uniform crossover, tournament selection and modified

uniform mutation as real value coding gives better and faster results in reaching known global optimum. The research demonstrated application of GA as an alternative to Stochastic Dynamic Programming (SDP) in real time operation of reservoirs.

Afshar et al. (2006) used swarm-based Honey-Bee Mating Optimization Algorithm for optimal reservoir operation. It is based on concept of mating process of the queen of hive. The algorithm has one pre-defined parameter and three user-defined parameters. The efficiency of algorithm was tested using nonlinear, continuous constrained problem with continuous decision and state variables.

Asgari et al. (2015) introduced weed optimization (WOA) algorithm which is based on life cycle of weeds, for optimal reservoir operation. The performance of WOA is tested using mathematical benchmark functions and a single reservoir operation problem - Bazoft reservoir in Iran and also a Discrete Time Four Reservoir Operation (DFRO) and Continuous Time Four Reservoir Operation (CFRO) system. The comparison of results with GA (Genetic Algorithm) showed that convergence of WOA is better and faster towards optimal solution. The functional value of WOA was 2.53% better than CFRO system, and 38.79% time better for single reservoir problem.

Haddad et al. (2015) used biography based optimization algorithm (BBO) for reservoir operation of Karun4 reservoir in Iran. Mathematical benchmark functions and a discrete time four reservoir operation system was also solved. The results were compared with results of Genetic algorithm which showed that BBO out-performed GA. For DFRO system, GA converged to 97.46% where BBO converged to 99.94%.

Sharma et al. (2015) studied the behaviour of Ukai reservoir system. Using historical data of reservoir, a simulation model based on standard operating policy was developed. Their study objected to minimize the flood damages and also ensure reliable water supply for various purposes. Stochastic Dynamic Programming model was implemented to develop target storage and releases with respect to certain flood constraints. Discretization of reservoir inflows and storage was done and optimal releases and optimal end period storages were reported by state variable combinations.

Patel et al. (2018) presented an efficient and reliable teaching-learning based approach, namely, teaching-learning based optimisation (TLBO) algorithm for optimisation of multi-reservoir operation policy. It was based on the teaching-learning process of the education

system. TLBO algorithm does not require any algorithm-specific parameters for obtaining optimal results; instead, it requires only the population size and number of iterations. The time required for obtaining the specific optimised algorithm parameter was reduced and results were also near the global-optimal solution. The number of function evaluations required, was less. This TLBO algorithm was implemented at five-reservoir model of the Upper Godavari River project in the city of Nashik in Maharashtra, India. The efficiency of the results of the TLBO algorithm was compared with the genetic algorithm (GA). The results showed that TLBO algorithm was considered to be a viable alternative to the operating policy of multi reservoir system and it avoided the local optimal solution.

Kumar and Yadav (2018) in their study evaluated three different benchmark problems to check the applicability and performance of TLBO and JAYA Algorithm (JA) in multi-reservoir operation problems. The benchmark problems were the discrete time four-reservoir operation (DFRO), the continuous time four-reservoir operation (CFRO), and the ten-reservoir operation (TRO). The results from the TLBO and JA were compared with different approaches from the literature. The optimal net benefits obtained from JA for DFRO, CFRO and TRO problems were 401.44, 308.40 and 1194.59, respectively, and that of TLBO algorithm were 401.33, 308.30 and 1194.44, respectively. It was found that both JA and TLBO algorithms provided a satisfactory solution as other optimization techniques, from literature. Their study concluded that JA out performed over TLBO.

3 STUDY AREA & DATA SOURCES

3.1 GENERAL

A brief description of the study area including its physiographic, climatic features are described. Also, the salient features of Dharoi reservoir including the capacity of elevation curve, area elevation curve and its command area are included. The data collected in present study related to meteorological, hydrological, topographical, soil, land use land cover and the data related to reservoir and command area are included.

3.1.1 Sabarmati River basin

Sabarmati River originates at an elevation of 762 meters from Aravalli hills of Udaipur district in the state of Rajasthan enrooting to Gulf of Khambhat in Gujarat. It is one of major west-flowing rivers located between 70°58' E to 73°51' E and 22°15' N to 24°47' N. After travelling a distance of 355.86 km from Gujarat (273.96 km) and Rajasthan state (81.9 km), it meets the Gulf of Cambay of Arabian sea in south-west direction. The Sabarmati basin (30,674 km^2) (Jain et al., 2007) is covered by by Rann of Kutch in the west, Aravalli hills in the north and north-east, and Gulf of Cambay in the south. The Sabarkantha, Kheda, Ahmedabad, Mahesana, Gandhinagar and Banaskantha districts of Gujarat and Udaipur, Sirohi, Pali and Dungarpur districts of Rajasthan falls in the basin. There are several major and minor dams located in the Sabarmati River and its tributaries. Among them, Dharoi dam is one of the major dam located in the main river, while other smaller dams, namely, Guhai, Harnav, Hathmati, Guhai, Meshwo, Watrak and Mazam, are located across its tributaries. The basin has recorded average annual rainfall of 689.90 mm. Due to sparse rainfall and a momentary river system; the entire study area depends heavily on ground water for its domestic, agriculture and industrial requirements. The basin is divided into two parts – *i) Sabarmati Upper Sub-Basin and ii) Sabarmati Lower Sub-Basin* (Figure 3.1b). They have been further clustered into 51 watersheds, each representing a different tributary system (WRIS).

The maximum temperature in the basin varies from 39°C to 48°C. The temperatures lies in the range of 11°C – 15°C in winters and 38-47°C in summers. The map of Köppen-Geiger climate classification for Sabarmati basin consists of three major climate types. Out of these, the dominant climate type is arid BSh (91.2%), followed by tropical AW (4.7%), and temperate Cwa (3.1%) (Rubel and Kottek 2010). In north, the basin is marked by hilly terrain whereas on south, it has large alluvium plains with gentle slope. Sei is the right bank tributary and Wakal, Hathmati, Harnav and Watrak are left bank tributaries of Sabarmati River. Out of total 9 major

and 11 medium irrigation projects; Dharoi irrigation project is located at 103 km from source of the river.

3.1.2 Salient features of Dharoi reservoir

Dharoi dam is located at 24° 0' 15.69" N and 72° 50' 33.72" E and it is the most important structure on Sabarmati. This Gravity dam (Earthen and Masonry) is located in Satlasana taluka, Mehsana District, Gujarat and constructed in June 1976. Dharoi Dam is 45.87 m high and 1207 m long with surface area of 107 sq. km at top. The earthen portion is 838.21 m long while the rest is masonry. The total capacity of reservoir is 907.88 MCM with live storage capacity of 775.89 MCM and dead storage capacity of 131.99 MCM. The dam is provided with Ogee Spillway of 219 m length and 12 radial gates and roller bucket type energy dissipator. Dharoi reservoir is a multipurpose reservoir constructed across Sabarmati River, located about 165 km upstream of Ahmedabad city, Gujarat. Mahesana, Sabarkantha, Patan and Gandhinagar districts of Gujarat are benefitted by this project for irrigation and domestic water demands. It is the major flood-controlling structure serving the purposes of drinking water supply, irrigation and hydroelectric power generation (till year 2000). The Dharoi command area is divided into two canals – Right Bank Main Canal (RBMC) and Left Bank Main Canal (LBMC) of 44 km and 29.52 km length respectively (Figure 3.1c-d). The discharge capacity of Right Bank Main Canal is 38.22 m^3/s and that of Left Bank Main Canal is 11.32 m^3/s. The cultural command area (CCA) of RBMC (LBMC) is 70454 (12145) ha and gross command area (GCA) is 81754 (15670) ha. Pearl Millet (Bajra), Cotton, Maize and Sorghum (Jowar) are major crops of Kharif season while Wheat, Rapeseed, Mustard and Castor are predominant in Rabi season. The basin is of hilly terrain in the upstream of Dharoi reservoir and in the downstream, the river flows in plains. The total catchment area of dam is 5540 km^2. The mean annual rainfall of Dharoi catchment is 633 mm. Most of the rainfall is received during monsoon season from June to September. It has total two stream gauging stations, i.e., Jotasan and Kheroj. In August 2017, the release from Dharoi Dam was approximately 3700 m^3/s water, thus submerging the lower walkway of Sabarmati Riverfront in Ahmedabad. Thus, to establish relationship between inflow and release of Dharoi reservoir, rainfall-runoff simulation is required in the region (https://www.deshgujarat.com). The index map of study is presented in **Figure 3.1.** The salient features of Dharoi reservoir are included in **APPENDIX-1** while the details Left bank main canal and Right bank main canal are included in **APPENDIX-2.**

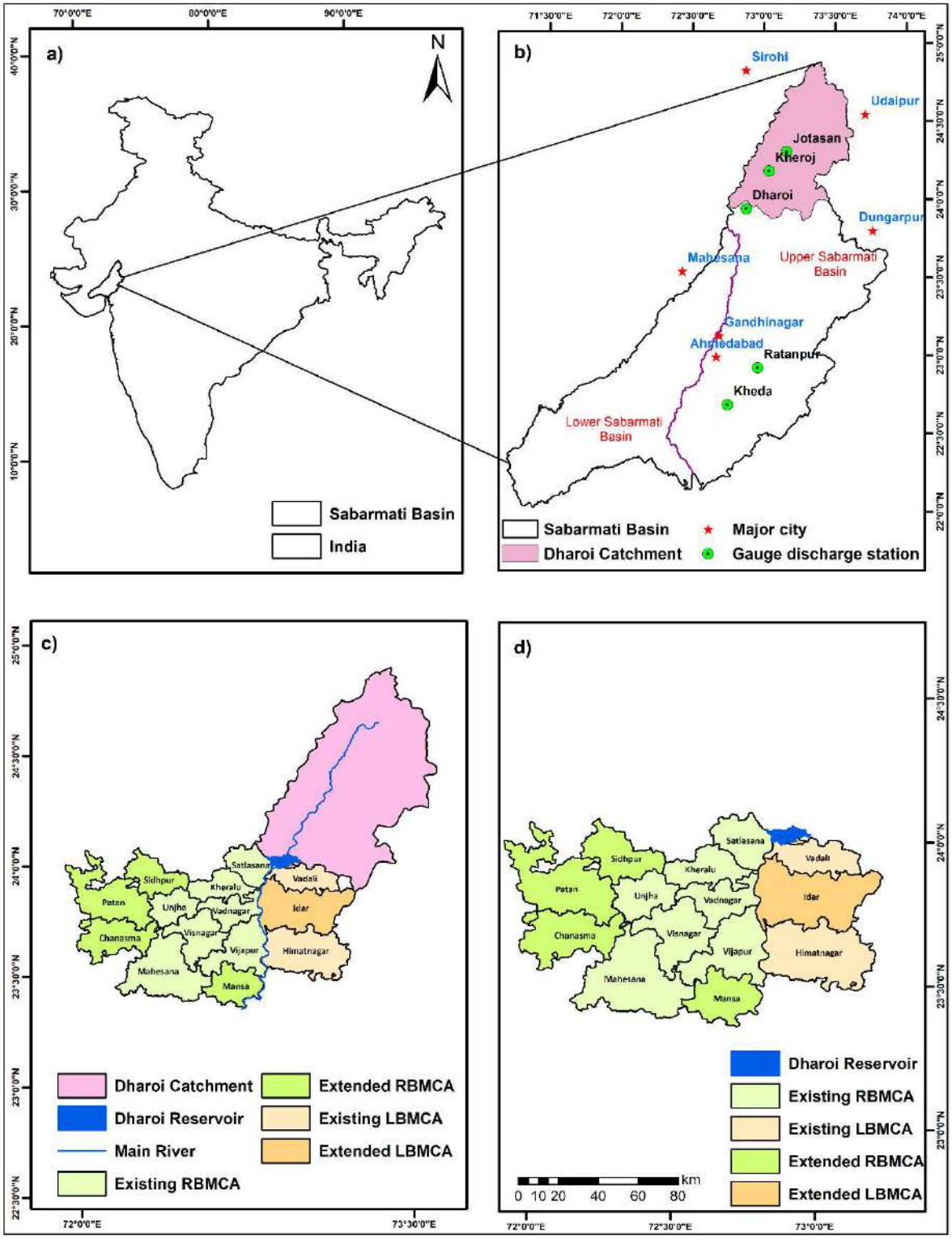

Figure 3.1 Index Map of Sabarmati River basin

3.2 DATA SETS AND THEIR SOURCES

The data collected in the present study for hydrological modelling like SRTM DEM, LULC maps, soil map, rainfall, temperature, stream flow, reservoir data and data of command areas are included in the Table 3.1. Further, the statistically downscaled precipitation and temperature data using Kernel regression for five GCMs were extracted from web link http://www.regclimindia.in/. These future downscaled data were used for getting the response of the basin for near, mid and far future.

The sedimentation survey by Gujarat Engineering research Institute (GERI) was conducted in 2006 which showed that average silting in the Dharoi reservoir in 31 years (1976 – 2006) was 3.054 m^3/year. Subsequently, changes in storage capacity of reservoir was also observed. The gross storage capacity of reservoir was reduced from 907.88 MCM to 813.14 MCM due to sedimentation during aforesaid period. The dead storage capacity of reservoir was changed to 67.51 MCM from 131.99 MCM. As a result, there was reduction of 30.26 MCM in live storage capacity of reservoir. The revised capacity elevation curve after 2006 is shown in Figure 3.2 which is based the sedimentation Survey of year 2006. The total monthly inflows into the reservoir and evaporation losses are included in Figure 3.3 and Figure 3.4 respectively. The cropping pattern in the Left bank main canal (LBMC) and Right bank Main Canal (RBMC) of Dharoi reservoir is included in **Appendix-3.**

Table 3.1 Nature of Data and their Sources

Data type	Data description	Temporal/ spatial resolution	Data source(s)
Shuttle Radar Topographic Mission (SRTM)	Slope, elevation	30 m	United States Geological Survey (USGS) website https://earthexplorer.usgs.gov/
Land-use and land-cover map	Description of land-use and land-cover classes, such as urban, scrub, agricultural land, forest	30 m and 56 m	USGS Earth Explorer and National Remote Sensing Centre (NRSC), Hyderabad, India
Soil map	Hydrologic soil group and its physical properties	1:250,000 scale	National Bureau of Soil Survey and Land Use Planning (NBSS & LUP), Nagpur, India
Rainfall	Gridded rainfall data	Daily (0.25° × 0.25°)	India Meteorological Department (IMD), Pune, India
Temperature	Gridded maximum and minimum temperatures	Daily (1° × 1°)	India Meteorological Department (IMD), Pune, India
Streamflow	Observed stage and discharge	Daily	India-WRIS web portal https://indiawris.gov.in/wris/#/
Reservoir data	Reservoir inflow	Daily and Monthly	Narmada, Water Resources, Water Supply and Kalpsar Department (NWRWS&KD), Government of Gujarat, India
Elevation - Area – Capacity Table (Last Sedimentation Survey carried out by GERI in November 2006)	Reservoir data	Average silting in Reservoir in 31 years (1976 – 2006)	Narmada, Water Resources, Water Supply and Kalpsar Department (NWRWS&KD), Government of Gujarat, India
Canal / District / Taluka wise Irrigated Command Area	Details of Original and Extended CA		Narmada, Water Resources, Water Supply and Kalpsar Department (NWRWS&KD), Government of Gujarat, India
Cropping Pattern	Type and area of crops in Kharif, Rabi and hot Weather in Dharoi command area		Dharoi Irrigation Office, Visnagar
Dharoi Regional Water Supply Scheme	Details of domestic water supplied to talukas		Gujarat Water Supply & Sewerage Board, Dharoi
Idar–Vadali Water Supply Scheme	Details of domestic water supplied to talukas under Idar - Vadali Water supply Scheme		Gujarat Water Supply & Sewerage Board, Idar
Meteorological Data	Minimum and Maximum Temperature Relative Humidity Average Wind Speed	Daily	State Water Data Center, Gandhinagar, Gujarat, India
Population Data	Human populations		District Census Handbook

Table 3.2 High Resolution GCMs (http://www.regclimindia.in/)

Experiment	Driving GCM	Institution
Scientific and Industrial Research Organization (CSIRO)	*BNU ESM*	Beijing Normal University Earth System Model
	CCCma CanESM2	Canadian Centre for Climate Modelling and Analysis
	CNRMCM5	Centre National de Recherches Météorologiques
	MPIESM_LR	Max Planck Institute for Meteorology
	MPIESM_MR	Max Planck Institute for Meteorology

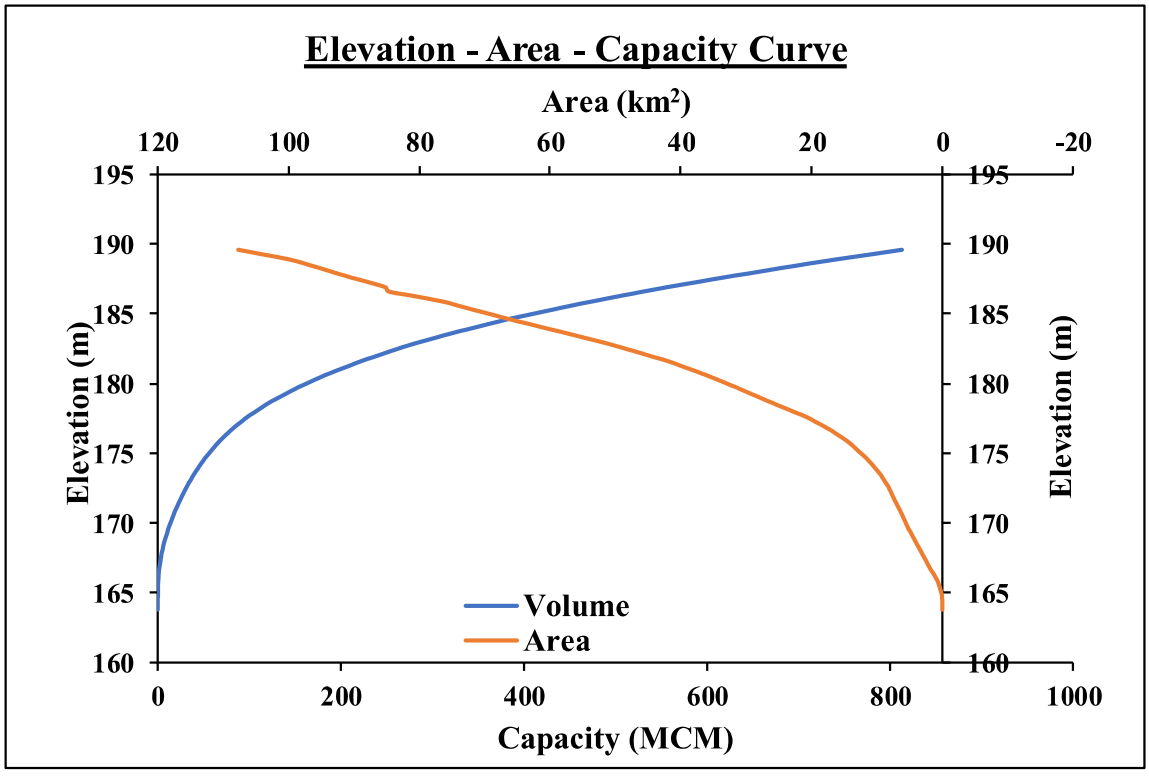

Figure 3.2 Elevation–Area–Capacity Curve of Dharoi reservoir as per Sedimentation Survey 2006

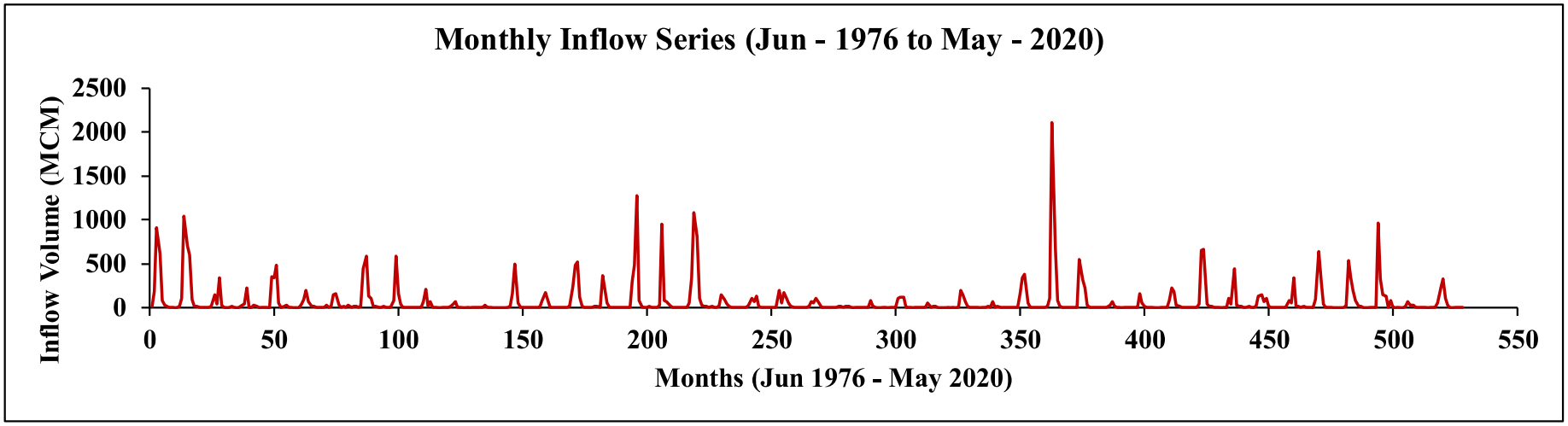

Figure 3.3 Time series of monthly inflow volume (Jun 1976 - May 2020)

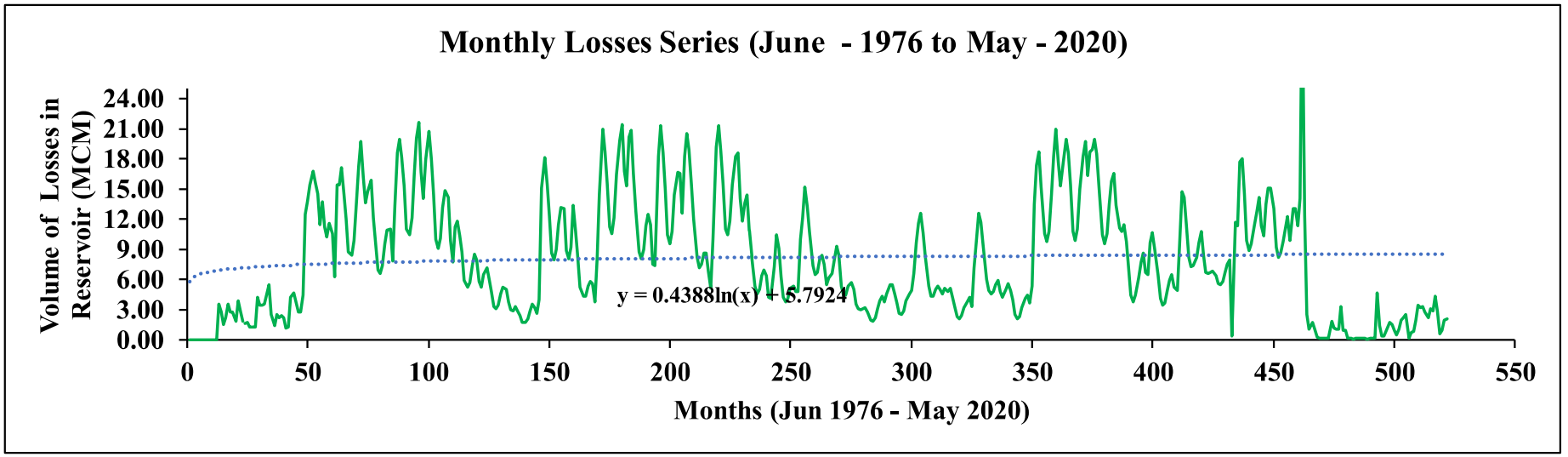

Figure 3.4 Time series of volume of total monthly reservoir losses (June 1976 – May 2020)

4 METHODOLOGY AND ANALYSIS OF DATA: TREND ANALYSIS

4.1 GENERAL

The methodology being adopted in present study for identifying the trend in historical data, particularly precipitation and temperature indices; hydrological modelling for computation of inflows into the Dharoi reservoir for baseline period, reservoir operation and their climate change impact analyses are described in Flow Chart in **Figure.4.1.**

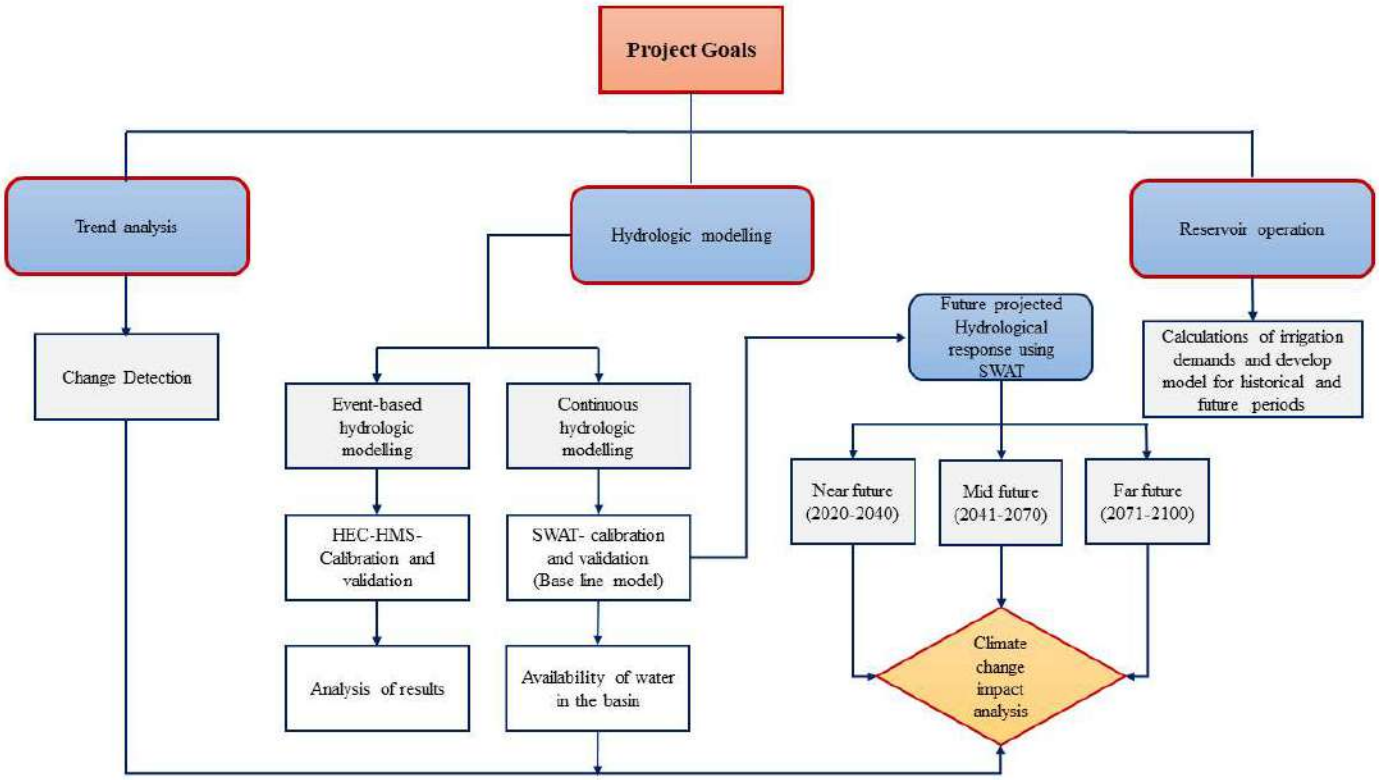

Figure 4.1 Methodology to achieve the objectives of project

This chapter contains the details of methodology adopted (Figure 4.2) and the results of trend analysis of SRB using IMD gridded daily rainfall data of 0.25° × 0.25° (1951-2019) and GCM downloaded daily precipitation data of 0.25° × 0.25° (2011-2100). Also, IMD gridded daily temperature data of 0.50° × 0.50° (1951-2017) has been used for trend analysis. The CMIP5 models are investigated for RCP4.5 and RCP8.5 for near (2020-2040), mid (2041-2070) and far (2071-2100) future.

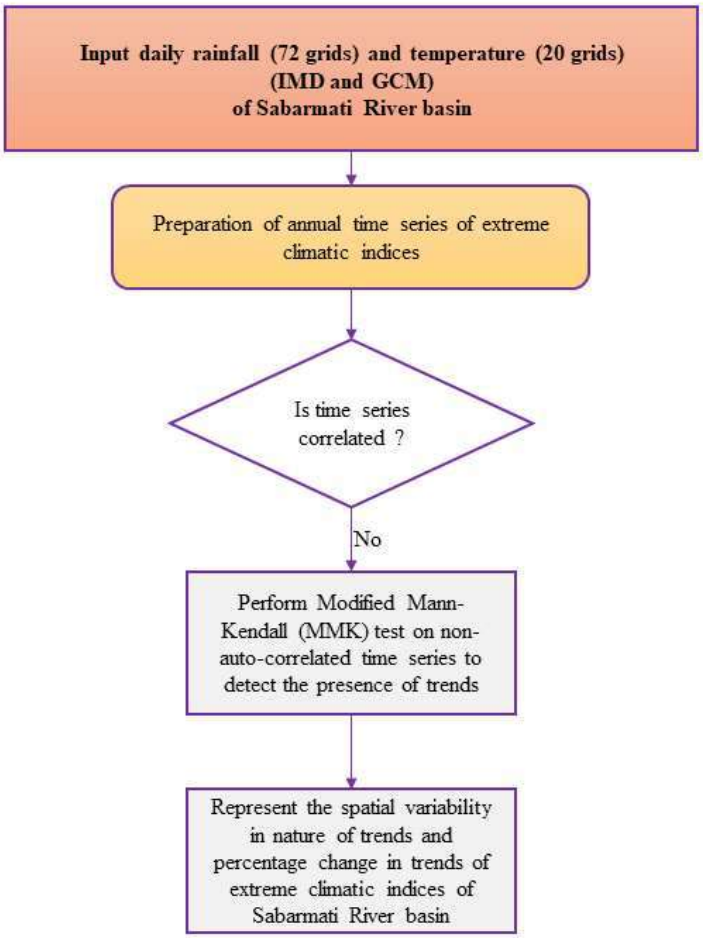

Figure 4.2 Methodology to detect trend in the SRB

4.1.1 Climate indices

In present study, thirteen precipitation extreme indices and six temperature extreme indices, (**Table 4.1**) defined by Expert Team on Climate Change Detection and Indices (ETCCDI) (Zhang et al., 2011) are selected which were used by several researchers in previous investigations (Revadekar and Kulkarni 2008; Zhang et al., 2011; Panda et al., 2016; Sharma et al., 2018; Dash and Maity 2019). Climate extreme events in SRB are studied for historical precipitation (1951 to 2019), temperature (1951 to 2017) and projected climate parameters (2020-2100) for investigating their tends. The Coupled Model Intercomparison Project (CMIP5) GCM models (BNU-ESM, CCCma-CanESM2, CNRM-CM5, MPIESM-LR, MPIESM-MR) under RCP4.5 and RCP8.5, were used for downscaling the climatic parameters like precipitation and temperature for future periods. These parameters were used further for identifying the impact of climate change in future period. Some indices, given by ETCCDI,

have been modified in present study with respect to the Indian Summer Monsoon Rainfall characteristics. The rainy days defines if rainfall equals or exceed 2.5 mm. Also, the light, moderate) and heavy rainy days are considered, when the daily rainfall amount is recorded in the range less than 2.5-7.5 mm; 7.5–64.5mm; and 64.5–124.5 mm (Sonar 2014).

Table 4.1 List of the ETCCDI Core Climate Indices used in This Study

Index	Indicator name	Definitions	Units
RD	Rainy days	Number of days when rainfall ≥2.5 mm	days
PRCPTOT	Annual total rainfall	Annual total rainfall from days ≥ 2.5 mm	mm
SDII	Simple daily intensity index	The ratio of annual total rainfall to the number of rainy days	mm/day
RX1day	Maximum 1-day rainfall amount	Annual maximum 1-day rainfall	mm
RX5day	Maximum 5-day rainfall amount	Annual maximum consecutive 5-day rainfall	mm
R95p	Extremely wet days	Annual total rainfall from days > 99th percentile	mm
R99p	Very wet days	Annual total rainfall from days > 95th percentile	mm
R5TOT	Rainfall extreme proportion	Proportion of annual rainfall from top 5 events in a year	%
Rlight	Number of light rainfall days	Number of days when annual rainfall ≥ 7.5	days
Rmod	Number of moderate rainfall days	Number of days when annual rainfall = 7.5 and < 64.5 mm	days
Rheavy	Number of heavy rainfall days	Number of days when annual rainfall = 64.5 and <124.5mm	days
CWD	Consecutive wet days	Maximum number of consecutive days when rainfall = 2.5 mm	days
CDD	Consecutive dry days	Maximum number of consecutive days when rainfall < 2.5mm	days
T_{max}	Maximum temperature	Annual maximum value of daily temperature	°C
T_{min}	Minimum temperature	Annual minimum value of daily temperature	°C
T_{av}	Average temperature	Annual average value of daily temperature	°C
DTR	Diurnal temperature range	Monthly/seasonal/annual mean difference between daily maximum and minimum temperature	°C
T40D	Very hot days	Number of days in a year on which max daily temperature ≥40°C	°C
T10D	Very cool days	Number of days in a year on which min daily temperature ≤ 10°C	°C

The description of non-parametric tests used for detection of trends in climatic variables are Modified Mann-Kendall (MMK) (Hamed and Rao 1998) and Sen's Slope tests (Hirsch et al., 1982). The statistical significance of the detected trends (using MMK test) has been assessed at 5% significance level. The selected climate indices have been calculated on an annual scale to improve knowledge and understanding of inter-annual extreme temperature and precipitation variability in SRB. The methods used for detection of trends on climate indices are presented in **APPENDIX-IV.**

4.2 TREND ANALYSIS OF PRECIPITATION USING EXTREME INDICES FOR HISTORIC PERIOD

The assessment of trends in the rainfall indices are undertaken using non-parametric test, viz., MMK (at 5% significance level). The distance weighting tool in ArcGIS®10.5, has been used for the generation of hydrologically correct digital elevation models (Hutchinson and Dowling 1991. Percentage grid contribution of historical rainfall (temperature) trend for the period 1951-2019 (1951-2017) are given in Table 4.3 and Table 4.4**.**

4.2.1 Basic rainfall indices

The PRCPTOT, RD and SDII defines the magnitude, rainy days and intensity of total rainfall respectively. The west coast of India exhibits high magnitude and large variability in observed in rainfall due to strong orographic influence of the Western Ghats (Goswami et al., 2006; Vittal et al., 2013). From the trend analyses, it has been found that 44% (35%) (32%) grids exhibit increasing trend including 33% (0%) (56%) grids showing increasing trend with statistically significance in PRCPTOT for period **1951 (O1), 1951-1985 (F1**) and **1985-2019** (S1) respectively Figure 4.3 (a-c). The increasing trend is more significant in S1 period, i.e., second half (1985-2019) of the whole period. Also, the number of rainy days is significantly increased in S1 (**Error! Reference source not found.** c) period with 10% (0%) (47%) grids for O1 (F1) (S1) period. The SDII is the ratio of PRCP and RD, O1 5 a) indicate that 53% grids are showing significantly increasing trend and, on the other hand, F1 (S1) exhibits 21% (22%) significantly increasing trend (Figure 4.5 b-c).

4.2.2 Extreme Rainfall Indices

The extreme rainfall indices, in present study, comprise of absolute indices (Rx1day and Rx5day), threshold-based indices (R95p and R99p) and a relative index (R5TOT). The Rx5day represents the maximum cumulative sum of 5-day rainfall in a year. The trends in Rx1day and

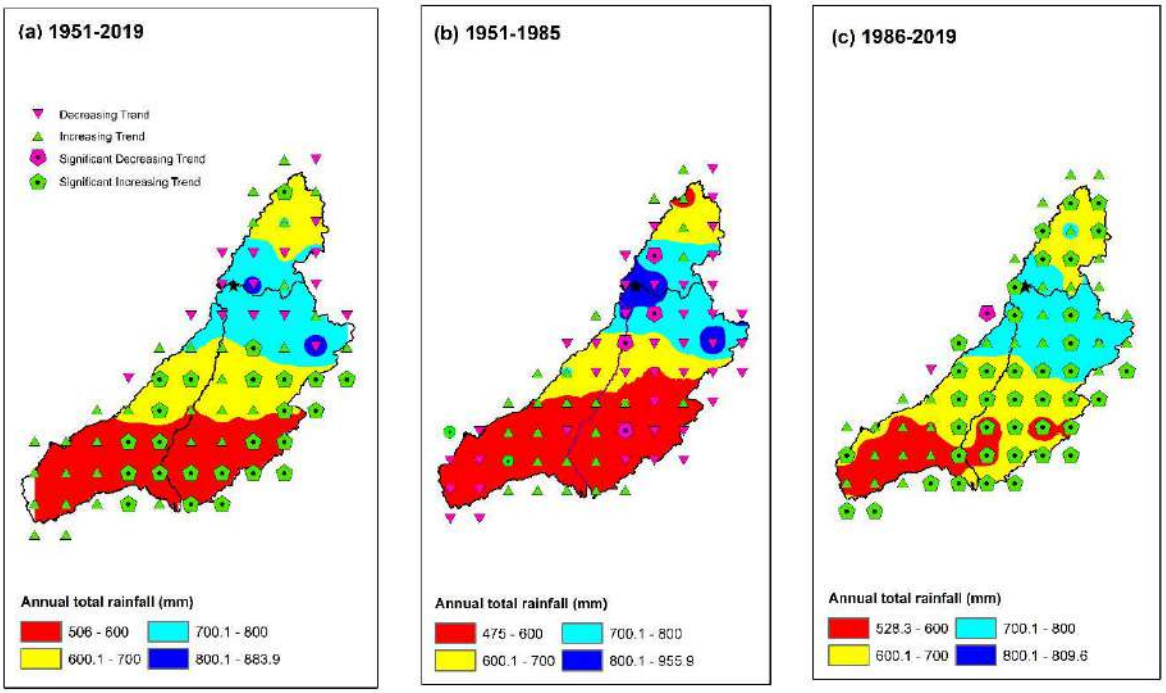

Figure 4.3 Spatial distribution of PRCPTOT over Sabarmati River basin

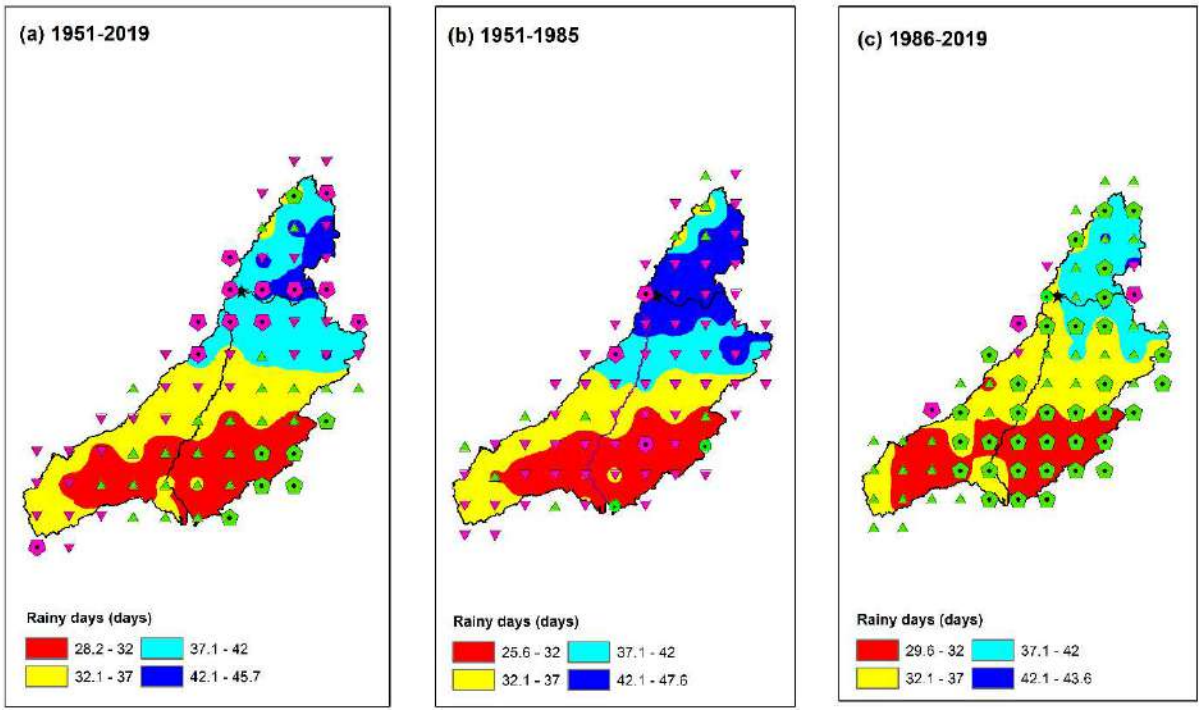

Figure 4.4 Spatial distribution of RD over Sabarmati River basin

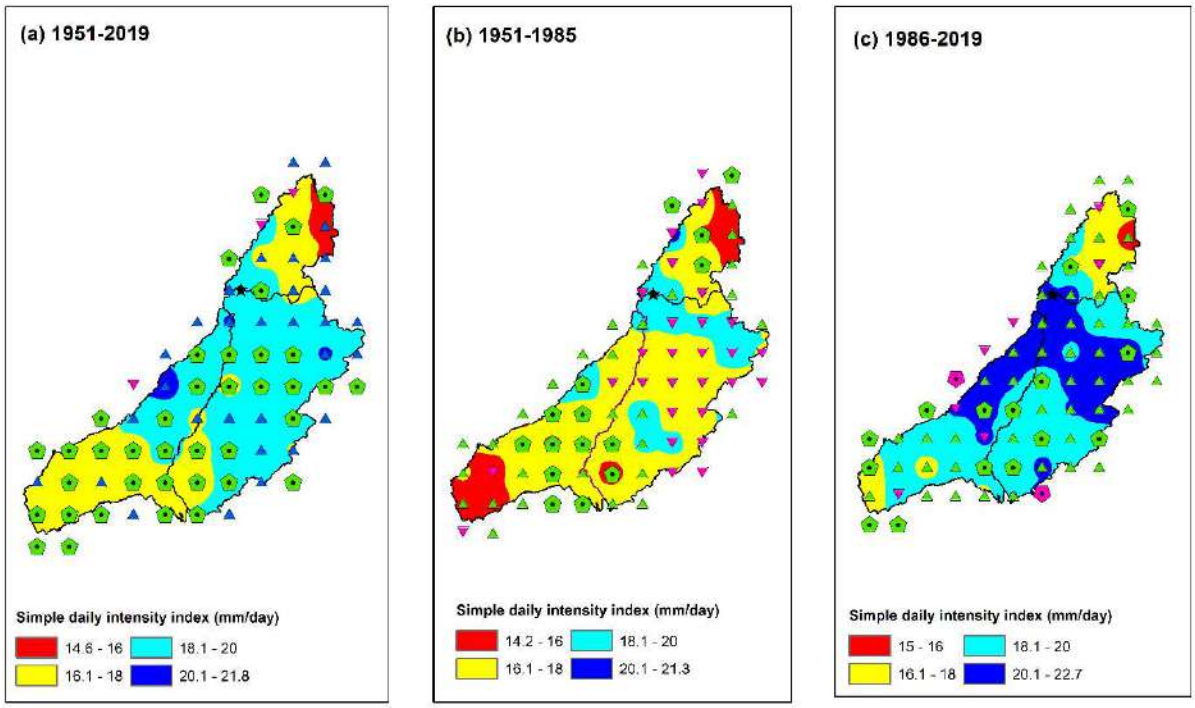

Figure 4.5 Spatial distribution of SDII over Sabarmati River basin

Rx5day are observed to increase for O1 and S1 periods (Figure 4.6 a and c and Figure 4.7 a and c).On the other hand, F1 period have not contributed much for these extreme indices (Figure 4.6 b and 4.7 b). The R95p (R99p) represent the sum of rainfall received in a single rainy day with magnitude equal to or more than 95th (99th) percentile value of rainfall for the period 1951–2019. The daily rainfall data of monsoon season (as it records 90% of total annual rainfall in the basin) has been considered for estimation of extreme rainfall thresholds, i.e., R95 and R99. The 19% (1%) (38%) grid points in the basin show significantly increasing trend and 74% (61%) (58%) are identified as increasing trend for O1 (F1) (S1) periods respectively for R99 (Figure 4.8 a-c). On other hand, 7% (36%) (4%) grids showed decreasing trend in R99p (Figure 4.8 a-c). In O1 (F1) (S1) period, 28% (0%) (34%) grid points in the basin show significantly increasing trend in R95p (Figure 4.9 a-c). The R5TOT, a relative index, represent the percentage contribution of top five rainfall events in a year, and reveals the degree of non-uniformity in temporal distribution of rainfall. The results of trend in R5TOT revealed that the 17% (13%) (3%) grids indicate significantly increasing trend while 8% (3%) (36%) grids show significantly decreasing trend in O1 (F1) (S1) (Figure 4.10 a-c).

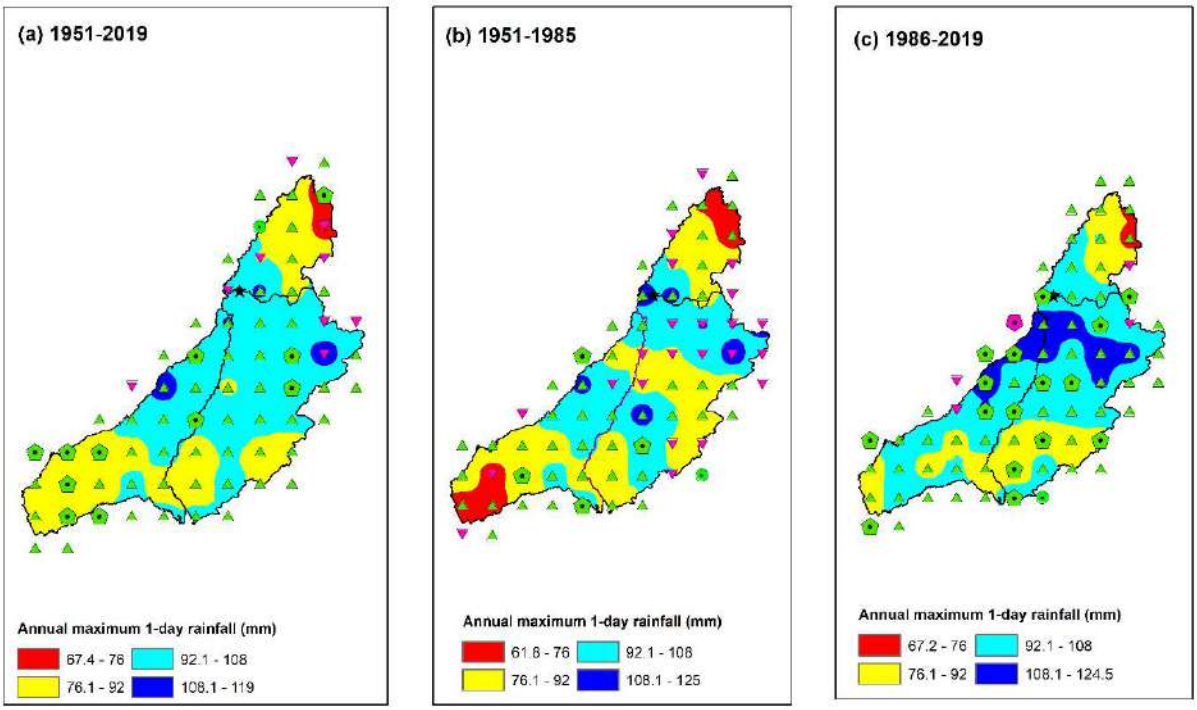

Figure 4.6 Spatial distribution of RX1day over Sabarmati River basin

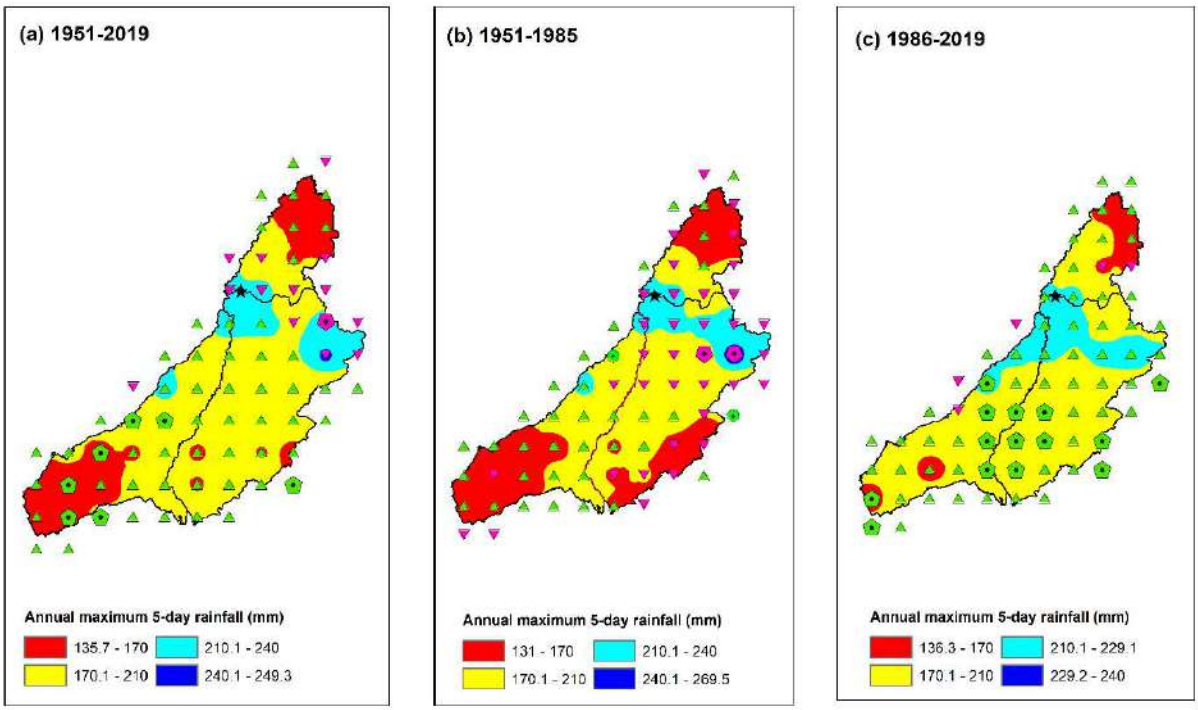

Figure 4.7 Spatial distribution of RX5day over Sabarmati River basin

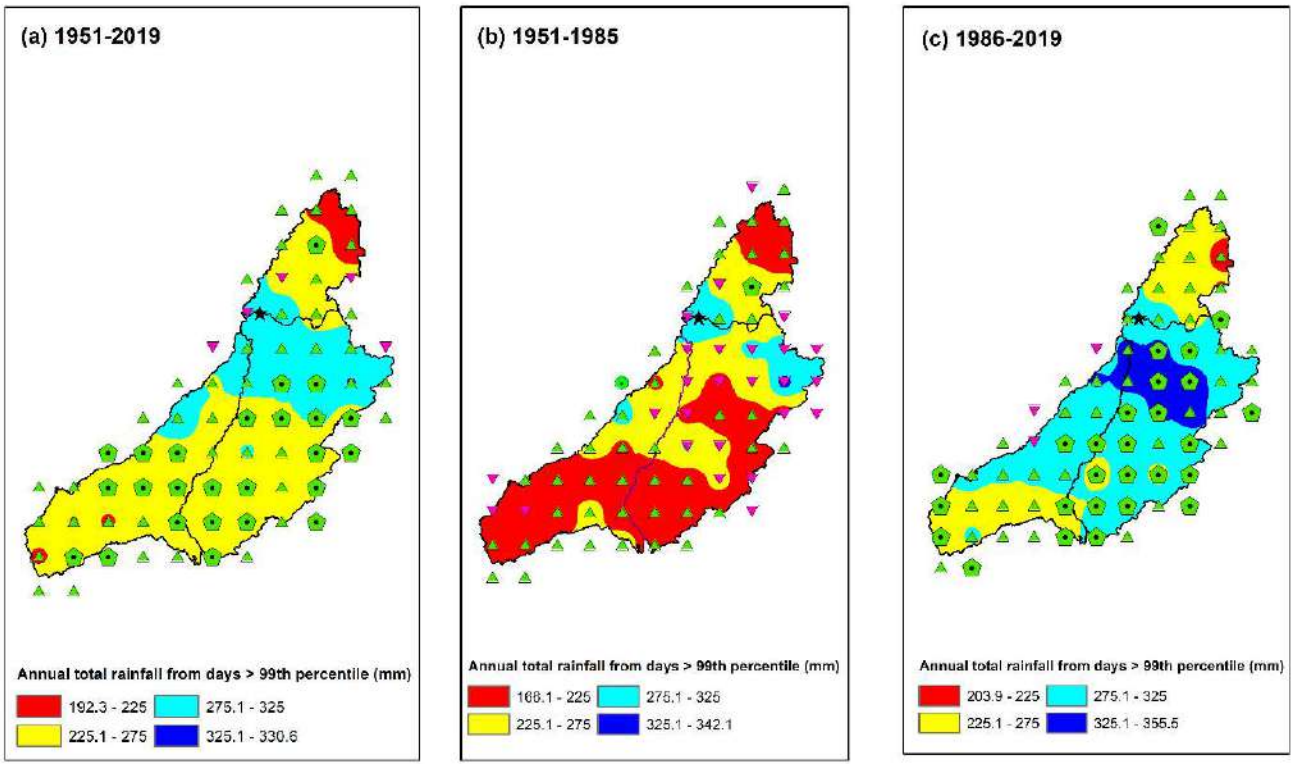

Figure 4.8 Spatial distribution of R99p over Sabarmati River basin

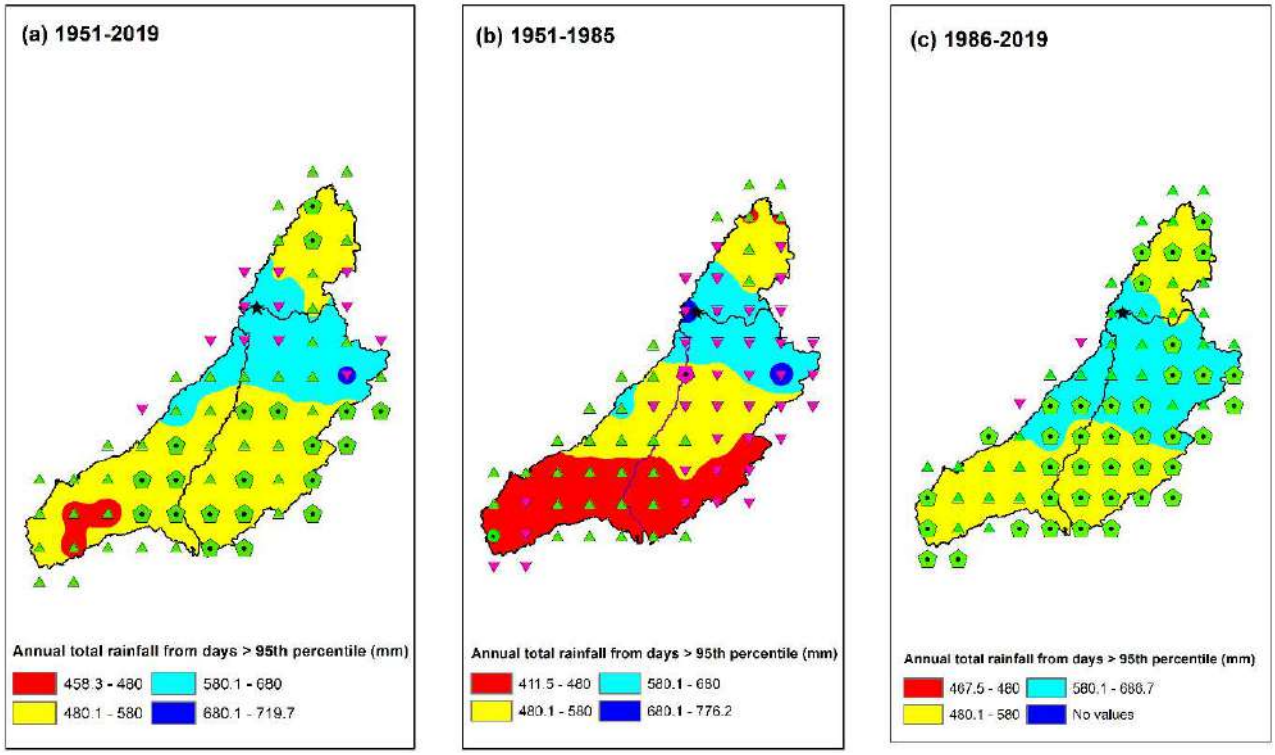

Figure 4.9 Spatial distribution of R95p over Sabarmati River basin

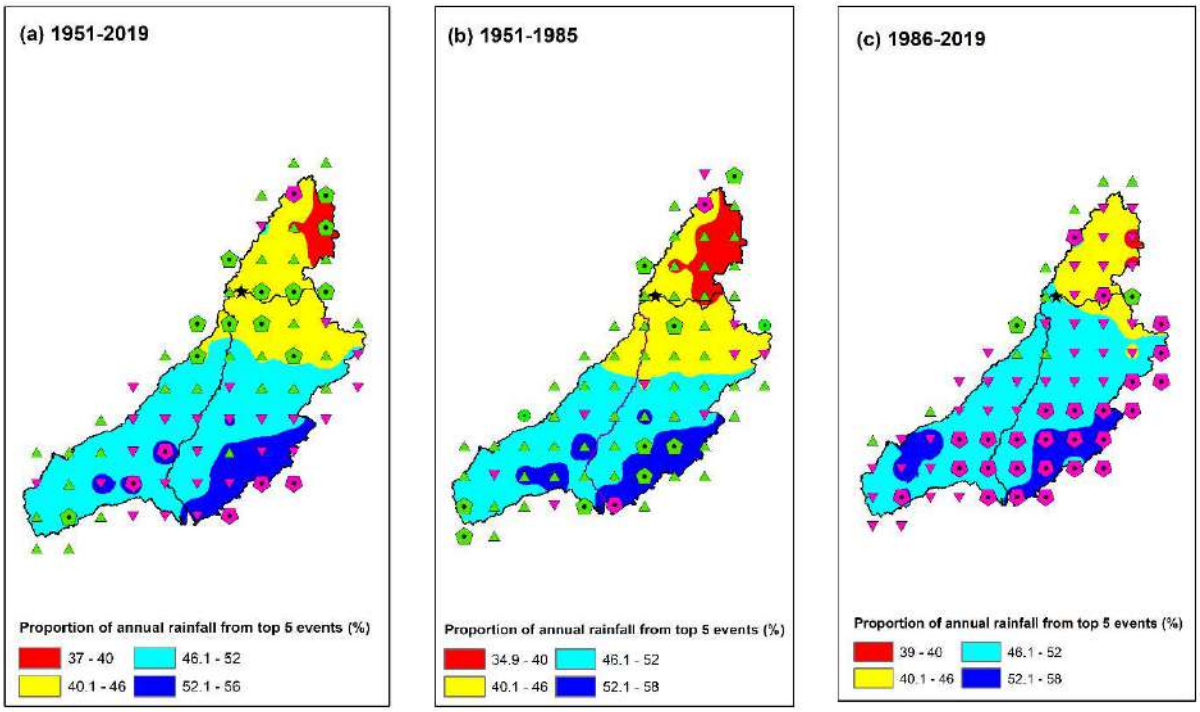

Figure 4.10 Spatial distribution of R5TOT over Sabarmati River basin

4.2.3 Duration-Based Indices

The duration or count-based indices used are light rainy days (LRF), moderate rainy days (MRF), heavy rainy days (HRF), consecutive dry days (CDD) and consecutive wet days (CWD). Three of the aforementioned indices, i.e., LRF, MRF and HRF are count and threshold-based indices respectively. In F1 period, LRF (MRF) (HRF) show significantly increasing trend only in 1% (0%) (0%) grid points (Figure 4.11 b, Figure 4.12 b and Figure 4.13 b) and S1 period reflects 26%, (30%) and (16%) grids (Figure 4.11 c, Figure 4.12 c and Figure 4.13 c) significantly increased, which shows the conversion of basin towards wetter zone. Consecutive dry days (CDD) and consecutive wet days (CWD) are duration-based indices which describes the drier and wetter conditions in a year. From Figure 4.14 and Figure 4.15 it is evident that dry spells have reduced and wet spells have increased for the S1 period, particularly in Upper Sabarmati basin. On other hand, in S1 period, the decreasing trend is observed for the CDD lower Sabarmati basin. As far as CWD is concerned for S1 period, invariably, the parameter shows increasing trend for the entire basin wherein significant increasing trend is observed in the lower Sabarmati basin.

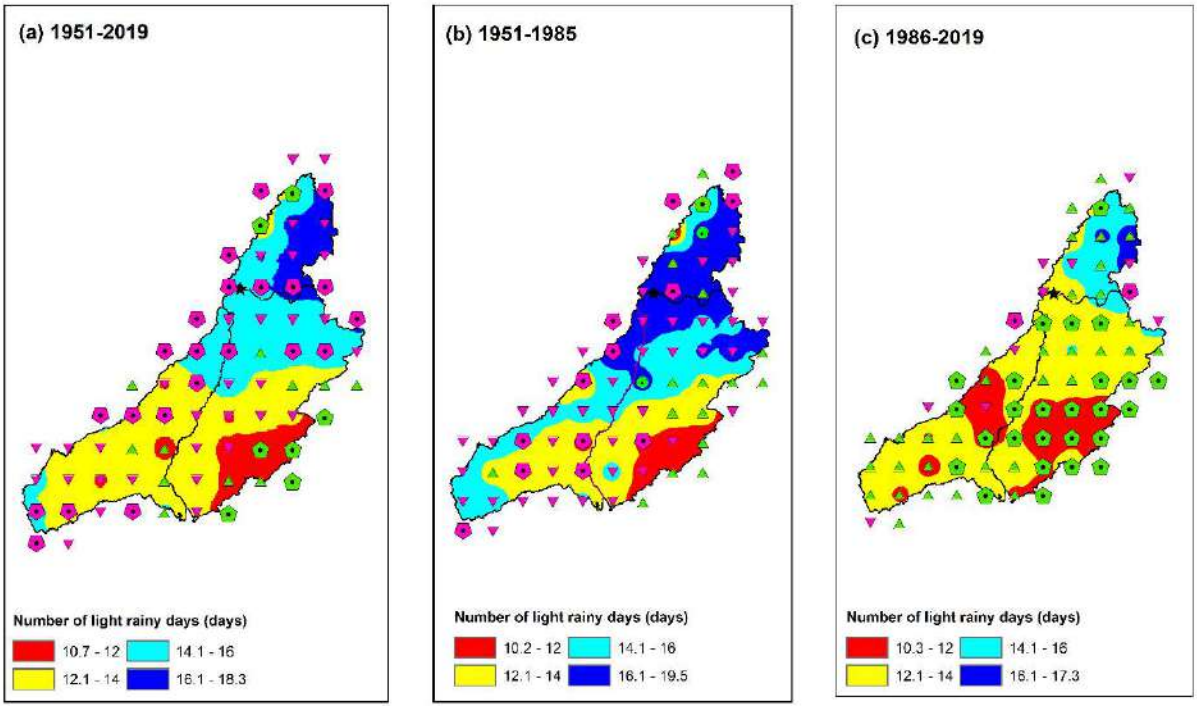

Figure 4.11 Spatial distribution of LRF over Sabarmati River basin

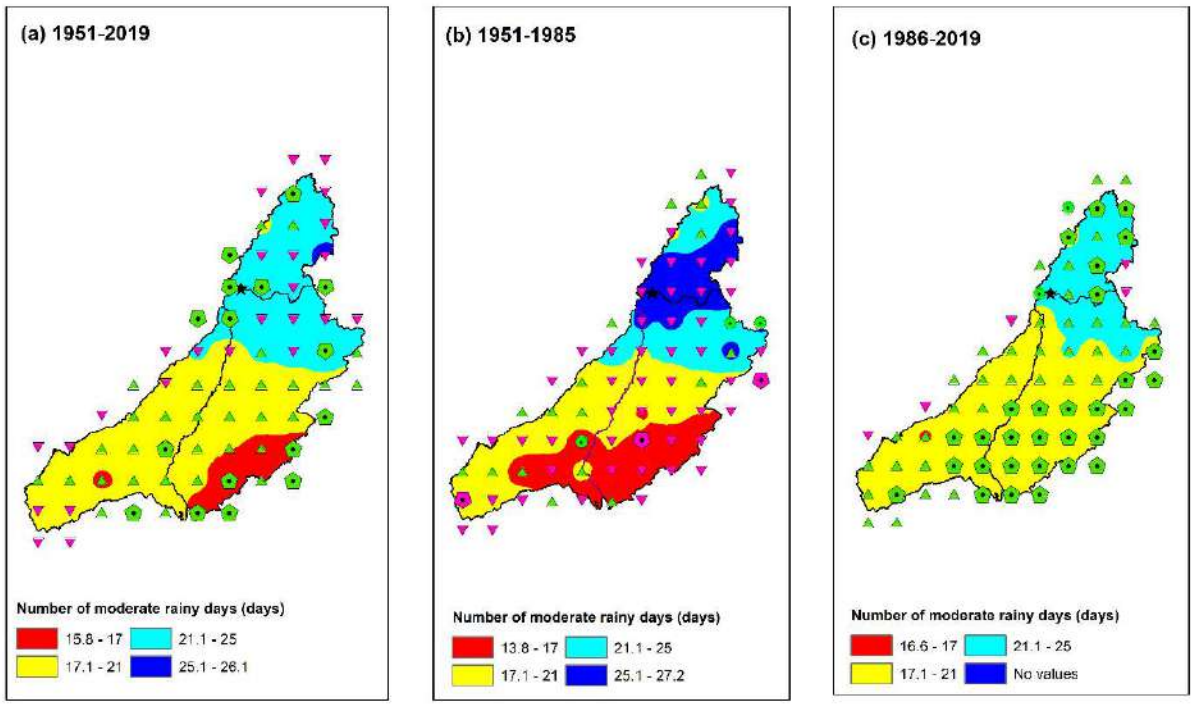

Figure 4.12 Spatial distribution of MRF over Sabarmati River basin

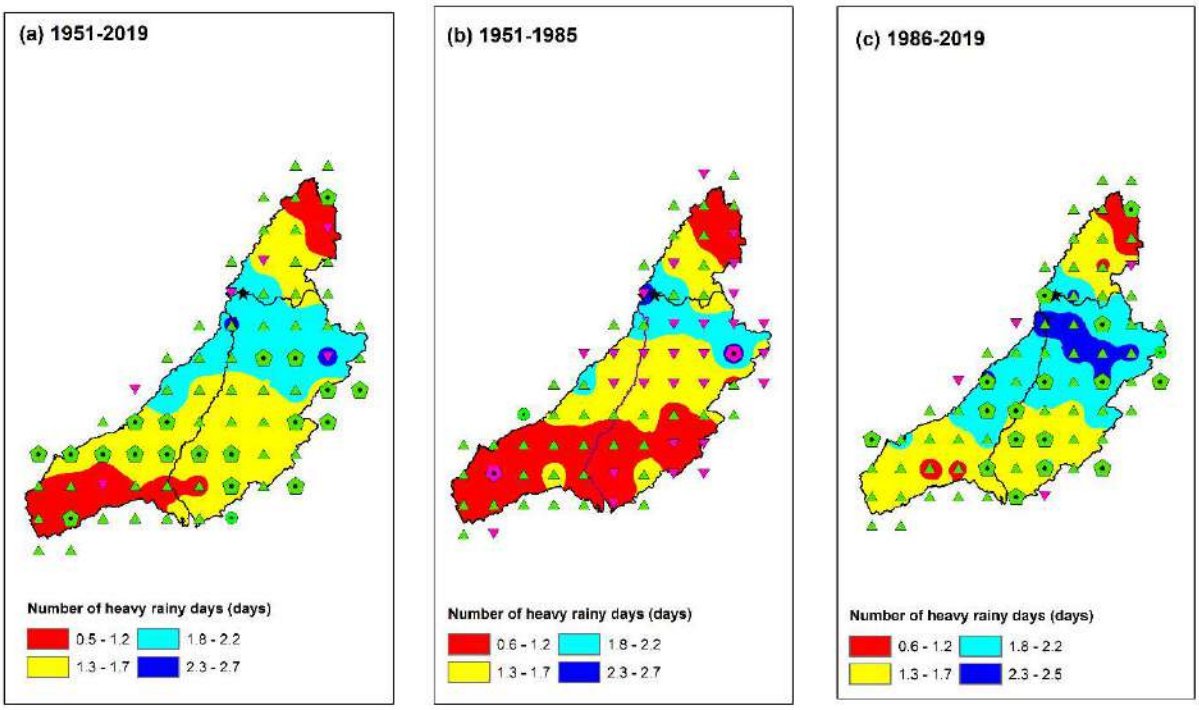

Figure 4.13 Spatial distribution of HRF over Sabarmati River basin

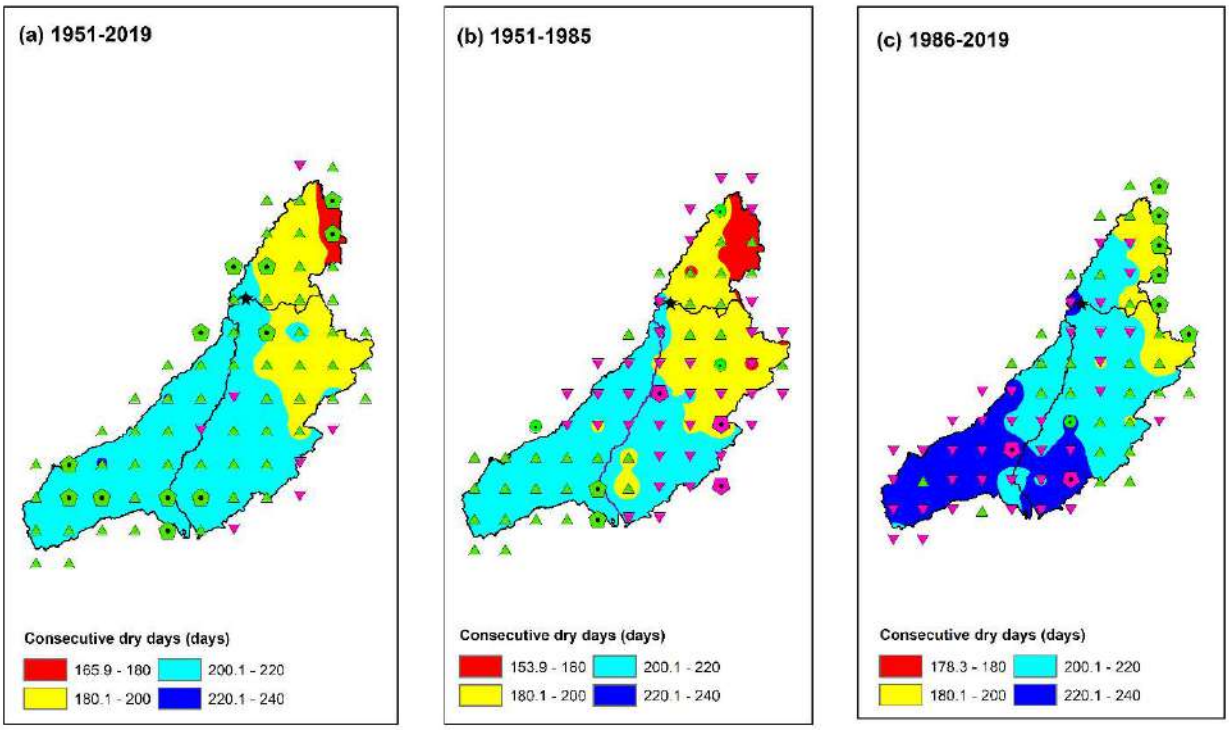

Figure 4.14 Spatial distribution of CDD over Sabarmati River basin

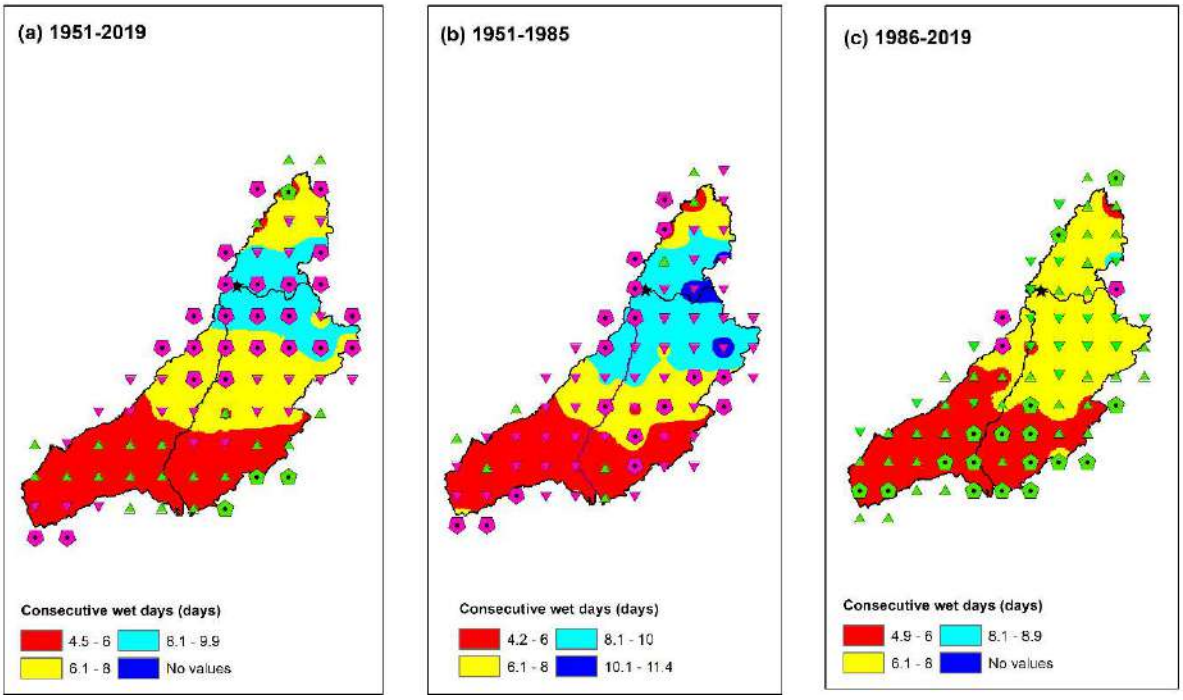

Figure 4.15 Spatial distribution of CWD over Sabarmati River basin

4.3 TREND ANALYSIS OF TEMPERATIURE USING EXTREME INDICES FOR HISTORIC PERIOD

The trends in extreme temperature indices, namely, maximum temperature (T_{max}), minimum temperature (T_{min}), average temperature (T_{av}), absolute indices--very hot days (T40D), very cold days T10D and diurnal temperature range (DTR), were analyzed. The spatial distribution of T_{max} and T_{av} indicates significantly increasing trend at all (100%) the grids during O1 period (Figure 4.16 and Figure 4.18 a). In F1, the T_{min} has been found to decrease with statistical significance at 30% grids (Figure 4.17 b). On the other hand, it has significantly increased at 100% grids of SRB in S1 period (Figure 4.17 c). The diurnal temperature (DTR), which is defined as the difference between daily maximum and minimum temperature on particular day. The DTR is an important meteorological indicator associated with urbanization and global climate change and reflects whether the weather was stable or not (Kalnay and Cai 2003). The DTR has been worked out from the daily data and the time series for the whole period was prepared. The spatial distribution of percentage change in trend in DTR for annual scales is shown in Figure 4.19. The DTR has been found to decrease in S1 period as nocturnal minimum temperatures have risen faster than day time maximum temperature in the context of global climate change (Vose et al., 2005; Li and Chen 2009; Easterling et al., 1997).

Table 4.2 Percentage grid contribution of historical rainfall trend for the period 1951-2019

Trend	Period	Significant Increasing Trend (% grid)	Significant Decreasing Trend (% grid)	Increasing Trend (% grid)	Decreasing Trend (% grid)	No Trend (% grid)
RD (days)	1951-2019	10	17	33	40	0
	1951-1985	0	4	14	79	3
	1986-2019	47	4	43	4	2
PRCPTOT (mm)	1951-2019	33	0	44	22	0
	1951-1985	0	6	35	57	2
	1986-2019	56	1	42	1	0
SDII (mm/day)	1951-2019	53	0	43	4	0
	1951-1985	21	0	40	39	0
	1986-2019	22	3	65	10	0
RX1day (mm)	1951-2019	15	0	71	13	1
	1951-1985	6	0	61	32	1
	1986-2019	22	1	69	6	1
Rx5day (mm)	1951-2019	10	1	71	18	0
	1951-1985	0	3	47	47	3
	1986-2019	19	0	74	7	0
R99p (mm)	1951-2019	19	0	74	7	0
	1951-1985	1	0	61	36	2
	1986-2019	38	0	58	4	0
R95p (mm)	1951-2019	28	0	56	17	0
	1951-1985	0	1	46	51	1
	1986-2019	54	0	43	3	0
R5TOT (%)	1951-2019	17	8	40	35	0
	1951-1985	13	3	69	13	2
	1986-2019	3	36	13	48	0
LRF (days)	1951-2019	10	31	15	44	0
	1951-1985	1	18	22	56	3
	1986-2019	36	3	47	14	0
MRF (days)	1951-2019	13	10	43	35	0
	1951-1985	0	4	24	68	4
	1986-2019	42	0	49	7	2
HRF (days)	1951-2019	26	0	64	8	2
	1951-1985	0	3	57	39	1
	1986-2019	22	0	71	6	1
CDD (days)	1951-2019	17	0	74	9	0
	1951-1985	3	4	40	49	4
	1986-2019	8	3	38	50	1
CWD (days)	1951-2019	6	33	29	32	0
	1951-1985	0	24	11	65	0
	1986-2019	24	4	46	26	0

The results of DTR concludes that SRB experiences a statistically decreasing (increasing) trend at 80% (0%) grids in S1 period (Figure 4.19 c), while in F1 30% (0%) grids indicate significant

increasing (decreasing) trend. DTR may have adverse effects on human health through its impacts on cardiovascular, nervous, and immunity system (Liang et al., 2008; Bull 1980;), thus resulting in the poor ability of accommodating to the wide variations in the temperature. A dominant increasing trend of hot days is indicated from the analysis of temperature indexes. Figure 4.20 depicts the significant increase (90% grids) in warming trend (T40d) across SRB for O1 period. The Lowest daytime temperature or cold days (T10D) shows significant decreasing trend across the SRB for O1 period (Figure 4.21 b).

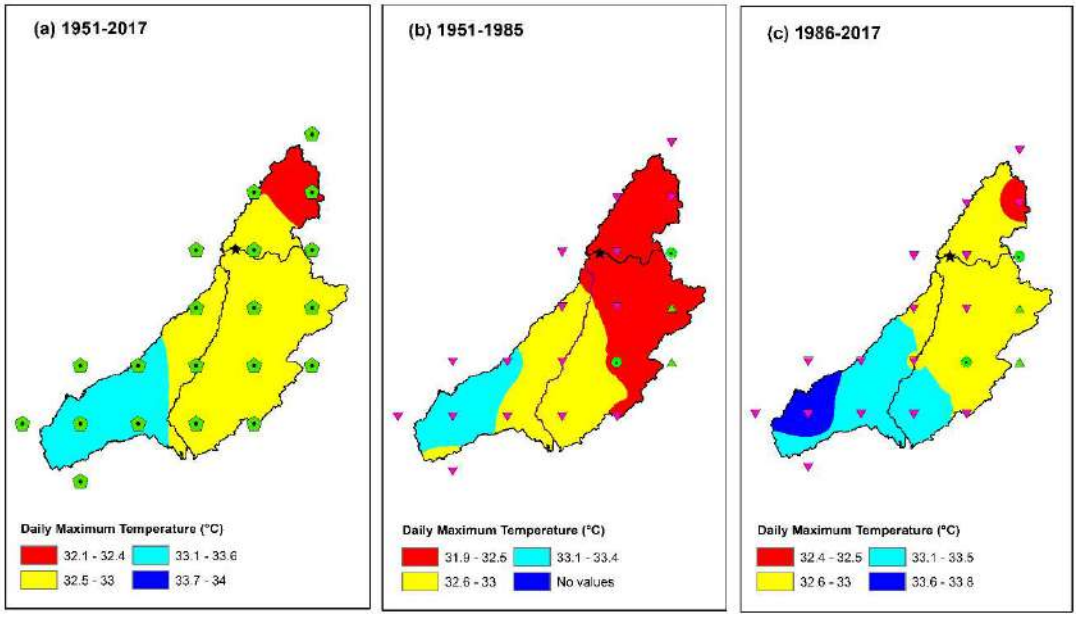

Figure 4.16 Distribution of T_{max} over Sabarmati River basin

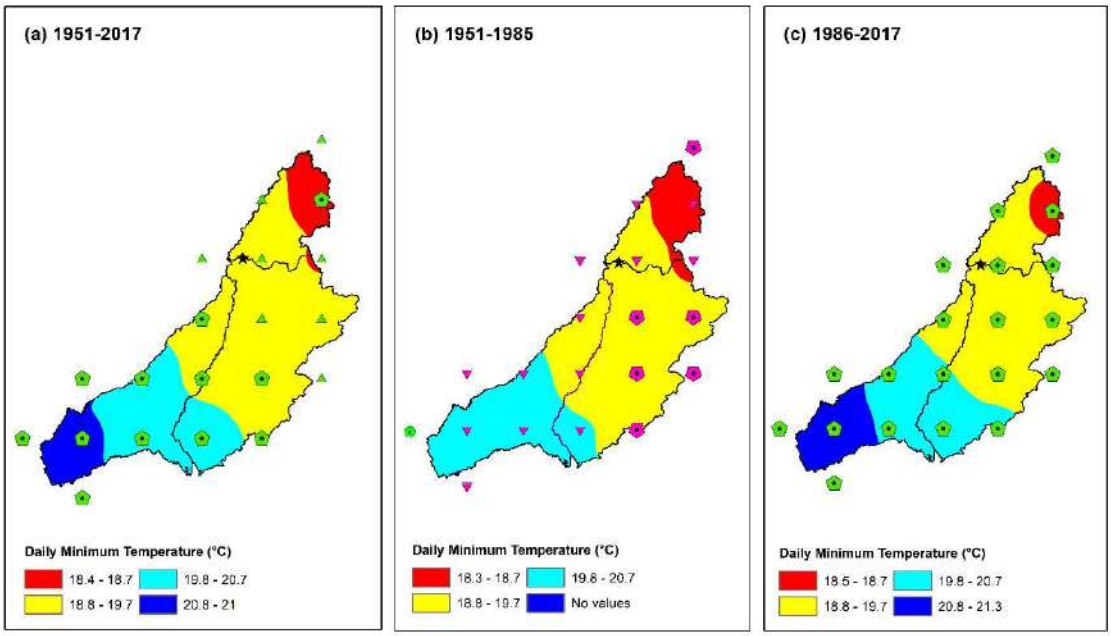

Figure 4.17 Distribution of T_{min} over Sabarmati River Basin

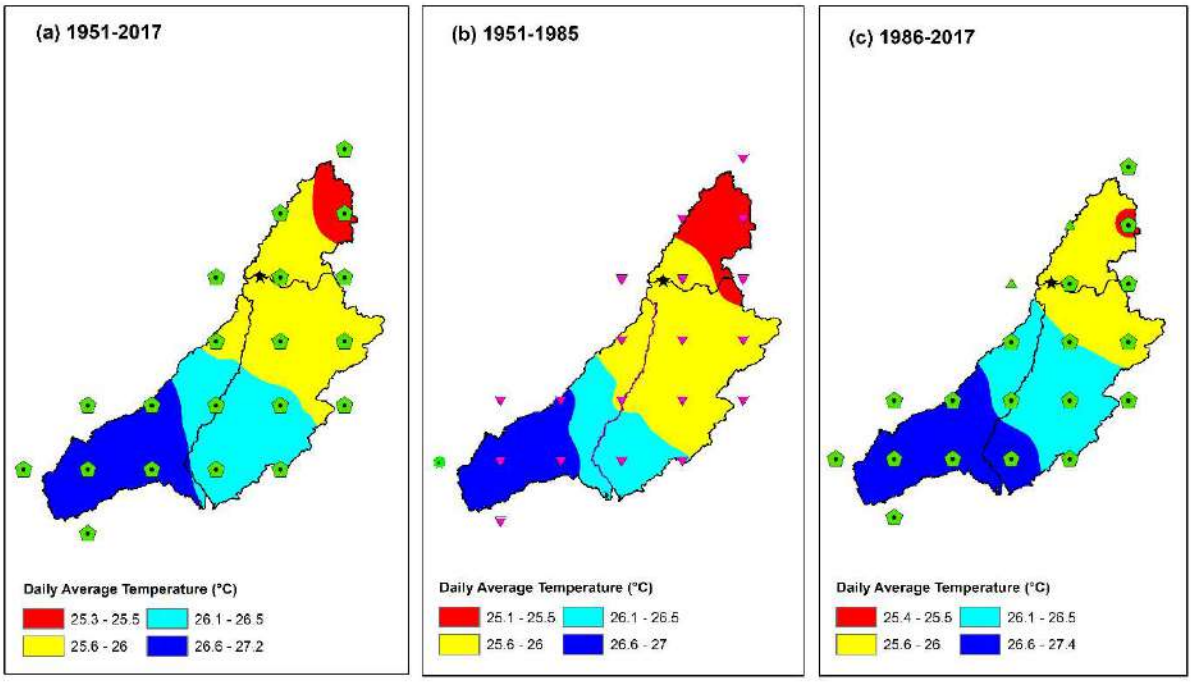

Figure 4.18 Distribution of T_{av} over Sabarmati River basin

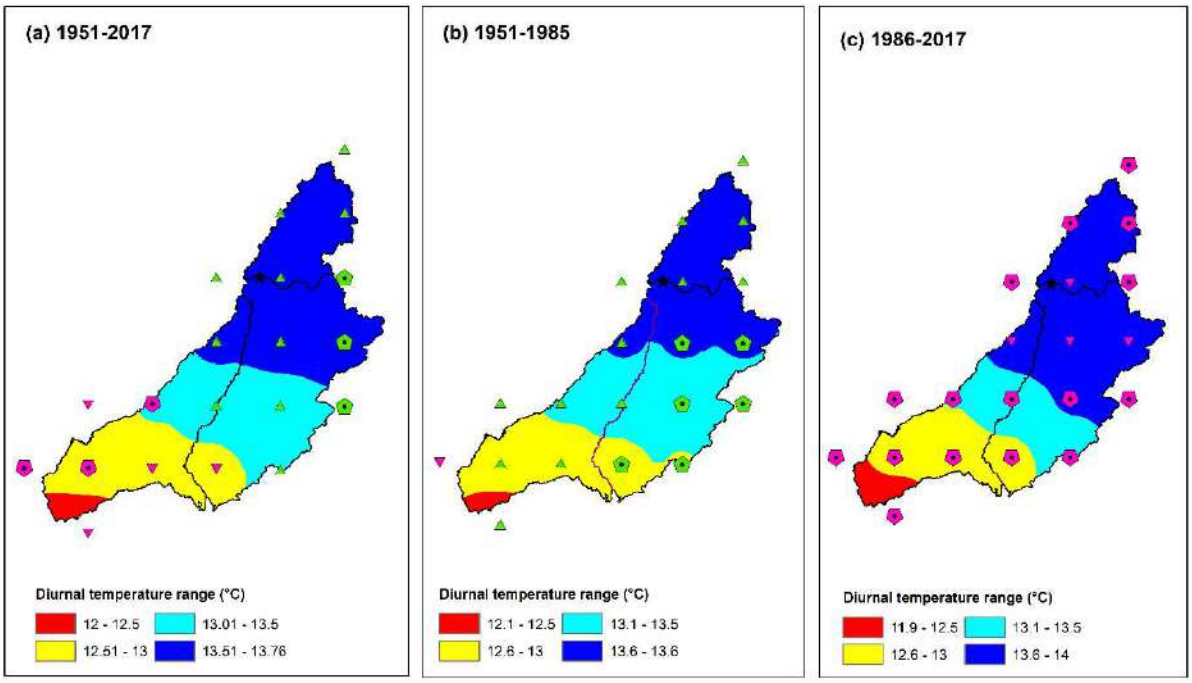

Figure 4.19 Distribution of DTR over Sabarmati River basin

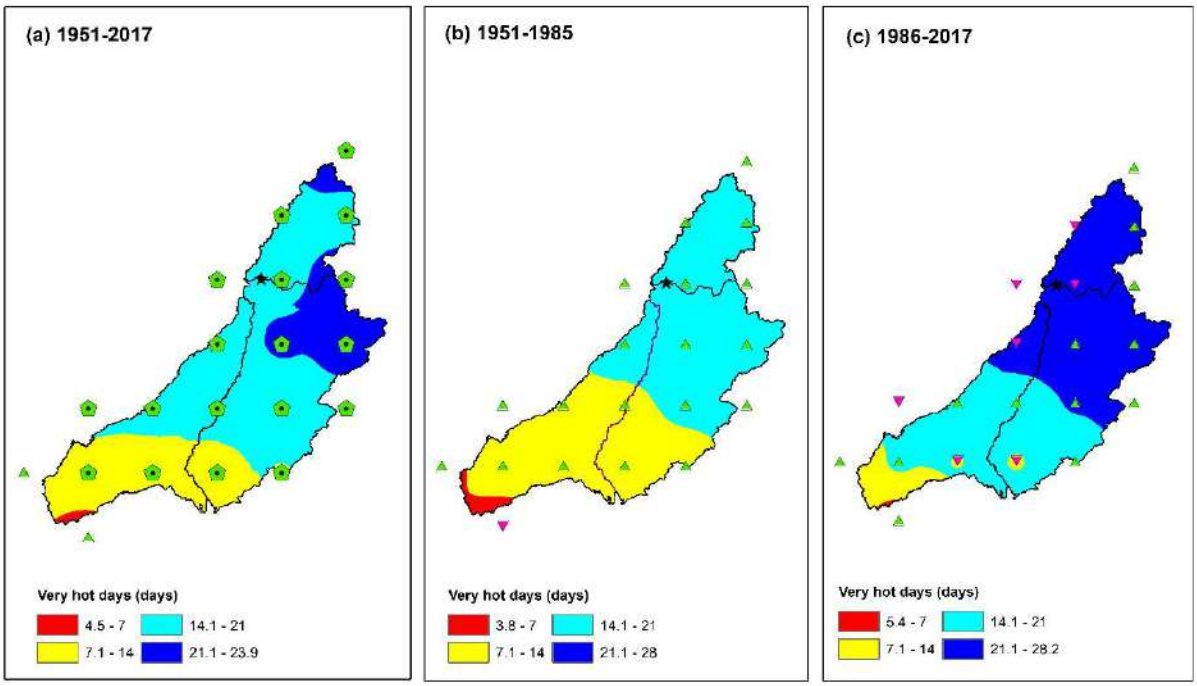

Figure 4.20 Distribution of T40D over Sabarmati River basin

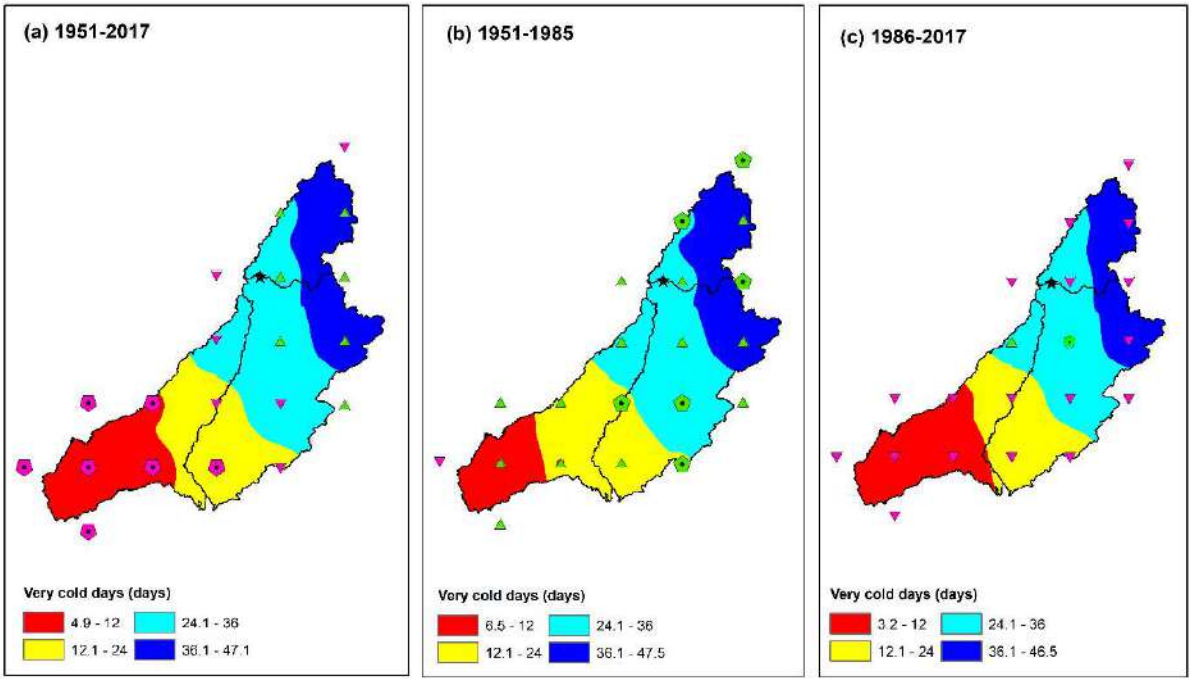

Figure 4.21 Distribution of T10D over Sabarmati River basin

Table 4.3 Percentage grid contribution of historical temperature trend for the period 1951-2017

Trend	Period	Significant Increasing Trend (% grid)	Significant Decreasing Trend (% grid)	Increasing Trend (% grid)	Decreasing Trend (% grid)	No Trend (% grid)
T_{max}	1951-2017	100	0	0	0	0
	1951-1985	0	0	10	80	10
	1986-2017	5	0	95	0	0
T_{min}	1951-2017	60	0	40	0	0
	1951-1985	0	30	0	65	5
	1986-2017	100	0	0	0	0
T_{av}	1951-2017	100	0	0	0	0
	1951-1985	0	0	0	95	5
	1986-2017	90	0	10	0	0
DTR	1951-2017	15	15	50	20	0
	1951-1985	30	0	65	5	0
	1986-2017	0	80	0	20	0
T40D	1951-2017	90	0	10	0	0
	1951-1985	0	0	95	5	0
	1986-2017	0	0	65	35	0
T10D	1951-2017	0	35	35	30	0
	1951-1985	30	0	65	5	0
	1986-2017	0	0	5	90	5

4.4 TREND ANALYSIS OF PRECIPITATION USING EXTREME INDICES FOR FUTURE PERIOD

The box and whisker plots present the values of extreme indices for projected precipitation of statistically downscaled Coupled Model Intercomparison Project (CMIP5) models (BNU ESM, CCCma-CanESM2, CNRM-CM5, MPIESM-LR, MPIESM-MR) under RCP4.5 and RCP8.5 for near (2020-2040), mid (2041-2070) and far (2071-2100) future. These plots graphically describe the statistical distribution in a way that is easy to understand for a wide range of users. The bottom and top horizontal lines in the boxes indicate the 25^{th} and 75^{th} percentiles, respectively. The location of the median line can suggest skewness in the distribution if it is noticeably shifted away from the center. The length of the interquartile range as shown by the box is a measure of the relative dispersion of the middle 50% of a dataset, just as the length of each whisker is a measure of the relative dispersion of outer range of data sets (Banacos, 2011). The PRCPTOT and RD projections of the GCM models, invariably, reflect increasing trend over SRB (Figure 4.22 a-b) and SDII projections indicate reduction for the RCP4.5 and RCP8.5 for near, mid and far future (Figure 4.22 c), when compared with the historical trend of the period 1951-2019. The rainfall extremes (SDII, RX1day, RX5day, R99p, R95p), show decreasing trends over the SRB for near, MID and far future. (Figure 4.22 d-f). Figure 4.23 (h) and Figure 4.24 (i) indicate that the LRF and MRF will increase in future (near, mid and fat future) with reference to base line period. On other hand, HRF would decrease with reference to the base line period (Figure 4.24 j). Thus, The LRF and MRF (HRF) projections indicate increase (reduction) in the present investigation in all the GCM models under RCP4.5 and RCP8.5 (Figure 4.23 h and Figure 4.24 i-j). The CDD (CWD) projections indicate reduction (increase) in the present investigation for all the GCM models under RCP4.5 and RCP8.5 (Figure 4.24 k-l). Thus, analysed results indicate that, in future, the SRB is becoming wetter while there would be reduction of extremes events. Table 4.4 shows the trend results of climate indices for historical and future period (ensemble of all GCMs). The future projections of all the GCM models show an increase in PRCPTOT, RD and CWD and reduction in CDD. This is an indication toward a wetter future climate in the study area.

Table 4.4 Projected changes in extreme indices for historical and future period (ensemble of all GCMs) under RCP4.5 and RCP8.5

Index	Historical (1951-2019)	RCP4.5 Near Future (2020-2040)	RCP4.5 Mid Future (2041-2070)	RCP4.5 Far Future (1971-2100)	RCP8.5 Near Future (2020-2040)	RCP8.5 Mid Future (2041-2070)	RCP8.5 Far Future (1971-2100)
RD (days)	34.2	58.1	57.7	59.7	60.6	61.3	68.6
PRCP (mm)	640.8	690.8	669.4	697.0	720.8	744.6	840.5
SDII (mm/day)	18.2	11.8	11.6	11.7	11.9	12.1	12.0
Rx1day (mm)	94.0	61.9	57.4	56.1	61.5	54.1	44.7
Rx5day (mm)	184.3	136.2	130.5	130.7	138.7	136.6	133.8
R99p (mm)	258.9	187.5	167.5	171.7	183.6	166.8	167.7
R95p (mm)	548.7	461.5	433.8	453.2	454.6	466.8	514.1
R5TOT (%)	47.8	31.8	30.7	29.2	30.4	28.2	23.5
LRF (days)	13.8	30.1	29.9	30.5	30.9	30.7	33.8
MRF (days)	19.9	27.5	27.3	28.7	29.0	30.1	34.2
HRF (days)	1.5	0.6	0.5	0.5	0.6	0.6	0.6
CDD (days)	204.7	152.8	153.1	151.5	151.5	150.2	147.3
CWD (days)	6.7	13.1	14.4	14.6	13.7	14.5	16.8

4.5 CONCLUDING REMARKS

The key findings of trend analyses on climatic variables, presented in the preceding section is appended in the following paragraph:

1. The extreme rainfall indices, on annual scale for S1 period, revealed an overall increasing trend in PRCPTOT, RD, RX1day, RX5day, R99p, R95p, LRF, MRF and CWD. On the other hand, the SDII and CDD has shown significant reduction in this period due to increase in number of rainy days. This is an indication that the Sabarmati River (SRB) basin is shifting towards the wet regime post 1985.
2. The T_{max} has shown significantly increasing trend in 100% (5%) grids across SRB in O1 (S1) period while T_{min} has shown increasing trend in 60% (100%) grids with statistical significance for period O1 (S1). It is also noticed that 100% (90%) grids have contributed significant increasing trend of T_{av} for O1 (S1) period at annual scale, which may be a matter of concern to the agriculture sector as it may have adverse impact on the yield of some of the crops in the SRB.

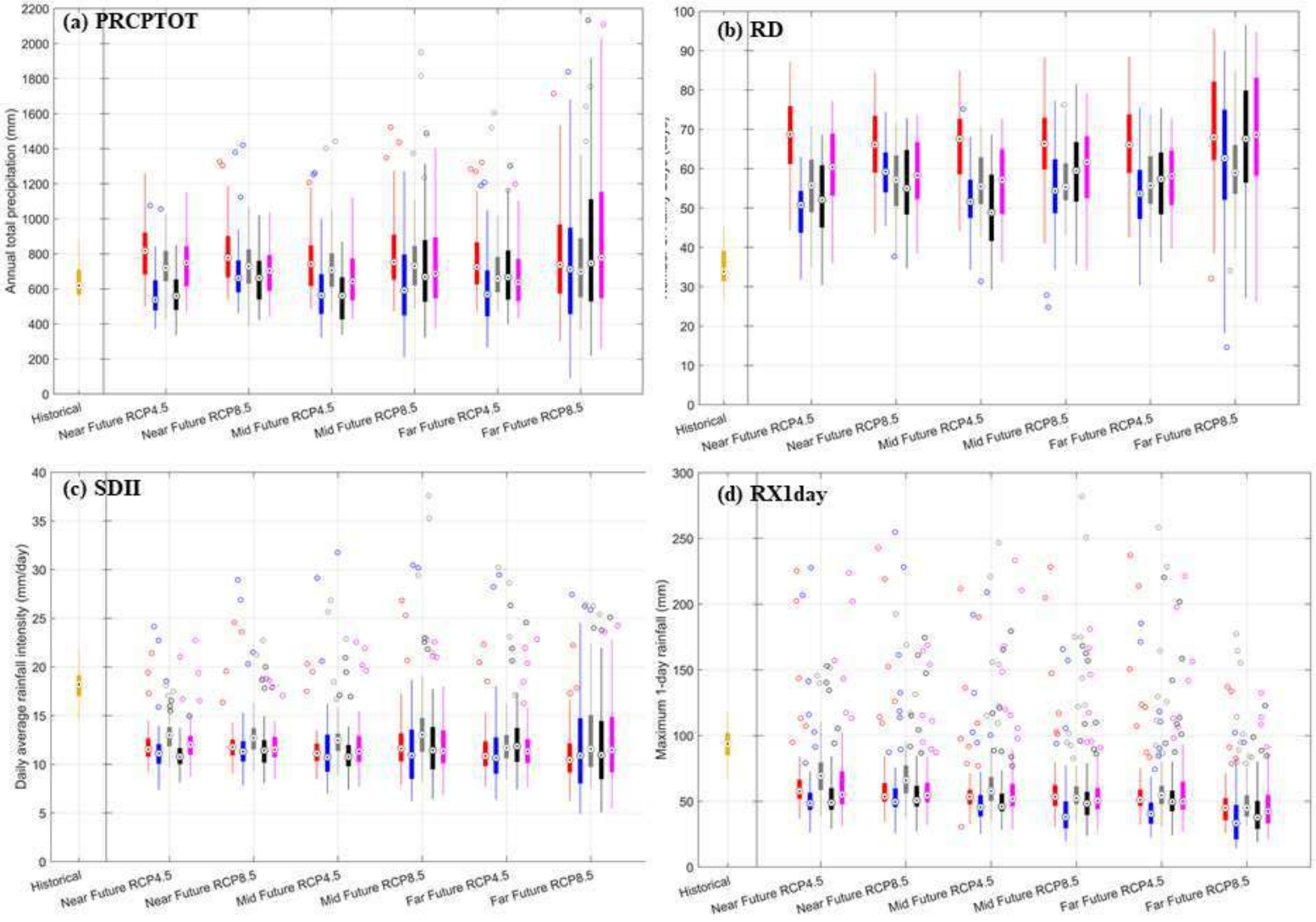

Figure 4.22 Projected trend investigation of CMIP5 climate models under RCP4.5 and 8.5

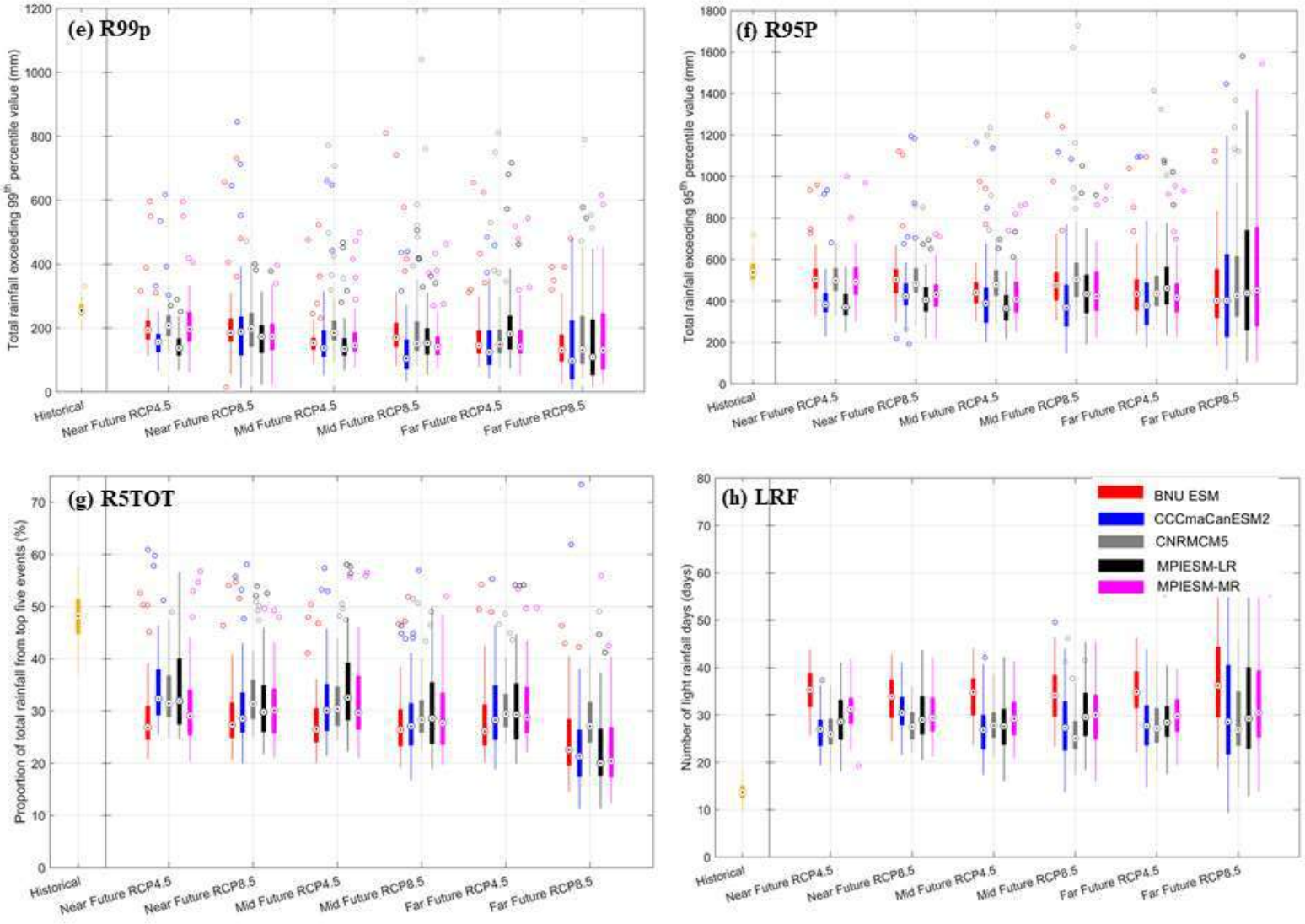

Figure 4.23 Projected trend investigation of CMIP5 climate models under RCP4.5 and RCP8.5

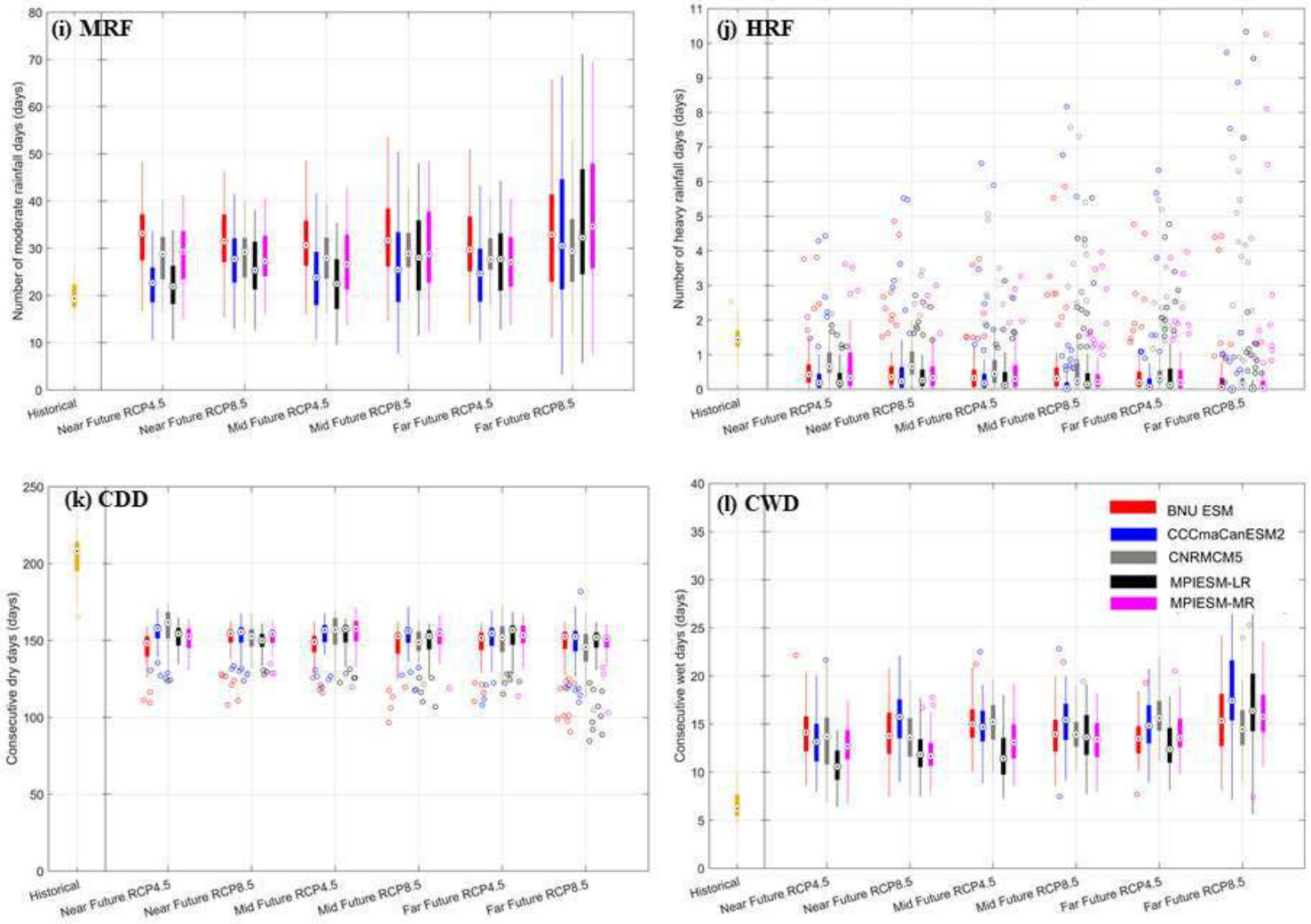

Figure 4.24 Projected trend investigation of CMIP5 climate models under RCP4.5 and RCP8.5

3. Due to increase in T_{min} and decrease in T_{max}, it is observed that 80% grids have indicated significantly decreasing trend of DTR in S1 period, i.e., post 1984. The change of DTR may have adverse effects on human health, i.e., through its impacts on cardiovascular, nervous, and immunity system (Liang et al., 2008; Bull 1980).

   The Heat stresses, during periods of high temperatures, may also exacerbate health problems, such as sunstrokes, muscle cramps and heat exhaustion, and may affect the work performance of the people in the basin.
4. The ensembled climatic parameters like RD, PRCPTOT, LRF, MRF and CWD, statistically downloaded from Five GCMs. are likely to increase in future (near, Mid and far future) for RCP 4.5 and RCP 8.5 scenarios. On the other hand, the climatic parameters like CDD, SDII and HRF are likely decrease in near, Mid and Far future. This trend indicates that the Sabarmati River Basin (SRB) is likely to become wetter in future. However, the extremes like flood and disasters may not likely to aggravate in future.
5. The Wetting conditions in future may reduce the drought events which may be favourable conditions for infilling the reservoir. The more available water in the reservoir can cover more command area for agriculture in future.

4.6 FUTURE SCOPE

Based on foregoing, following may form the future scope of work:

With reference to the analyses

1. Change in climate will affect the soil moisture, groundwater recharge, and frequency of flood or drought, and finally groundwater level in different areas (Huntington 2003; Eckhardt 2003; Alen et al., 2004). The present study can be related to understand the impact of climate change on soil moisture, and groundwater recharge.
2. Establish the linkages between changes in extreme climatic indices with anthropogenic influences such as changes in land use-land cover and human population and their associated effects in SRB.

5 METHODOLOGY AND ANALYSIS OF DATA: HYDROLOGIC MODELLING

5.1 GENERAL

This section includes results and analysis of hydrologic modelling to predict the inflow in Dharoi reservoir using HEC-HMS and SWAT models for event and continuous basis respectively. The SWAT model is calibrated from historically observed data for period 1995-2014 and validated for the period 2015-2019. The calibrated and validated model for prediction of inflows into the Dharoi reservoir has been used for predicting the possible response of the basin for inflows into the Dharoi reservoir.

5.2 EVENT BASED HYDROLOGIC MODEL USING HEC-.HMS

5.2.1 General

HEC-HMS 4.2.1, a semi-distributed hydrologic model has been used to predict the inflow in Dharoi reservoir. The HEC-Geo HMS interface, an extension in Arc-GIS, is used for watershed delineation and generating the inputs to perform hydrologic modelling. To compute runoff volume, peak runoff rate and flow routing, SCS CN method, SCS unit hydrograph method and Muskingum routing methods are chosen, respectively. The model was calibrated and validated for event based hydrologic modelling.

5.2.2 Data analysis

The high spatial resolution (0.25°× 0.25°) daily gridded rainfall data from IMD were procured for the period 2000-2013 of Dharoi catchment for present study. After downloading the DEM of the study area, relevant tiles were merged/mosaiced in single tile of DEM, which is further used for the delineation of watershed. The DEM is pre-processed in HEC-Geo HMS for the delineation of watershed in which “adjoint catchment processing” was the last step (Figure 5.2). The Landsat image of year 2008 has been utilized, which was downloaded from the USGS website, and supervised classification was carried out in ERDAS IMAGINE 2014. The most prominent land use in the catchment is forest (43%), followed by agricultural land (22%), built-up (1.3%) water bodies (1.03%), and barren land (32.67%). Soil map is obtained by Food and Agriculture Organization (FAO) world soil map in ARC-GIS 10.2. In present study, lag time and time of concentration of the sub basin is calculated using Kirpich equation. The calculation of lag time is presented Table 5.1. Wet, dry, and normal years are categorized as suggested by Yoo (2006) and analysed results of the time series between 1901-2013 are shown in Appendix

-V. If annual basin rainfall is more than P_{mean}+ 0.75*Standard deviation (SD), it can be classified as wet year, if it is less than P_{mean}- 0.75*SD, it can be classified as dry year and the one which lies in between (P_{mean}+ 0.75*SD) and (P_{mean}- 0.75*SD) can be considered as normal year. (Yoo, 2006).

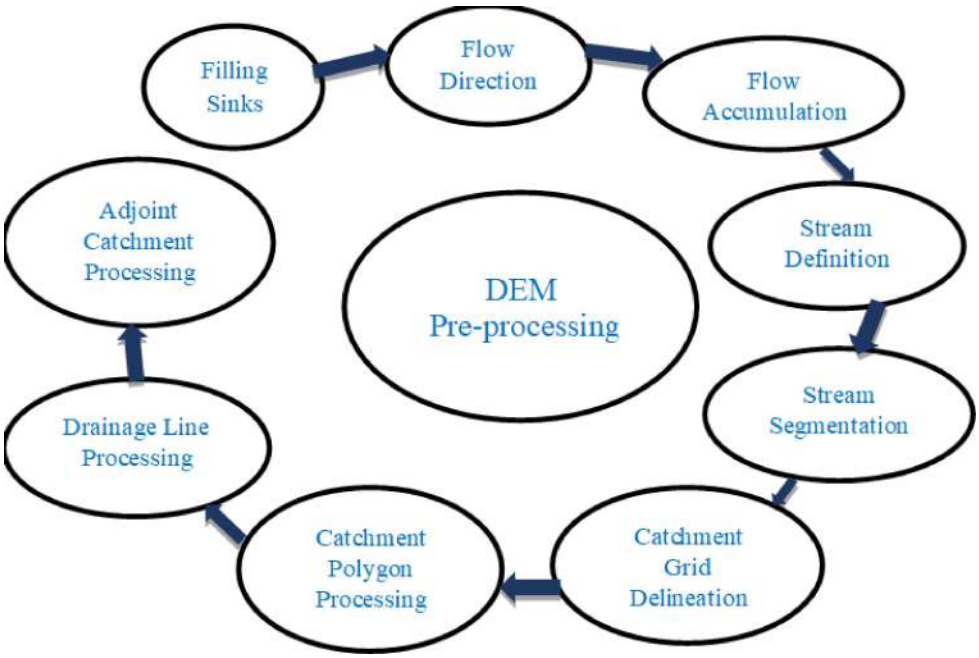

Figure 5.1 Pre-processing in HEC-Geo HMS

Table 5.1 Lag time calculation

S N	Station	Time of Concentration (min)	Lag time (min)
1	Jotasan	315.7	189.4
2	Kheroj	302.2	181.3
3	Dharoi	213.1	127.8

5.2.3 Calibration of event-based hydrologic model

The calibration of HEC-HMS model is performed using gridded rainfall data for prediction of inflows into Dharoi reservoir for the period 2000-2013. Initial values of the model parameters are based on land use land cover, soil type, digital elevation model and channel characteristic within the basin. Accordingly, the sets of parameters obtained during the calibration period are used for validation. In the present study, peak weighted root mean square error objective function was used. For minimizing the objective function, univariate search algorithm was used. Manual calibration was used to obtain the optimized parameters in the study.

The values of optimized parameters obtained after calibration using SCS CN loss method for event based hydrologic modelling are given in Table 5.2Figure 5.2. It is observed that curve number is higher and Muskingum "k" is lower for wet year as compared to normal and dry years for event-based hydrologic model. During wet years, the antecedent soil moisture is higher, which increases the runoff potential, thereby, leading to higher values of curve number during such years. On other hand, the higher streamflow discharge in the channel results into increase in velocity, which has led to lower Muskingum "k" value vis-à-vis normal and dry years.

Table 5.2 Optimized Parameters of Dharoi catchment using SCS CN method

Year	Average curve number	Initial abstraction (mm)	Storage time constant, k (hr)	Lag time (min)	Weighing factor, x
Dry year	45	58	4.2	166.1	0.2
Normal year	57.3	35	4	166.1	0.2
Wet year	70	10	3	166.1	0.2

5.2.4 Validation and performance of event based hydrologic model

The calibrated model was validated and the results are given in **Error! Reference source not found.**. The evaluation criteria (NSE > 0.5), given by Moriasi et al. (2007), suggests that model performs reasonably well when NSE is greater than 0.5. The results indicated that NSE values for Dharoi is in the satisfactory range of 0.58-0.72 and 0.65-0.74 during calibration and validation periods respectively. The coefficient of determination (R^2) and percent error in volume (PEV) of the predicted model is found to be good. It has also been observed that the observed peak discharge was found greater than the simulated peak which may occur as baseflow was neglected during model development.

5.2.5 Concluding remarks for event based hydrological modelling

- The most prominent land use in the catchment is forest (43%), followed by agricultural land (22%). According to FAO soil, 80 % most part of the basin is covered by hydrologic soil group "C", i.e., sandy loam soil which possesses moderate high runoff potential.
- From the event based hydrologic modelling using SCS-CN method, the curve number, initial abstraction and Muskingum "k" were found to be the most sensitive parameters.

- Further, it is also observed that curve number is higher and Muskingum “k” is lower for wet year as compared to normal and dry years for event-based hydrologic model. During wet years, the antecedent soil moisture is higher, which increases the runoff potential, thereby, leading to higher values of curve number during such years. On other hand, the higher streamflow discharge in the channel results into increase in velocity, which has led to lower Muskingum “k” value vis-à-vis normal and dry years.
- The evaluation criteria (NSE > 0.5), given by Moriasi et al., (2007), fitted in results obtained in event based and continuous model.

Table 5.3 Performance indicators of Dharoi catchment for event based modelling

Classification	Event	Cumulative rainfall before the event (mm)	Cumulative rainfall during the event (mm)	Observed peak discharge (m^3/sec)	Computed peak discharge (m^3/sec)	Performance indices		
						R^2	NSE	PEV (%)
Dry year	July 10 to Jul 23 2000 (Calibration)	95.2	193.4	112.1	70.5	0.69	0.67	-5.5
	Aug 01 to Aug 16 2002 (Calibration)	125.6	102	37.1	38.2	0.74	0.72	20.1
	July 30 to Aug 18 2004 (Calibration)	122.9	288.1	94.6	112.9	0.62	0.61	16.1
	Aug 10 to Aug 16 2008 (Validation)	240.7	77.6	15.4	11.1	0.64	0.65	14.2
Normal year	July 05 to July 18 2001 (Calibration)	191.6	192.4	612.3	627.5	0.66	0.64	22
	Aug 21 to Sep 05 2003 (Calibration)	480.3	133.7	237.6	237.4	0.68	0.68	4
	July 25 to Aug 11 2005 (Calibration)	101.2	380.7	1737.6	1841.4	0.62	0.60	21
	Aug 29 to Sep 18 2012 (Validation)	487.1	296.2	1237.7	1032.8	0.74	0.74	16
Wet year	Aug 11 to Sep 06 2006 (Calibration)	617.4	536.9	4384.1	3943.7	0.73	0.72	4.1
	Sep 06 to Sep 20 2011 (Validation)	677.2	150.1	1815.1	1031.8	0.71	0.70	-35.1

5.3 CONTINUOUS HYDROLOGIC MODEL USING SWAT

5.3.1 SWAT model development

In present study, Arc-GIS extension of Soil and Water Assessment tool (SWAT), ARC-SWAT 2012 interfaced with Arc-GIS 10.5 has been used to develop the model. The methodology for continuous hydrologic modelling is presented in Figure 5.2. The inputs required for the development of SWAT model are spatially distributed topographic, climatic, land-use and soil data of the basin. The topographic data was in the form of digital elevation model (DEM), land-use map was taken from the classified from satellite imagery, and soil map was extracted National Bureau of Soil Survey and Land Use Planning (NBSS & LUP), Nagpur, India. All layers of these inputs were overlayed in ARC-SWAT to create the Hydrologic Response Unit (HRU). Brief description of the aforesaid data sets are included in the following paragraphs:

5.3.1.1 Digital elevation model (DEM)

In present study, Shuttle Radar Topographic Mission DEM (SRTM DEM) with 1arc second (~ 30 m) horizontal resolution and ±16 m vertical resolution was used which was downloaded from the United States Geological Survey (https://earthexplorer.usgs.gov/) (Figure 5.4 (b)). SWAT uses DEM for the delineation of stream network and watershed boundary and, then computes slope of the catchment.

5.3.1.2 Land use land cover map

Land-use/land-cover imagery of years 1999, 2004, 2009 and 2014 obtained from NRSC, Hyderabad, and reclassified into six classes which are forest, water bodies, agricultural land, built-up area, fallow land and scrub land are shown in Figure 5.3. The most dominant land class is forest, followed by agricultural land, fallow land, scrub land, water bodies and built-up area.

5.3.1.3 Soil map

The soil map of the study area was procured from the National Bureau of Soil Survey and Land Use Planning (NBSS & LUP), Nagpur, India. The existing soil properties for different soil are categorized according to Challa et al. (1999). About 68% of the soil in the Dharoi catchment consists of soil hydrologic group B (sandy loam) followed by soil hydrologic group D (clay - 19%) and C (clay loam - 13%) (Figure 5.4 (c)).

5.3.1.4 Climate zone

As per the Köppen-Geiger climate classification, the Dharoi catchment includes hot semi-arid, (BSh) and monsoon influenced humid subtropical, (Cwa) climate zones (Rubel and Kottek, 2010).

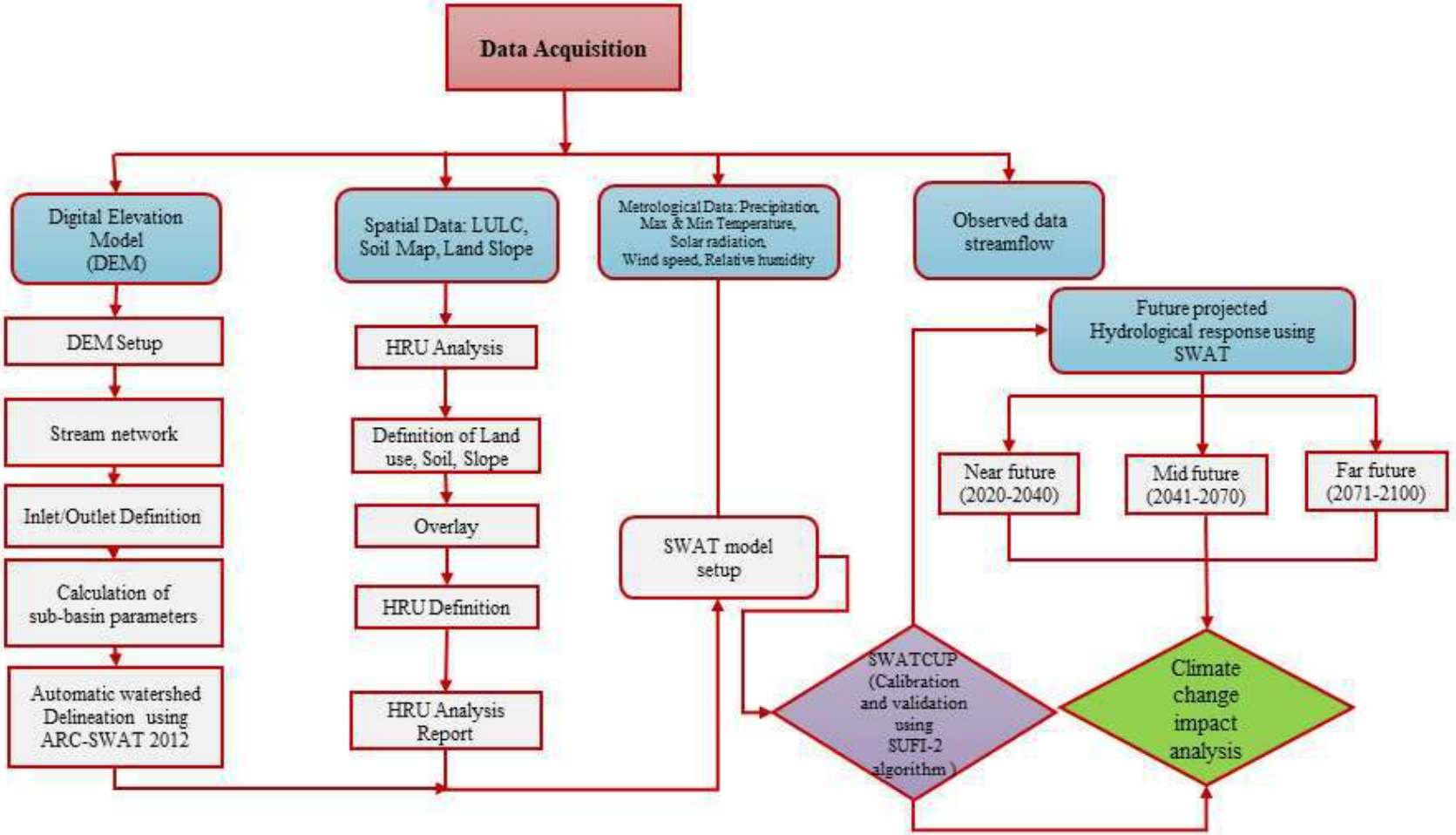

Figure 5.2 Methodology for continuous hydrologic modelling

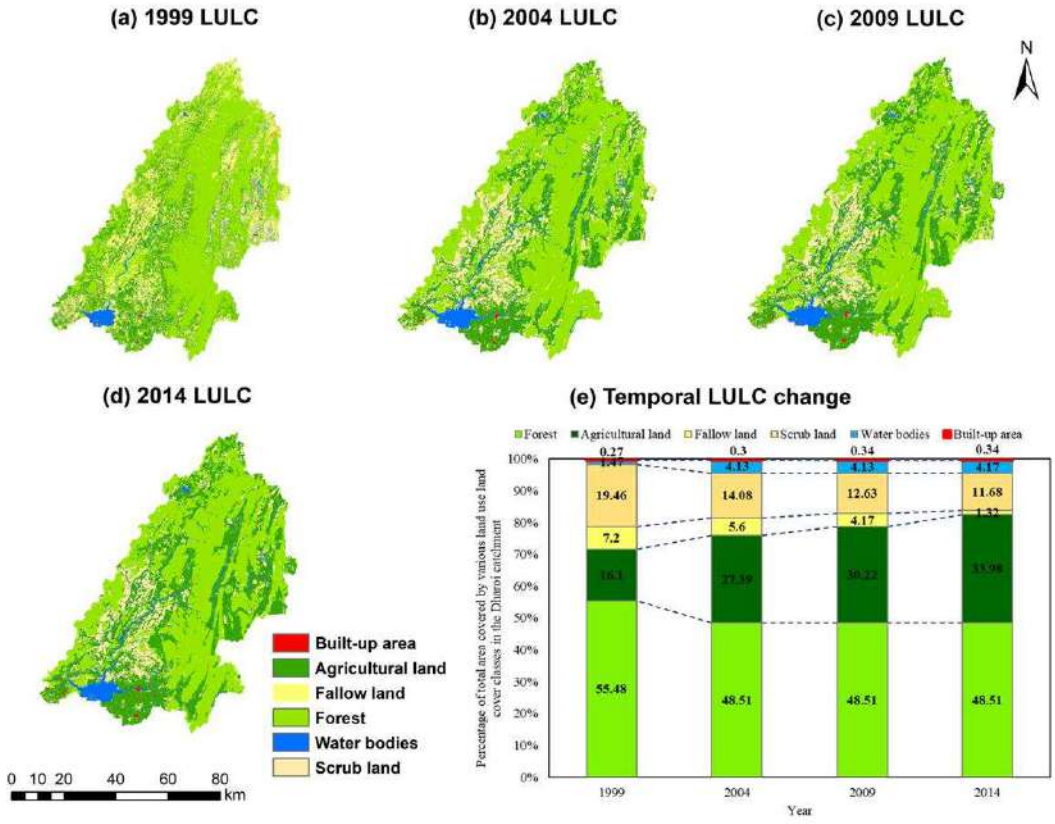

Figure 5.3 Land use land cover map of the Dharoi catchment for the year (a) 1999, (b) 2004, (c) 2009, and (d) 2014

5.3.1.5 Rainfall and temperature data

The Rainfall data as input for SWAT model requires two tables, i.e., "precipitation gauge location table" to specify the location of the rain gauge stations in Universal Transverse Mercator (UTM) projected coordinate system and "precipitation data table" containing daily rainfall data in the format given in the SWAT-2012 user guide. The daily gridded rainfall data of 0.25° × 0.25° spatial resolution of Dharoi catchment for the period 1995 to 2019 is analyzed in the present study. From the rainfall data, it is observed that the wet and dry seasons in the study area extend from June to September and October to May months, respectively. The daily maximum (T_{max}) and minimum (T_{min}) temperatures of 1° × 1° spatial resolution are used for the period 1995 to 2019 in the present study.

5.3.1.6 SWAT model simulation

In the present study, SWAT model has been developed for Dharoi catchment. The files prepared as per the previous section, is given as input to the model such as DEM in .tiff format, land use map in grid format, soil map in shapefile format and climatic parameters in .txt format. In ArcGIS platform, using ARC-SWAT extension, SWAT project setup need to be created first for SWAT model run. In

watershed delineator tab in ARC-SWAT, the first input need to be given is DEM. Then the stream network will get generated. After the generation of stream network, sub-basin outlet point is allocated where the tributaries meet in the main channel. On the basis of outlet point and stream network, watershed is delineated. The stream network and 15 sub basin created on the basis of threshold given is created for Dharoi catchment as shown in Figure 5.5.

The threshold values for land uses, soil type and slope classes are used to create the HRUs for the study are given in Table 5.4.

Table 5.4 Threshold values for land uses, soil type and slope classes for HRU definition

Parameter	Threshold area in %
Landuse/landcover	5%
Soil type	10%
Slope	10%

5.3.2 Calibration and validation

After the successful SWAT model simulation, .TXTINOUT file is exported to stand-alone tool developed for the SWAT model, namely, SWAT Calibration and Uncertainty Program (SWAT-CUP) for calibration, validation, and sensitivity analyses (Abbaspour et al., 2004) using Sequential Uncertainty Fitting (SUFI-2) algorithm. The parameters considered for the present study are given in **Error! Reference source not found.**. In all, fourteen parameters have been identified based on the literature available on SWAT modelling for the Indian rivers (Narsimlu et al., 2012; Saraf and Regulwar, 2018), which were then used for hydrological model calibration and validation.

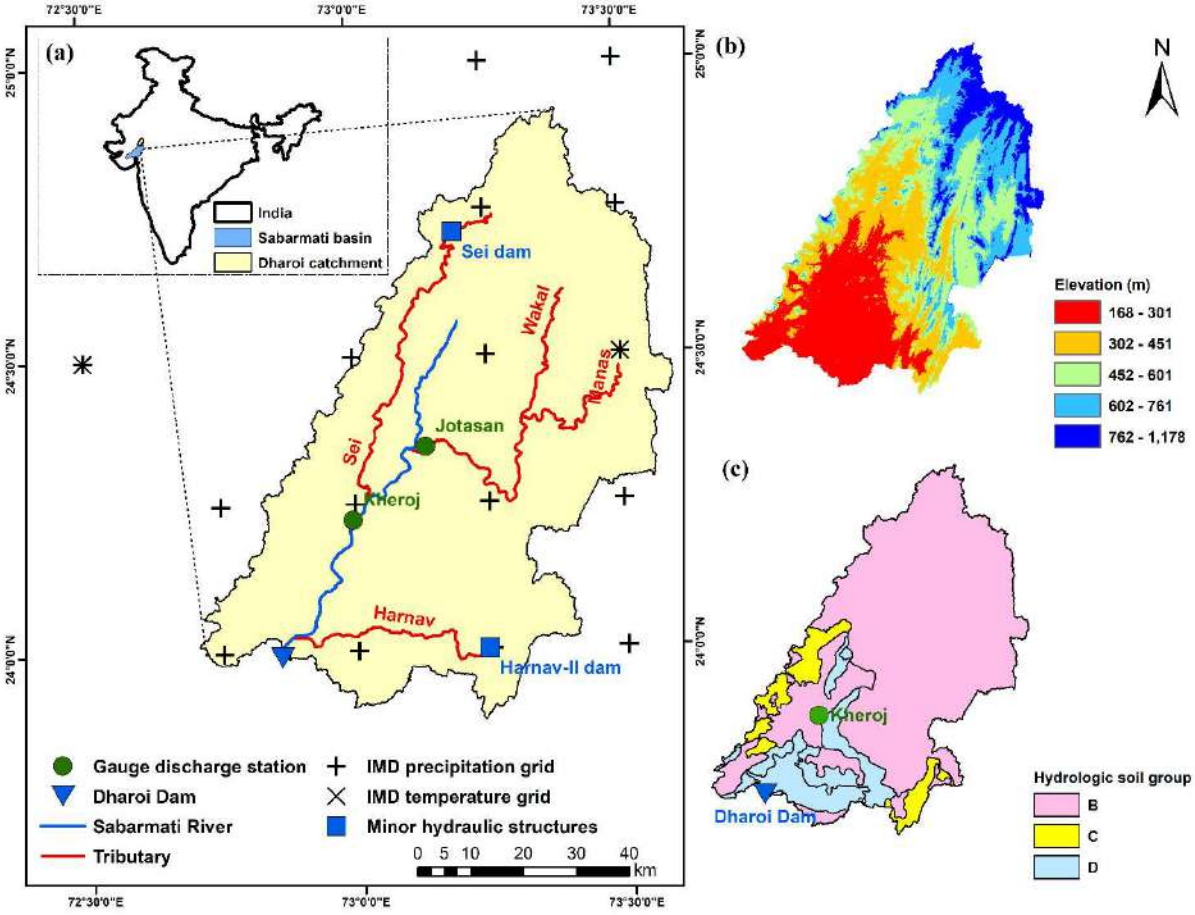

Figure 5.4 (a)

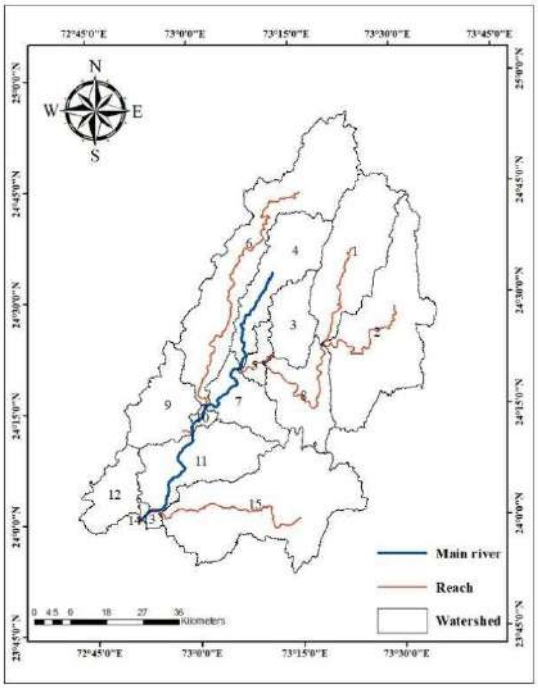

Figure 5.5 Sub basin configuration in SWAT model

Table 5.5 Description of the parameters adopted in SWAT model with their absolute ranges and initial values

Parameter Name	Description	Absolute ranges	Initial value
	Parameters controlling surface water response		
rCN2	SCS runoff curve number for moisture condition II	35-98	55-94
vEPCO	Plant uptake compensation factor	0-1	1
vESCO	Soil evaporation compensation factor	0-1	0.95
rCH_N2	Manning's *n* value for the main channel	-0.01-0.3	-0.0103
vCH_K2	Effective hydraulic conductivity in main channel alluvium (mm/hr)	-0.01-500	0.015-100
vSURLAG	Surface runoff lag coefficient	0.05-24	4
	Parameters controlling subsurface water response		
vALPHA_BNK	Baseflow alpha factor for bank storage (days)	0-1	0
vALPHA_BF	Baseflow alpha factor (days)	0-1	0.048
vGWQMN	Threshold depth of water in the shallow aquifer required for return flow to occur (mm)	0-5000	1000
vGW_DELAY	Groundwater delay (days)	0-500	31
vGW_REVAP	Groundwater revap coefficient	0.02-0.2	0.02
	Parameters controlling soil properties		
rSOL_AWC	Available water capacity of the soil layer (mm H_2O/ mm soil)	0-1	0.054-0.26
rSOL_BD	Moist bulk density mm layer (g/cm^3)	0.9-2.5	1.4-1.7
rSOL_K	Saturated hydraulic conductivity (mm/hr)	0-2000	0.58-41.27

5.3.2.1 Objective function for calibration and statistical performance indices

In present study, Kling Gupta Efficiency (KGE) (Gupta et al., 2009) has been adopted as the objective function. Nash-Sutcliffe Efficiency (NSE) has been also adopted by the researchers as the objective function (Narsimlu et al., 2013; Saraf and Regulwar et al., 2018). However, adopting KGE instead of NSE leads to improvement in the bias and variability measure while only slightly decreasing the correlation (Ma et al., 2020). The KGE gives equal weightage to all three components (correlation, bias, and variability measures). The value of KGE ranges from $-\infty$ to 1. KGE values at or above 0.75 and 0.50 denote good and intermediate performance of the model, respectively, while the ideal value is one. The model performance is also assessed using several statistical performance indices, viz., NSE, RSR (root mean squared error to standard deviation ratio) and PBIAS (percent bias). The mathematical expressions for KGE, NSE, RSR and PBIAS are described in Equations (1) - (4).

$$KGE = 1 - \sqrt{(r-1)^2 + \left(\frac{Q\sigma_{sim}}{Q\sigma_{obs}} - 1\right)^2 + \left(\frac{\bar{Q}_{sim}}{\bar{Q}_{obs}} - 1\right)^2} \quad (5.1)$$

$$NSE = 1 - \left\{\frac{\sum_{i=1}^{n}\left(Q_{obs_i} - Q_{sim_i}\right)^2}{\sum_{i=1}^{n}\left(Q_{obs_i} - \bar{Q}_{obs}\right)^2}\right\} \quad (5.2)$$

$$RSR = \left\{\frac{\sqrt{\sum_{i=1}^{n}\left(Q_{obs_i} - Q_{sim_i}\right)^2}}{\sqrt{\sum_{i=1}^{n}\left(Q_{obs_i} - \bar{Q}_{obs}\right)^2}}\right\} \quad (5.3)$$

$$PBIAS = \left\{\frac{\sum_{i=1}^{n}\left(Q_{obs_i} - Q_{sim_i}\right)}{\sum_{i=1}^{n} Q_{obs_i}} \times 100\right\} \quad (5.4)$$

where, Q_{obs_i} = observed streamflow at time i; Q_{sim_i} = simulated (predicted or forecasted) streamflow at time i; $\bar{Q}_{obs}$ = mean of the observed streamflows; $\bar{Q}_{sim}$ = mean of the simulated streamflows; $Q\sigma_{obs}$ = standard deviation of the observed streamflows; $Q\sigma_{sim}$ = standard deviation of the simulated streamflows; r = linear correlation coefficient.

5.3.2.2 Results and Discussions

The SWAT model has been calibrated for baseline period (1995-2014) and validated (2015-2019) at monthly time-step using LULC of 2004 to evaluate best model parameters and water balance components. Total 14 parameters (mentioned in Table 5.5) were adopted for calibration of the SWAT model using the SUFI-2 algorithm. As the SWAT model involves a vast domain of parameters, the global sensitivity analysis method was adopted to screen out the sensitive parameters. Six out of fourteen parameters, namely, CN2, SOL_AWC, ESCO, SOL_K, GWQMN, and GW_REVAP, exhibit sensitivity for baseline period. While other parameters, such as GW_DELAY, EPCO, SURLAG, SOL_BD, ALPHA_BNK, CH_N2, and CH_K2, showed insignificant variations in the global sensitivity analysis during the calibration process. The global sensitivity results at the catchment outlet indicate CN2 as the most sensitive parameter. The higher sensitivity of the CN2 is driven by the heterogeneous hydrologic soil conditions in the Dharoi catchment, ranging from moderate to high runoff potential. The fitted value of the parameters, obtained during calibration of hydrologic model for the baseline period using LULC of year 2005 at monthly scale are included in Table 5.6.

The calibrated model is validated for the period 2015-2019). The model performance indicator results are presented in Table 5.7. The Table 5.7 shows good results for both calibration and validation period as per the criteria given by Moriasi et al. (2007). The comparison of simulated hydrographs derived from single site and multisite calibration approach with observed hydrographs at the Dharoi dam is

shown in Figure 5.6 which reveals that the observed and simulated streamflow show good agreement during calibration (1995-2014) and validation (2015-2019) periods. The period 1995-2004 is predominantly dominated by low magnitude flows, wherein the maximum monthly flow observed was less than 100 m^3/s.

Based on the SWAT model simulations, the key water balance components, viz., rainfall (P), surface flow or runoff (Q_s), lateral flow (Q_{lat}), actual evapotranspiration (E_a) and percolation ($Perc$), recharge to deep aquifer ($Rech_{deepaq}$) are analysed. The change in soil water storage (ΔS) is estimated using Equation (6). The relative error can be estimated using the Equation (5). The model simulation errors (-1.9%) in water balance estimation for baseline period are within satisfactory limit. It is to be noted that maximum part of the precipitation is lost due to evapotranspiration (60.4%), followed by percolation (19.8%) and surface runoff (17.05%) in the catchment for the baseline period (Table 5.8 a).

$$Relative\ Error(\%) = (P - Q_s - Q_{lat} - E_a - Perc - \Delta S)/P \times 100 \quad (5.5)$$

$$\Delta S = (Perc - Rech_{deepaq} - Revap - Return\ flow) \quad (5.6)$$

Table 5.6 Final fitted value of the parameters

Parameters	Fitted Value	Parameters	Fitted Value
[r]CN2	0.12	[r]SOL_K	-0.18
[v]ALPHA_BF	0.71	[r]SOL_AWC	-0.06
[v]GW_DELAY	76.85	[v]CH_N2	0.3
[v]GW_GWQMN	1137.84	[v]CH_K2	56.42
[v]ESCO	0.13	[v]ALPHA_BNK	0.74
[v]EPCO	0.42	[v]GW_REVAP	0.05
[r]SOL_BD	0.012	[v]SURLAG	5.59

Table 5.7 Model simulation results based on the values of the objective function (KGE) and statistical performance indices (NSE, RSR and PBIAS) during model calibration and validation

	Calibration				Validation			
	KGE	NSE	RSR	PBIAS (%)	KGE	NSE	RSR	PBIAS (%)
Baseline period	0.95	0.91	0.30	1.1	0.94	0.95	0.23	-4.5

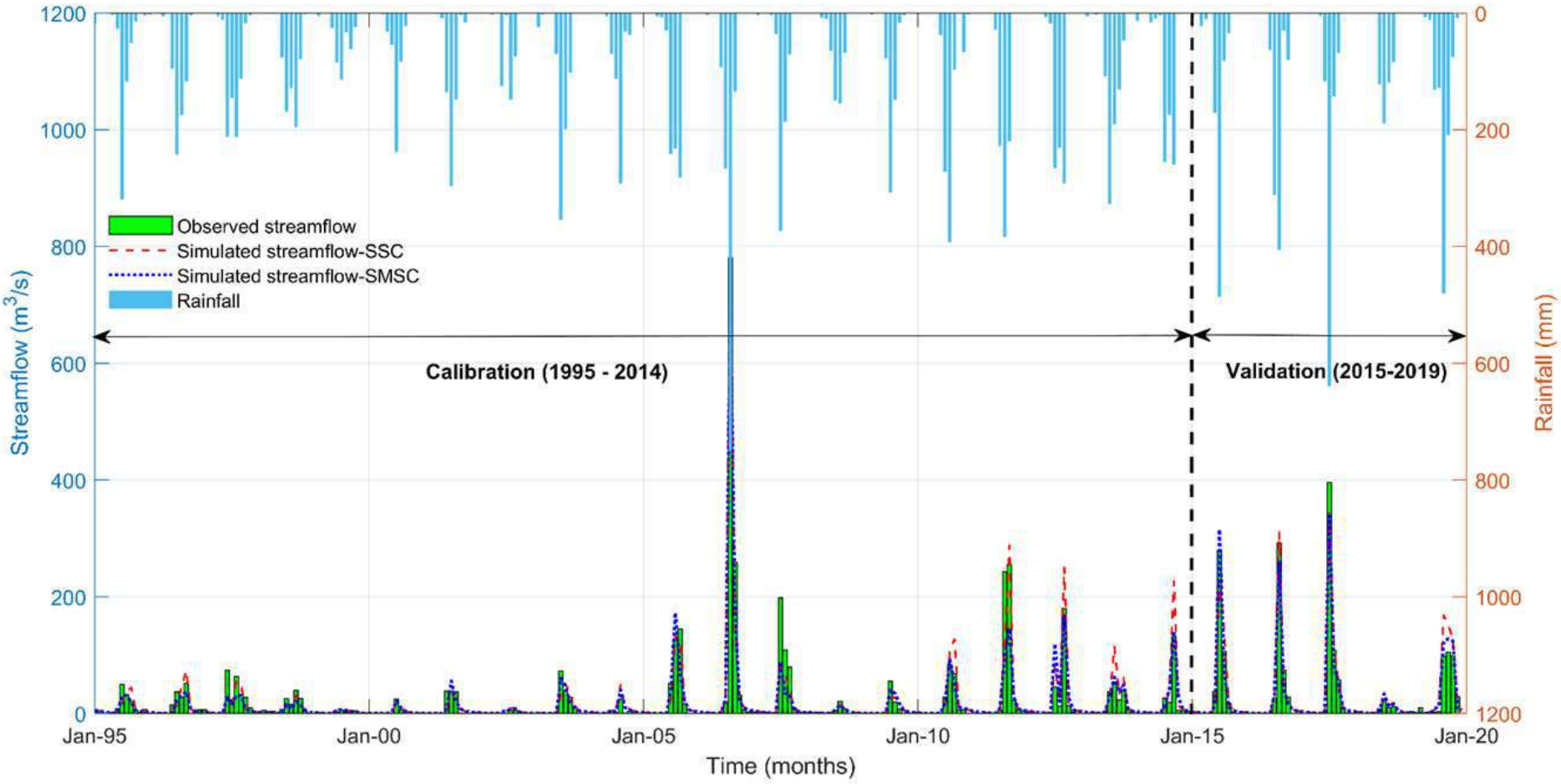

Figure 5.6 Comparison of simulated hydrographs derived from single-site and simultaneous multi-site calibration techniques with observed hydrograph at the Dharoi dam

Table 5.8a Future projected annual water balance components in Dharoi catchment for RCP4.5 scenario of GCM models

Baeline period		P (mm)	Q_s (mm)	Q_{lat} (mm)	E_a (mm)	$Perc$ (mm)	$Rech_{deepaq}$ (mm)	$Revap$ (mm)	$Return\ flow$ (mm)	$\Delta S = (Perc - Rech_{deepaq} - Revap - Return\ flow)$ (mm)	**Relative error (%)**
Calibration (1995-2014)		**659.8**	**112.5**	**15.5**	**398.9**	**142.2**	**8.2**	**128.2**	**2.2**	**-12.9**	**-1.9**
Validation (2015-209)		**846.2**	**202.68**	**21.17**	**440.4**	**202.11**	**11.2**	**180.4**	**20.3**	**-9.79**	**-1.22**
GCM model	**Scenario**	P (mm)	Q_s (mm)	Q_{lat} (mm)	E_a (mm)	$Perc$ (mm)	$Rech_{deepaq}$ (mm)	$Revap$ (mm)	$Return\ flow$ (mm)	$\Delta S = (Perc - Rech_{deepaq} - Revap - Return\ flow)$ (mm)	**Relative error (%)**
BNU - ESM	Near Future (2020-2040)	858.70	178.30	10.49	461.70	221.94	10.95	185.59	22.48	2.92	-1.94
	Mid Future (2041-2070)	785.70	132.79	9.20	474.60	189.46	9.74	177.13	8.76	-6.17	-1.80
	Far Future (2071-2100)	749.40	110.05	8.30	479.60	171.04	8.50	157.51	4.53	0.50	-2.68
CCCma - CanESM2	Near Future (2020-2040)	612.90	78.12	6.42	425.00	127.97	6.54	125.44	0.32	-4.33	-3.31
	Mid Future (2041-2070)	525.30	42.88	4.80	412.10	94.00	4.81	90.75	1.35	-2.91	-4.87
	Far Future (2071-2100)	545.50	49.57	5.03	419.10	95.59	5.03	95.59	0.57	-5.60	-3.33
CNRM -CM5	Near Future (2020-2040)	813.50	191.22	9.99	413.00	214.22	10.47	180.29	18.78	4.68	-2.41
	Mid Future (2041-2070)	719.60	137.89	8.58	415.60	179.88	9.24	166.89	9.20	-5.45	-2.35
	Far Future (2071-2100)	670.50	99.94	7.39	432.10	152.77	7.55	142.05	1.15	2.02	-3.54
MPIESM - LR	Near Future (2020-2040)	627.70	81.79	6.52	433.30	131.00	6.83	130.68	0.90	-7.41	-2.79
	Mid Future (2041-2070)	548.00	49.75	4.85	425.40	94.44	4.73	89.59	0.31	-0.19	-4.79
	Far Future (2071-2100)	590.00	61.50	5.59	437.30	110.41	5.60	106.42	0.44	-2.05	-3.86
MPIESM - MR	Near Future (2020-2040)	781.10	139.39	9.41	452.10	198.06	10.02	178.40	12.54	-2.90	-1.92
	Mid Future (2041-2070)	650.10	79.41	6.76	448.00	137.82	6.81	128.56	1.09	1.36	-3.58
	Far Future (2071-2100)	632.90	66.73	5.92	466.20	117.22	5.91	111.97	0.47	-1.13	-3.48

Table 5.8b Future projected annual water balance components in Dharoi catchment for RCP8.5 scenario of GCM models

Baeline period		P (mm)	Q_s (mm)	Q_{lat} (mm)	E_a (mm)	$Perc$ (mm)	$Rech_{deepaq}$ (mm)	$Revap$ (mm)	$Return\ flow$ (mm)	$\Delta S = (Perc - Rech_{deepaq} - Revap - Return\ flow)$ (mm)	Relative error (%)
Calibration (1995-2014)		**659.8**	**112.5**	**15.5**	**398.9**	**142.2**	**8.2**	**128.2**	**2.2**	**-12.9**	**-1.9**
Validation (2015-2009)		**846.2**	**202.68**	**21.17**	**440.4**	**202.11**	**11.2**	**180.4**	**20.3**	**-9.79**	**-1.22**
GCM model	**Scenario**	**P (mm)**	**Q_s (mm)**	**Q_{lat} (mm)**	**E_a (mm)**	**$Perc$ (mm)**	**$Rech_{deepaq}$ (mm)**	**$Revap$ (mm)**	**$Return\ flow$ (mm)**	**$\Delta S = (Perc - Rech_{deepaq} - Revap - Return\ flow)$ (mm)**	**Relative error (%)**
BNU - ESM	Near Future (2020-2040)	788.60	134.95	9.34	466.90	195.02	9.77	170.97	22.48	-8.20	-1.19
	Mid Future (2041-2070)	773.70	121.85	8.74	483.80	179.41	8.95	163.39	7.99	-0.92	-2.48
	Far Future (2071-2100)	778.40	116.73	8.68	496.40	176.68	8.84	159.97	7.97	-0.10	-2.57
CCCma - CanESM2	Near Future (2020-2040)	709.10	107.72	8.22	440.40	172.57	8.41	153.92	4.15	6.09	-3.65
	Mid Future (2041-2070)	518.30	29.18	4.50	427.70	86.66	4.55	87.49	0.24	-5.62	-4.65
	Far Future (2071-2100)	545.50	52.21	5.66	421.70	112.20	5.66	105.41	1.41	-0.28	-8.43
CNRM -CM5	Near Future (2020-2040)	792.10	168.41	9.32	438.90	193.79	9.81	175.13	12.05	-3.20	-1.91
	Mid Future (2041-2070)	689.30	101.26	7.31	459.30	145.41	7.44	140.16	2.13	-4.32	-2.85
	Far Future (2071-2100)	617.30	52.35	5.49	482.30	101.70	5.06	94.54	0.92	1.18	-4.17
MPIESM - LR	Near Future (2020-2040)	661.60	86.25	7.06	448.60	142.74	7.25	136.34	2.14	-2.99	-3.03
	Mid Future (2041-2070)	578.10	43.08	4.88	459.60	94.52	4.69	88.73	0.11	0.99	-4.32
	Far Future (2071-2100)	604.60	52.34	5.53	462.40	108.39	5.42	102.19	0.80	-0.02	-3.98
MPIESM - MR	Near Future (2020-2040)	707.40	104.14	7.75	460.40	156.73	8.09	150.25	3.46	-5.07	-2.34
	Mid Future (2041-2070)	643.40	64.97	6.08	477.30	119.40	6.10	116.41	0.57	-3.68	-3.21
	Far Future (2071-2100)	622.30	36.64	5.15	505.80	98.76	4.94	93.60	0.13	0.09	-3.88

5.3.2.3 Analysis of stream flows for future scenarios

The calibrated and validated hydrological model (SWAT) for the Dharoi catchment has been used for simulating the response of the catchment for the rainfall statistically downscaled from five GCMs, i.e., BNU-ESM, CCCma-CanESM2, CNRM-CM5, MPIESM-LR and MPIESM-MR for RCP 4.5 and 8.5 scenarios.

The RCP4.5 indicates intermediate pathway scenario which indicates good agreement with the latest policy of lower greenhouse gas emission by the global community. Therefore, it is often considered as a very-good-case scenario in the context of recent policy directions (Wang et al., 2016). On other hand, RCP8.5 is the scenario which provides the possible highest impact on climate change. Therefore, RCP4.5 and RCP8.5 are selected as these two scenarios can provide a possible complete range of impact. The water balance component indicated that the amount of precipitation was lost mainly due to evapotranspiration for all GCM model under RCP4.5 and RCP8.5 scenario, which may be possible due to the semi-arid characteristic of the Dharoi catchment and increase in temperature in the catchment.

The relative error in water balance estimation is within the range of -1.80 to -4.8%, for all GCM model scenario which are within satisfactory limits (Table 5.8a and Table 5.8b). The simulated results showed that the 53-81% of precipitation is expected to returned to atmosphere through evapotranspiration. On the other hand, 5-23% (12-37%) contributes to surface runoff (percolation) in GCM model for RCP4.5 and RCP8.5 scenarios (Table 5.8a and Table 5.8b).

The flow duration curve for Dharoi catchment is plotted in Figure 5.7 at monthly scale. The flow duration curve was found to be the most informative way of representing the complete range of river discharges for the selected period (Smakhtin 2001). From the flow duration curves derived from different GCMs for both RCP4.5 and RCP8.5, indicate that high dependable flows (low discharges) are likely to increase in future while the low dependable flows (floods) are likely to decrease in future. This condition could be favourable to the water users as reservoir is likely to get more water for the usage in future.

The streamflow variation of IMD and GCM historical along with future projected GCM models at monthly scale for RCP4.5 is presented in Figure 5.8. From the Figure 5.8, it is seen that stream flows in the basin is likely to increase in near future (2020-2041) under RCP4.5 scenario. After wards the stream flow may reduce during 2041-2070 and 2071-2100 periods.

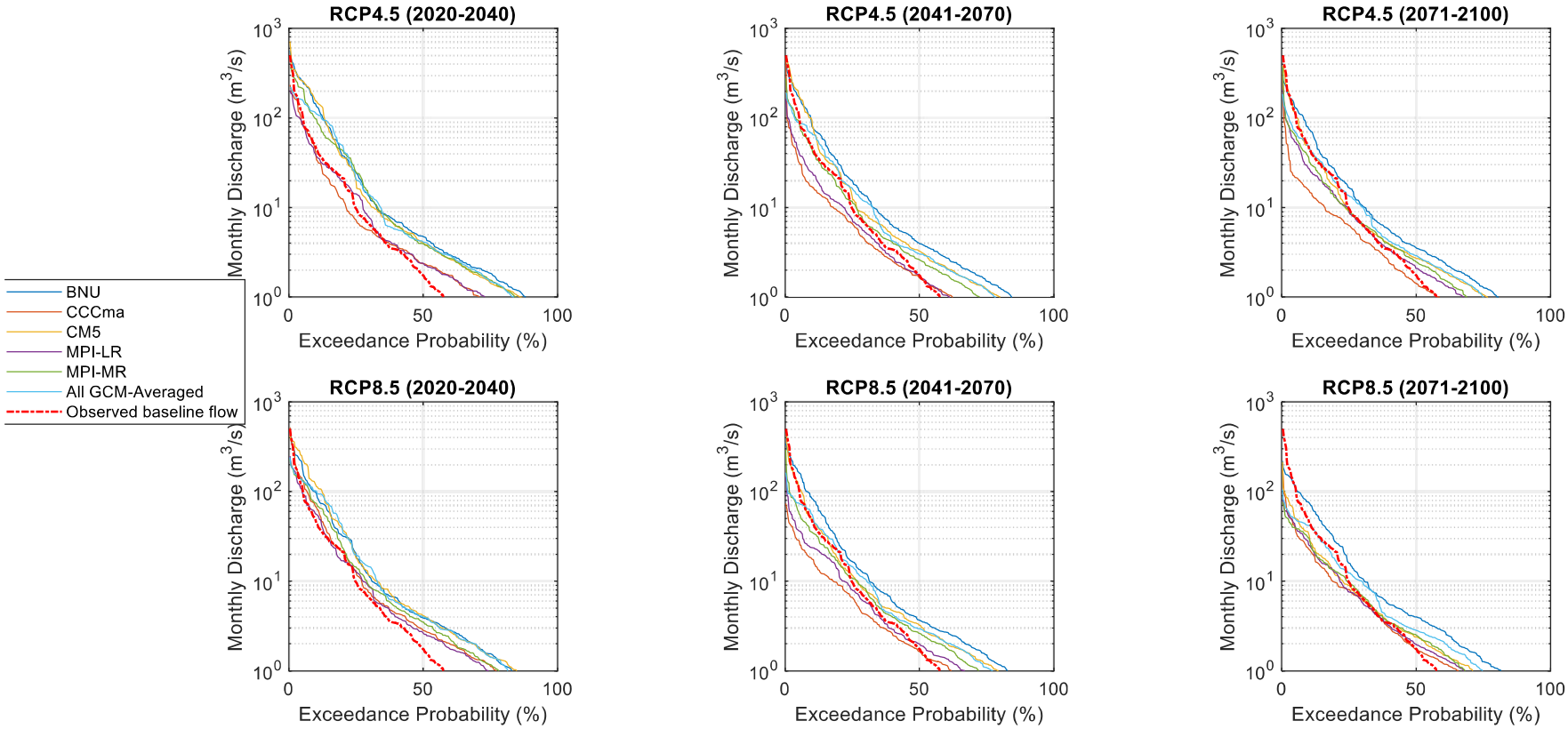

Figure 5.7 Flow duration curve for RCP4.5 and RCP8.5 of GCM model

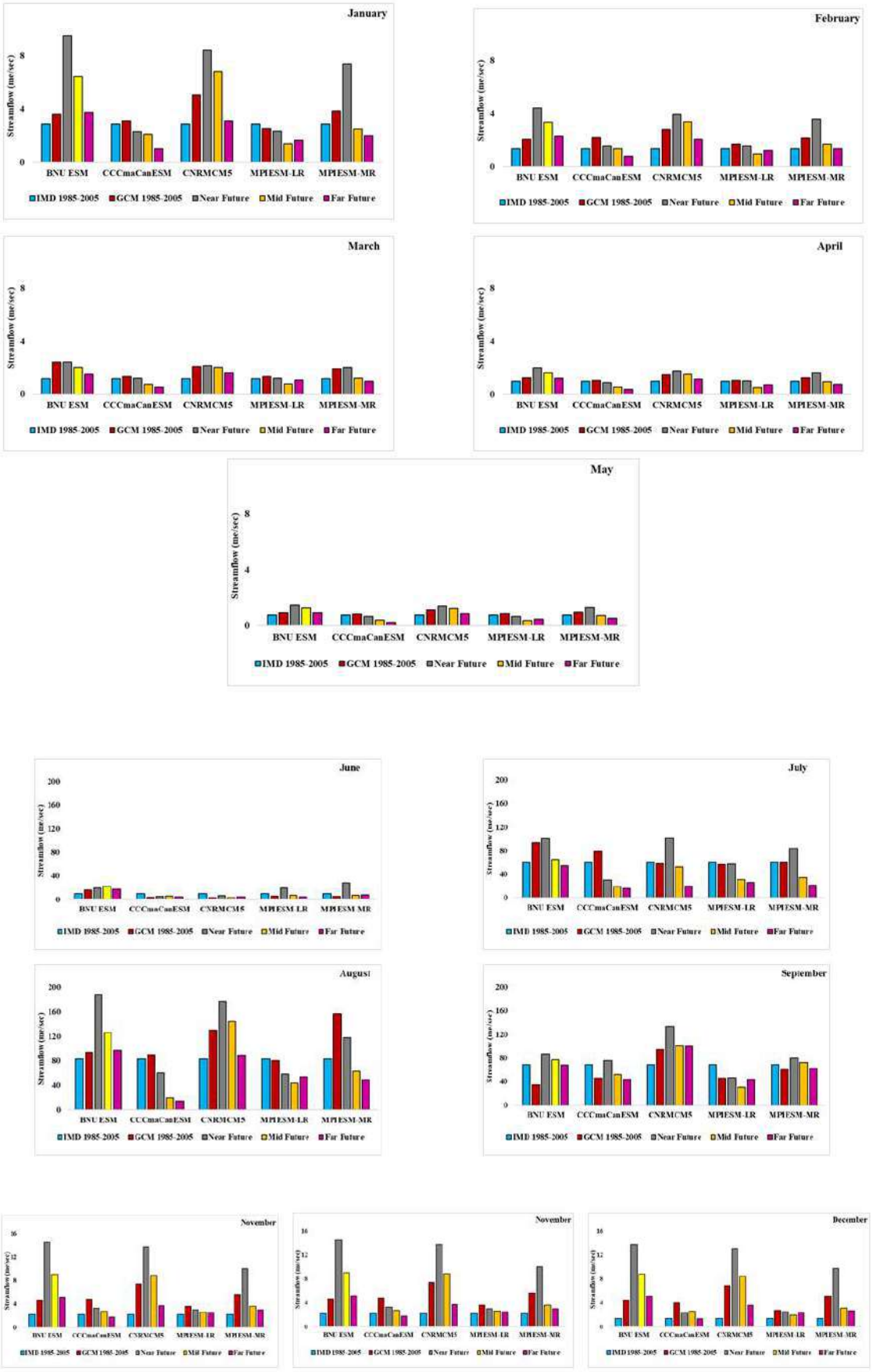

Figure 5.8 Streamflow variation of historical and future period for RCP4.5

5.3.2.4 Concluding remarks

- ✓ The SWAT model for baseline period has been calibrated for period 1995-2014 and validated for period 1995-2014. Out of the 14 parameters analyzed, CN2, SOL_AWC, ESCO, SOL_K, GWQMN, and GW_REVAP, have been found to be sensitive as compared to rest of the parameters. The global sensitivity results at the catchment outlet indicates CN2 as the most sensitive parameter. The SWAT model simulation results showed good capability to simulate the discharges, wherein the value of the objective function, Kling-Gupta efficiency (KGE), ranged from 0.94-0.95 in calibration as well as validation periods. The other statistical performance indices, such as, RSR, NSE and PBIAS also suggested better performances of the model.
- ✓ The comparison of simulated hydrographs derived from single site and multisite calibration approach with observed hydrographs at the Dharoi dam which indicate that the observed and simulated streamflow show good agreement during calibration (1995-2014) and validation (2015-2019). It is noted that maximum part of the precipitation is lost due to evapotranspiration (60.4%), due to Semi-arid characteristics of Dharoi catchment.
- ✓ The simulated results showed that the 53-81% of precipitation is expected to returned to atmosphere through evapotranspiration. On the other hand, 5-23% (12-37%) would contribute to surface runoff (percolation) in GCM model for RCP4.5 and RCP8.5 scenarios. The relative error in water balance estimation is within the range of -1.80 to -4.8%, for all GCM model and scenarios, which are within satisfactory limits.
- ✓ From the flow duration curves derived from different GCMs for both RCP 4.5 and 8.5, indicate that high dependable flows (low discharges) are likely to increase in future while the low dependable flows (floods) are likely to decrease in future.
- ✓ The streamflow variation of IMD and GCM historical along with future projected GCM models at monthly scale indicate that stream flows in the basin are likely to increase in near future (2020-2041) under RCP 4.5 scenario. After wards, the stream flows may reduce during mid (2041-2070) and far (2071-2100) future.

6 METHODOLOGY AND ANALYSIS OF DATA: IMPACT ON IRRIGATION DEMAND

6.1 GENERAL

In this chapter, the methodology for computation of irrigation demand in Dharoi command area is included. The meteorological data, statistical downloaded for future periods (near, mid and far future), were used to calculate the changes in the irrigation demands in future with reference to the base line period. The calculated irrigation demands for base line period and future periods are compared to assess the impact of climate change on irrigation demand in the command area.

6.2 METHODOLOGY

The amount of water required for irrigation or the prediction of irrigation demand for a command area is critical for the design and operation of an irrigation projects. The water need, also known as the irrigation requirement, is most frequently described as the total quantity of water required by the crops in the command area from the time of their initial watering to the time of harvesting or last watering (base period) (Garg 2005). The Gross Irrigation Requirements are dependent on Net Irrigation Requirements (NIR) of crops. The Gross irrigation demand is a function of Reference Evapotranspiration, Crop Water Requirement (CWR), Effective Rainfall (Peff), water application efficiency and conveyance efficiency. The calculation procedure is explained in further sections.

- **Hargreaves Method**

The reference evapotranspiration was estimated using a modified Hargreaves approach (Samani 2000) to estimate solar radiation and crop evapotranspiration with use of minimum climatological data.

The difference between maximum and minimum air temperature is proportional to the amount of cloud cover in a certain region. Clear-sky circumstances result in high temperatures during the day (T_{max}) as the atmosphere is transparent to incoming solar radiation and low temperatures at night (T_{min}) as the atmosphere absorbs less outgoing longwave radiation. The T_{max} is less under overcast situations as considerable portion of the incoming solar energy never reaches the earth's surface and is absorbed and reflected by the clouds. Similarly, T_{min} will be substantially greater because cloud cover acts as a blanket, reducing net outgoing longwave radiation. As a result, the difference between maximum and minimum air temperatures (T_{max} - T_{min}) may be used to estimate the proportion of extra-terrestrial radiation that reaches the earth's surface.

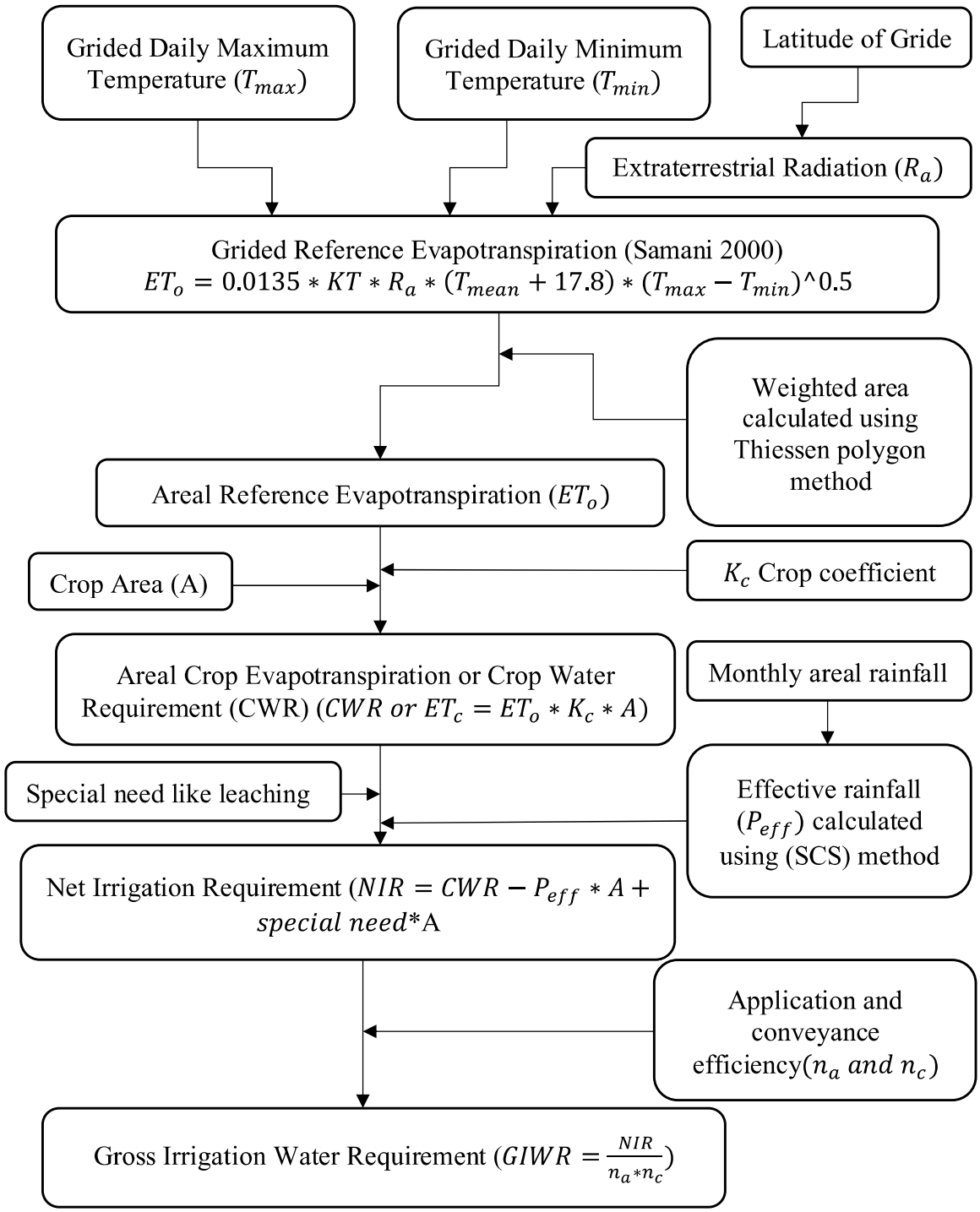

Figure 6.1 Methodology adopted for estimation of irrigation water demand

Hargreaves and Samani used the concept to produce estimations of (ET_o using only air temperature data. Furthered, (Samani 2000) modified the approach by minimizing the error associated with

estimation of solar radiation, thus, improving the estimation of reference evapotranspiration. Samani (2000) proposed Equation (6.1) for computation of Evapotranspiration (ET_o),

$$ET_o = 0.0135 * KT * R_a * (T_{mean} + 17.8) * (T_{max} - T_{min})\text{^}0.5 \quad (6.1)$$

where

$$KT = 0.00185 * (T_{max} - T_{min})^{0.5} - 0.0433 * (T_{max} - T_{min}) + 0.4023 \quad (6.2)$$

Radiation (R_a) (mm/day) = 0.408 * radiation (MJ/m^{2}day),

R_a is extra-terrestrial radiation (MJ/m^{2}day),

T_{max} is maximum air temperature (^{o}C),

T_{max} is minimum air temperature (^{o}C),

T_{mean} is mean air temperature (^{o}C),

ET_o is evapotranspiration (mm/day).

- **Crop Water Requirement (CWR)**

Consumptive usage of a crop, also known as crop evapotranspiration, is the total quantity of water consumed by the plant in transpiration (building of plant tissues) plus evaporation from neighboring soils and plant leaves. The CWR varies for various crops and can also vary for the same crop at different locations and times. This is also known as crop water requirement (CWR), which may be determined using Equation 6.3.

$$CWR = ET_c = K_c \times ET_o \quad (6.3)$$

Here, ETc denotes crop evapotranspiration (mm), *Kc* denotes crop coefficient at a certain development stage (dimensionless), and *ETo* denotes reference evapotranspiration (mm).

- **Effective Precipitation (P_{eff})**

Effective rainfall is the precipitation that falls during crop growth and is available to supply the crop evapotranspiration demands while eliminating precipitation lost through deep percolation below the root zone and surface drainage. The Soil Conservation Service (SCS) Method, as defined in Equation 6.4, was used to determine effective rainfall.

$$P_{eff_t} = \frac{P_t}{125} * (125 - 0.2 * P_t) \qquad P_t \leq 250\,mm$$
$$P_{eff_t} = 125 + 0.1 * P_t \qquad P_t > 250\,mm \quad (6.4)$$

where, P_{eff_t}=effective rainfall in tth month; and P_t=rainfall in tth month.

- **Net Irrigation Requirement (NIR)**

Net irrigation requirement is the amount of irrigation water required to fulfil the crop water requirement and additional needs such as leaching (Special needs), as expressed in Equation 6.5.

$$NIR = CWR - P_{eff} + Special\ needs \tag{6.5}$$

The filed irrigation requirement (*FIR*) and Gross irrigation water requirement are calculated as per Equation 6.6 and Equation 6.7 respectively.

$$FIR = \frac{NIR}{n_a} \tag{6.6}$$

$$GIWR = \frac{FIR}{n_c} \tag{6.7}$$

where, *NIR*=Net Irrigation Requirement; *FIR* = Field irrigation requirement; *GIWR*= Gross irrigation water requirement; n_a= Application efficiency (60% for flood irrigation); and n_c=Conveyance efficiency (70% considered for present study).

The climatic parameters like maximum, minimum temperature and rainfall were obtained from the statistically downscaled data of Dharoi command area. The extra-terrestrial radiations were estimated as per the FAO approach. The cropping patterns for calculation of irrigation demand for base line and future were taken as per **APPENDIX III.**

The predicted irrigation demand for current cropping pattern for base line period and future periods are included in following sections.

6.3 RESULTS AND DISCUSSIONS

The absolute values of the long-term mean rainfall, reference evapotranspiration, crop water demand and gross irrigation water requirement in the Dharoi command area for RCP 4.5 and RCP 8.5 scenarios, using ensembled downscaled climatic variables for five GCMs, were estimated on monthly scales see Figure 6.2. The values indicated in Figure 6.2, shows the changes in the variables with reference to their respective values for observed IMD data for the base line period. From Figure 6.1 (b), it is revealed that reference evapotranspiration (ET_o) values decrease for February, March, April, October, November and December months with reference to their corresponding values of IMD data for historical period. On the other hand, the value of the parameter decreases during January, May, June, July, August and September months. Such increase/ decrease in the ET_o values are due to monthly variations in (T_{max}-T_{min}) parameters in their respective months. The crop water requirement for different months, depending upon the stage of Kharif, Rabi and two seasonal crops, were

estimated from the estimated reference crop evapotranspiration (ET_o. The net irrigation demands values were subsequently computed by subtracting the effective rainfall for each month and adding additional irrigation requirement such as leaching etc. Subsequently, from Net irrigation requirement, the field irrigation requirement and gross irrigation requirement are obtained by giving due consideration of water application efficiency and conveyance efficiency respectively. From Figure 6.2(d), it is apparent that, the gross irrigation requirement (GIR) would increase (decrease) in future for January and October months (September, November and December months) with reference to the base line period. This increase in GIR in January month is due to increase in ET_o in the same month (Figure 6.2(b)). Similarly, the decrease in GIR in September, November and December months is due to increase in effective rainfall in future in such months (See Figure 6.2(a)). In the remaining months, the GIR remains invariant with reference to the base line period in future.

6.4 CONCLUDING REMARKS

The Gross irrigation requirements in few months are likely to increase (decrease), particularly for January and October months (September, November and December) months with reference to the base line period. Due to change in the gross irrigation requirement (GIR) for future periods, and increase in the inflows into the Dharoi reservoir, suitable muti-objective techniques need to be implemented for changing conditions in near, mid and far future.

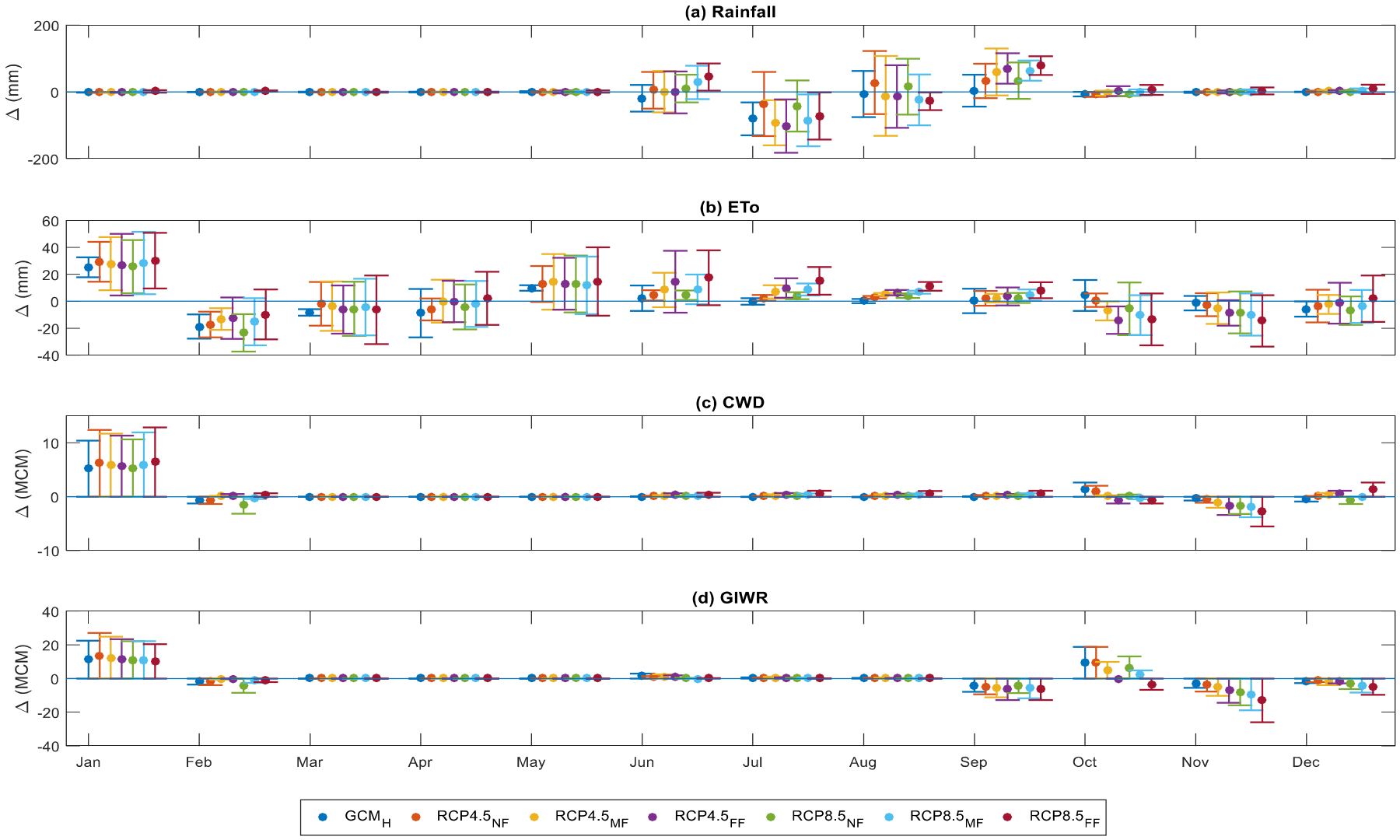

Figure 6.2 Mean change in Rainfall, ETo, CWD and GIWR in Dharoi command area with reference to their respective values for base line period during near-, mid-, and far-future under RCP 4.5 and RCP 8.5 scenarios for ensembled output of GCM Models

7 CONCLUSIONS AND ADAPTIVE MEASURES

7.1 SUMMARY OF WORK

The work related with Impact of climate change on water resources of Sabarmati basin are presented. Firstly, the trend in the climatic parameters, like Extreme precipitation and temperature indices have been analyzed and the results are discussed for base line period and future periods. Subsequently, the hydrological modelling using the data of base line period and statistically downloaded climatic variables were used to calibrate, validate the same and use to see the response of upper Sabarmati basin under changing climatic scenarios. Further, the command area of Dharoi reservoir have been analysed for existing cropping pattern, and the irrigation demand for the base line period and future periods are estimated to assess the impact of climatic variables on future irrigation demand. The Key conclusions, derived from foregoing study are described in following paragraphs:

7.2 CONCLUSIONS

The key findings of trend analyses on climatic variables, presented in the preceding section is appended in the following paragraph:

a) The extreme rainfall indices, on annual scale for S1 period, revealed an overall increasing trend in PRCPTOT, RD, RX1day, RX5day, R99p, R95p, LRF, MRF and CWD. On the other hand, the SDII and CDD have shown significant reduction in this period due to increase in number of rainy days. This is an indication that the Sabarmati River (SRB) basin is shifting towards the wet regime post 1985.

   The T_{max} has shown significantly increasing trend in 100% (5%) grids across SRB in O1 (S1) period while T_{min} has shown increasing trend in 60% (100%) grids with statistical significance for period O1 (S1). It is also noticed that 100% (90%) grids have contributed significant increasing trend of T_{av} for O1 (S1) period at annual scale, which may be a matter of concern to the agriculture sector as it may have adverse impact on the yield of some of the crops in the SRB. The Heat stresses, during periods of high temperatures, may also exacerbate health problems, such as sunstrokes, muscle cramps and heat exhaustion, and may affect the work performance of the people in the basin.

b) Due to increase in T_{min} and decrease in T_{max}, it is observed that 80% grids have indicated significantly decreasing trend of DTR in S1 period, i.e., post 1984. The change of DTR may have adverse effects on human health, i.e., through its impacts on cardiovascular, nervous, and immunity system (Liang et al., 2008; Bull 1980).

c) The ensembled climatic parameters like RD, PRCPTOT, LRF, MRF and CWD, statistically downloaded from Five GCMs. are likely to increase in future (near, Mid and far future) for

RCP 4.5 and RCP 8.5 scenarios. On the other hand, the climatic parameters like CDD, SDII and HRF are likely decrease in near, Mid and Far future. This trend indicates that the Sabarmati River Basin (SRB) is likely to become wetter in future. However, the extremes like flood and disasters may not likely to aggravate in future.

d) The Wetting conditions in future may reduce the drought events which may be favourable conditions for infilling the reservoir. The more available water in the reservoir can cover more command area for agriculture in future.

e) The SWAT model for baseline period has been calibrated for period 1995-2014 and validated for period 1995-2014. Out of the 14 parameters analyzed, CN2, SOL_AWC, ESCO, SOL_K, GWQMN, and GW_REVAP, have been found to be sensitive as compared to rest of the parameters. The global sensitivity results at the catchment outlet indicates CN2 as the most sensitive parameter. The SWAT model simulation results showed good capability to simulate the discharges, wherein the value of the objective function, Kling-Gupta efficiency (KGE), ranged from 0.94-0.95 in calibration as well as validation periods. The other statistical performance indices, such as, RSR, NSE and PBIAS also suggested better performances of the model.

f) The comparison of simulated hydrographs derived from single site and multisite calibration approach with observed hydrographs at the Dharoi dam which indicate that the observed and simulated streamflow show good agreement during calibration (1995-2014) and validation (2015-2019). It is noted that maximum part of the precipitation is lost due to evapotranspiration (60.4%), due to Semi-arid characteristics of Dharoi catchment.

g) The simulated results showed that the 53-81% of precipitation is expected to returned to atmosphere through evapotranspiration. On the other hand, 5-23% (12-37%) would contribute to surface runoff (percolation) in GCM model for RCP4.5 and RCP8.5 scenarios. The relative error in water balance estimation is within the range of -1.80 to -4.8%, for all GCM model and scenarios, which are within satisfactory limits.

h) From the flow duration curves derived from different GCMs for both RCP 4.5 and 8.5, indicate that high dependable flows (low discharges) are likely to increase in future while the low dependable flows (floods) are likely to decrease in future.

i) The streamflow variation of IMD and GCM historical along with future projected GCM models at monthly scale indicate that stream flows in the basin are likely to increase in near future (2020-2041) under RCP 4.5 scenario. After wards, the stream flows may reduce during mid (2041-2070) and far (2071-2100) future.

j) The Gross irrigation requirements in few months are likely to increase (decrease), particularly for January and October months (September, November and December) months with reference to the base line period.

7.3 ADAPTIVE MEASURES

On the basis of results reported in the preceding section, the following are recommended adoptive measures in Sabarmati basin and Dharoi reservoir:

(a) The increasing trend in T_{min} and T_{av} across the Sabarmati basin needs special investigations with reference to their likely effects on human health due to heat stress, and crop yield in the basin. Also, the changing trends in diurnal temperature range (DTR) and its possible effects needs to be addressed.

(b) The increasing trends total annual rainfall (PRCPTOT), rainy days (RD), Low rainfall (LRF) and medium rain fall (MRF), indicated that Sabarmati basin is shifting towards wet regime in future. The flow duration curves for inflow into the Dharoi reservoir indicated that inflows into the reservoir are likely to increase in future, particularly, low and medium discharges. Such increase in inflows into the reservoir may require changing the operating rules of Dharoi reservoir in future.

(c) The irrigation demands are likely to change due to increase in reference crop evapotranspiration, precipitation and, subsequent, changes in Gross irrigation requirement (GIR) of Dharoi command area. The changes in GIR and increase in inflows into the Dharoi reservoir indicate that optimal cropping pattern in the command area, using suitable multiobjective optimization model, has to be estimated to meet both the demands, i.e., irrigation and water supply for domestic and industrial needs, in future.

REFERENCES

Abbasnia, M., and Toros, H. (2016). Future changes in maximum temperature using the statistical downscaling model (SDSM) at selected stations of Iran. *Modeling Earth Systems and Environment*, *2*(2), 1-7.

Abbaspour, K. C., Faramarzi, M., Ghasemi, S. S., and Yang, H. (2009). Assessing the impact of climate change on water resources in Iran. *Water resources research*, *45*(10).

Abbaspour, K. C., Johnson, C. A., and Van Genuchten, M. T. (2004). Estimating uncertain flow and transport parameters using a sequential uncertainty fitting procedure. *Vadose zone journal*, *3*(4), 1340-1352.

Abushandi, E., and Merkel, B. (2013). Modelling rainfall runoff relations using HEC-HMS and IHACRES for a single rain event in an arid region of Jordan. *Water resources management*, *27*(7), 2391-2409.

Afshar, A., Haddad, O. B., Mariño, M. A., and Adams, B. J. (2007). Honey-bee mating optimization (HBMO) algorithm for optimal reservoir operation. *Journal of the Franklin Institute*, *344*(5), 452-462.

Allen, R. G., Pereira, L. S., Raes, D., and Smith, M. (1998). FAO Irrigation and drainage paper No. 56. *Rome: Food and Agriculture Organization of the United Nations*, *56*(97), e156.

Anandhi, A., Srinivas, V. V., Kumar, D. N., and Nanjundiah, R. S. (2009). Role of predictors in downscaling surface temperature to river basin in India for IPCC SRES scenarios using support vector machine. International Journal of Climatology: A Journal of the Royal Meteorological Society, 29(4), 583-603.

Asgari, H. R., Bozorg Haddad, O., Pazoki, M., and Loáiciga, H. A. (2016). Weed optimization algorithm for optimal reservoir operation. *Journal of Irrigation and Drainage Engineering*, *142*(2), 04015055.

Avila-Diaz, A., Benezoli, V., Justino, F., Torres, R., and Wilson, A. (2020). Assessing current and future trends of climate extremes across Brazil based on reanalyses and earth system model projections. *Climate Dynamics*, *55*(5), 1403-1426.

Babar, S., and Ramesh, H. (2015). Streamflow response to land use–land cover change over the Nethravathi River Basin, India. *Journal of Hydrologic Engineering*, *20*(10), 05015002.

Bennett, T. H., and Peters, J. C. (2000). Continuous soil moisture accounting in the hydrologic Engineering Center Hydrologic Modeling System (HEC-HMS). In *Building partnerships* (pp. 1-10).

Chen, L., Xu, J., Wang, G., Liu, H., Zhai, L., Li, S., ... and Shen, Z. (2018). Influence of rainfall data scarcity on non-point source pollution prediction: Implications for physically based models. *Journal of Hydrology*, *562*, 1-16.

Choudhari, K., Panigrahi, B., and Paul, J. C. (2014). Simulation of rainfall-runoff process using HEC-HMS model for Balijore Nala watershed, Odisha, India. *International Journal of Geomatics and Geosciences*, *5*(2), 253.

CWC (2014). Sabarmati Basin Watershed Atlas. Central Water Commission, New Delhi.

De Silva, M. M. G. T., Weerakoon, S. B., and Herath, S. (2014). Modeling of event and continuous flow hydrographs with HEC–HMS: case study in the Kelani River Basin, Sri Lanka. *Journal of Hydrologic Engineering*, *19*(4), 800-806.

Deng, C., Liu, P., Wang, W., Shao, Q., and Wang, D. (2019). Modelling time-variant parameters of a two-parameter monthly water balance model. *Journal of Hydrology*, *573*, 918-936.

Deng, C., Liu, P., Wang, W., Shao, Q., and Wang, D. (2019). Modelling time-variant parameters of a two-parameter monthly water balance model. *Journal of Hydrology*, *573*, 918-936.

Du, J., Rui, H., Zuo, T., Li, Q., Zheng, D., Chen, A., ... and Xu, C. Y. (2013). Hydrological simulation by SWAT model with fixed and varied parameterization approaches under land use change. *Water resources management*, *27*(8), 2823-2838.

Fleming, M., and Neary, V. (2004). Continuous hydrologic modeling study with the hydrologic modeling system. *Journal of hydrologic engineering*, *9*(3), 175-183.

Gehlot, L. K., Jibhakate, S. M., Sharma, P. J., Patel, P. L., and Timbadiya, P. V. (2021). Spatio-temporal variability of rainfall indices and their teleconnections with El Niño-Southern oscillation for Tapi Basin, India. *Asia-Pacific Journal of Atmospheric Sciences*, *57*(1), 99-118.

Ghosh, S., Das, D., Kao, S. C., and Ganguly, A. R. (2012). Lack of uniform trends but increasing spatial variability in observed Indian rainfall extremes. *Nature Climate Change*, *2*(2), 86-91.

Ghosh, S., Das, D., Kao, S. C., and Ganguly, A. R. (2012). Lack of uniform trends but increasing spatial variability in observed Indian rainfall extremes. *Nature Climate Change*, *2*(2), 86-91.

Goswami, B. N., Venugopal, V., Sengupta, D., Madhusoodanan, M. S., and Xavier, P. K. (2006). Earth by comets and meteorites. Further studies of these objects may elucidate whether their composition and membrane-like structures were important building blocks for the origin of life. *Science*, *314*(December), 1442-1445.

Gupta, H. V., Kling, H., Yilmaz, K. K., and Martinez, G. F. (2009). Decomposition of the mean squared error and NSE performance criteria: Implications for improving hydrological modelling. *Journal of hydrology*, *377*(1-2), 80-91.

Haddad, O. B., Hosseini-Moghari, S. M., and Loáiciga, H. A. (2016). Biogeography-based optimization algorithm for optimal operation of reservoir systems. *Journal of Water Resources Planning and Management*, *142*(1), 04015034.

Haque, S., Hossain, M. A., Salehin, M., and Rahman, M. (2017). Sensitivity analysis of SMA based continuous hydrologic simulation for SariGowain river basin. In *International Conference on Engineering Research, Innovation and Education*.

Hargreaves, G. H., and Samani, Z. A. (1985). Reference crop evapotranspiration from temperature. *Appl. Eng. Agric., 1*(2), 96-99.

Heidari, M., Chow, V. T., Kokotović, P. V., and Meredith, D. D. (1971). Discrete differential dynamic programing approach to water resources systems optimization. *Water Resources Research*, *7*(2), 273-282.

Huntington, T. G. (2006). Evidence for intensification of the global water cycle: Review and synthesis, *Journal of Hydrology, 319*(1–4), 83–95.

Huntington, T. G. (2006). Evidence for intensification of the global water cycle: review and synthesis. *Journal of Hydrology*, *319*(1-4), 83-95.

IPCC (2013) Climate change 2013: the physical science basis. In: Stocker TF, Qin D, Plattner G-K, Tignor M, Allen SK, Boschung J, Nauels A, Xia Y, Bex V, Midgley PM (eds) Contribution

of working group I to the fifth assessment report of the intergovernmental panel on climate change. Cambridge University Press, Cambridge.

Jain, S. K., Goel, M. K., and Agarwal, P. K. (1998). Reservoir operation studies of Sabarmati system, India. *Journal of water resources planning and management*, *124*(1), 31-37.

Kendall, M. G. (1975). Rank Correlation Measures. Charles Griffin, London, pp. 220.

Knowlton, K., Kulkarni, S. P., Azhar, G. S., Mavalankar, D., Jaiswal, A., Connolly, M., ... and Ahmedabad Heat and Climate Study Group. (2014). Development and implementation of South Asia's first heat-health action plan in Ahmedabad (Gujarat, India). *International journal of environmental research and public health*, *11*(4), 3473-3492.

Krishna Kumar, K., Hoerling, M., and Rajagopalan, B. (2005). Advancing dynamical prediction of Indian monsoon rainfall. *Geophysical Research Letters*, *32*(8).

Kumar, R., and Gautam, H. R. (2014). Climate change and its impact on agricultural productivity in India. *Journal of Climatology and Weather Forecasting*.

Kumar, V., and Yadav, S. M. (2018). Optimization of reservoir operation with a new approach in evolutionary computation using TLBO algorithm and Jaya algorithm. *Water Resources Management*, *32*(13), 4375-4391.

Kundzewicz, Z. W., Mata, L. J., Arnell, N. W., Döll, P., Jimenez, B., Miller, K., ... and Shiklomanov, I. (2008). The implications of projected climate change for freshwater resources and their management. *Hydrological sciences journal*, *53*(1), 3-10.

Lehmann, E. L., and D'Abrera, H. J. (1975). *Nonparametrics: statistical methods based on ranks*. Holden-day.

Lucas-Borja, M. E., Carrà, B. G., Nunes, J. P., Bernard-Jannin, L., Zema, D. A., and Zimbone, S. M. (2020). Impacts of land-use and climate changes on surface runoff in a tropical forest watershed (Brazil). *Hydrological Sciences Journal*, *65*(11), 1956-1973.

Ma, D., Xu, Y. P., Xuan, W., Gu, H., Sun, Z., and Bai, Z. (2020). Do model parameters change under changing climate and land use in the upstream of the Lancang River Basin, China?. *Hydrological Sciences Journal*, *65*(11), 1894-1908.

Majidi, A., and Shahedi, K. (2012). Simulation of rainfall-runoff process using Green-Ampt method and HEC-HMS model (Case study: Abnama Watershed, Iran). *International Journal of Hydraulic Engineering*, *1*(1), 5-9.

Mann, H. B. (1945). Non-Parametric Tests against Trend. Econmetrica, 13, 245-259. *Mantua, NJ, SR Hare, Y. Zhang, JM Wallace, and RC Francis (1997), A Pacific Decadal*.

Mazdiyasni, O., AghaKouchak, A., Davis, S. J., Madadgar, S., Mehran, A., Ragno, E., ... and Niknejad, M. (2017). Increasing probability of mortality during Indian heat waves. *Science advances*, *3*(6), e1700066.

Mekonnen, D. F., Duan, Z., Rientjes, T., and Disse, M. (2018). Analysis of combined and isolated effects of land-use and land-cover changes and climate change on the upper Blue Nile River basin's streamflow. *Hydrology and earth system sciences*, *22*(12), 6187-6207.

Merz, R., Parajka, J., and Blöschl, G. (2009). Scale effects in conceptual hydrological modeling. *Water resources research*, *45*(9).

Meselhe, E. A., Habib, E., Oche, O. C., and Gautam, S. (2004). Performance evaluation of physically based distributed hydrologic models and lumped hydrologic models. In *Critical Transitions in Water and Environmental Resources Management* (pp. 1-10).

Mokhtari, E. H., Remini, B., and Hamoudi, S. A. (2016). Modelling of the rain–flow by hydrological modelling software system HEC-HMS–watershed's case of wadi Cheliff-Ghrib, Algeria. *Journal of Water and Land Development*, (30).

Monteith, J. L. (1965). Evaporation and environment. In *Symposia of the society for experimental biology* (Vol. 19, pp. 205-234). Cambridge University Press (CUP) Cambridge.

Moriasi, D. N., Arnold, J. G., Van Liew, M. W., Bingner, R. L., Harmel, R. D., and Veith, T. L. (2007). Model evaluation guidelines for systematic quantification of accuracy in watershed simulations. *Transactions of the ASABE*, *50*(3), 885-900.

Narsimlu, B., Gosain, A. K., and Chahar, B. R. (2013). Assessment of future climate change impacts on water resources of Upper Sind River Basin, India using SWAT model. *Water resources management*, *27*(10), 3647-3662.

NBSS and LUP (National Bureau of Soil Survey and Land Use Planning, Nagpur) (2008). Soil Survey Report. Rajasthan and Gujarat State, India.

NMSA (2001). Initial National Communication of Ethiopia to the United Nations Framework Convention on Climate Change (UNFCCC). National Meteorological Services Agency (NMSA) Addis Ababa Ethiopia.

Patel, J. N., and Balve, P. N. (2018). Optimisation of Multireservoir Operation Policy using Teaching-Learning Based Optimisation Algorithm. *Pertanika Journal of Science and Technology*, *26*(3).

Pettitt, A. N. (1979). A non-parametric approach t Stat. *Soc, Ser. C*, *28*, 126-135.

Pingale, S. M., Khare, D., Jat, M. K., and Adamowski, J. (2014). Spatial and temporal trends of mean and extreme rainfall and temperature for the 33 urban centers of the arid and semi-arid state of Rajasthan, India. *Atmospheric Research*, *138*, 73-90.

Rajeevan, M., Bhate, J., and Jaswal, A. K. (2008). Analysis of variability and trends of extreme rainfall events over India using 104 years of gridded daily rainfall data. *Geophysical research letters*, *35*(18).

Razmkhah, H. (2016). Comparing performance of different loss methods in rainfall-runoff modeling. *Water resources*, *43*(1), 207-224.

Rodell, M., Velicogna, I., and Famiglietti, J. S. (2009). Satellite-based estimates of groundwater depletion in India. *Nature*, *460*(7258), 999-1002.

Rubel, F., and Kottek, M. (2010). Observed and projected climate shifts 1901-2100 depicted by world maps of the Köppen-Geiger climate classification. *Meteorologische Zeitschrift*, *19*(2), 135.

Saha, K. R., Mooley, D. A., and Saha, S. (1979). The Indian monsoon and its economic impact. *GeoJournal*, *3*(2), 171-178.

Sahana, V., and Timbadiya, P. V. (2020). Spatiotemporal variation of water availability under changing climate: Case study of the upper Girna Basin, India. *Journal of Hydrologic Engineering*, *25*(5), 05020004.

Saleh, A., Ghobad, R., and Noredin, R. (2011). Evaluation of HEC-HMS methods in surface runoff simulation (Case study: Kan watershed, Iran). *Advances in Environmental Biology*, 1316-1322.

Samani, Z. (2000). Estimating solar radiation and evapotranspiration using minimum climatological data. *Journal of irrigation and drainage engineering*, *126*(4), 265-267.

Saraf, V. R., and Regulwar, D. G. (2018). Impact of climate change on runoff generation in the Upper Godavari River Basin, India. *Journal of Hazardous, Toxic, and Radioactive Waste*, *22*(4), 04018021.

Seneviratne, S., Nicholls, N., Easterling, D., Goodess, C., Kanae, S., Kossin, J., ... and Zwiers, F. W. (2012). Changes in climate extremes and their impacts on the natural physical environment.

Sharma, P. J., Loliyana, V. D., SR, R., Timbadiya, P. V., and Patel, P. L. (2018). Spatiotemporal trends in extreme rainfall and temperature indices over Upper Tapi Basin, India. *Theoretical and Applied Climatology*, *134*(3), 1329-1354.

Sharma, P. J., Patel, P. L., and Jothiprakash, V. (2015). A simulation–optimization approach in development of operation policy for a multipurpose reservoir. In *E-proceedings of the 36thIAHR World Congress. The Hague, the Netherlands*.

Shastri, H., Paul, S., Ghosh, S., and Karmakar, S. (2015). Impacts of urbanization on Indian summer monsoon rainfall extremes. *Journal of Geophysical Research: Atmospheres*, *120*(2), 496-516.

Siebert, S., Burke, J., Faures, J. M., Frenken, K., Hoogeveen, J., Döll, P., and Portmann, F. T. (2010). Groundwater use for irrigation–a global inventory. *Hydrology and earth system sciences*, *14*(10), 1863-1880.https://www.un.org/en/climatechange

Sonali, P., and Kumar, D. N. (2013). Review of trend detection methods and their application to detect temperature changes in India. *Journal of Hydrology*, *476*, 212-227.

Sonali, P., and Kumar, D. N. (2013). Review of trend detection methods and their application to detect temperature changes in India. *Journal of Hydrology*, *476*, 212-227.

Tabari, H., Marofi, S., Aeini, A., Talaee, P. H., and Mohammadi, K. (2011). Trend analysis of reference evapotranspiration in the western half of Iran. *Agricultural and forest meteorology*, *151*(2), 128-136.

Tan, M. L., Ibrahim, A. L., Yusop, Z., Duan, Z., and Ling, L. (2015). Impacts of land-use and climate variability on hydrological components in the Johor River basin, Malaysia. *Hydrological Sciences Journal*, *60*(5), 873-889.

Teegavarapu, R. S. V. A. Goly, and J. Obeysekera, 2013: Influences of Atlantic multidecadal oscillation phases on spatial and temporal variability of regional precipitation extremes. *J. Hydrol*, *495*, 74-93.

Vijay, A., Sivan, S. D., Mudbhatkal, A., and Mahesha, A. (2021). Long-term climate variability and drought characteristics in tropical region of India. *Journal of Hydrologic Engineering*, *26*(4), 05021003.

Vörösmarty, C. J., McIntyre, P. B., Gessner, M. O., Dudgeon, D., Prusevich, A., Green, P., and Davies, P. M. (2010). Global threats to human water security and river biodiversity. *nature*, *467*(7315), 555-561.

Vorosmarty, C. J., Greenv P., Salisbury, J., and Lammers, R. B. (2000), Global Water Resources: Vulnerability from Climate Change and Population Growth, *Science, 289*(5477), 284–288.

Wardlaw, R., and Sharif, M. (1999). Evaluation of genetic algorithms for optimal reservoir system operation. *Journal of water resources planning and management*, *125*(1), 25-33.

Wei, X., Liu, W., and Zhou, P. (2013). Quantifying the relative contributions of forest change and climatic variability to hydrology in large watersheds: a critical review of research methods. *Water*, *5*(2), 728-746.

Wisser, D., Frolking, S., Douglas, E. M., Fekete, B. M., Vörösmarty, C. J., and Schumann, A. H. (2008). Global irrigation water demand: Variability and uncertainties arising from agricultural and climate data sets. *Geophysical Research Letters*, *35*(24).

WRIS (Water Resources Information System of India). http://indiawris.gov.in/wris/#/ (Accessed on April 2021)

Ye, J. S., Gong, Y. H., Zhang, F., Ren, J., Bai, X. K., and Zheng, Y. (2018). Which temperature and precipitation extremes best explain the variation of warm versus cold years and wet versus dry years?. *Journal of Climate*, *31*(1), 45-59.

Hydrologic details of Dharoi reservoir

A)	**Catchment Area**			
	1	Total Catchment Area at Dam site	:	5540 km^2
	2	Catchment Area in Rajasthan Territory	:	2901 km^2
	3	Catchment Area in Gujarat Territory	:	2639 km^2
B)	**Mean Annual Runoff in Catchment**		:	1052 Mm^3
C)	**Mean Annual Rainfall**		:	633 mm
D)	**Floods**			
	1	Maximum Flood & Released from Dam (Dt. 2-9-1973)	:	14158 m^3/s
	2	Maximum Probable Flood (M.P.F.)	:	21662 m^3/s
	3	Standard Probable Flood (S.P.F.)	:	18179 m^3/s
	4	Moderated outflow corresponding to M.P.F.	:	16225 m^3/s
	5	Design flood with full opening (12 Nos. Gate)		
		@ RL 622' (189.559 m)	:	13226 m^3/s
		@ RL 630' (192.02 m)	:	18427 m^3/s

Key features of Dharoi reservoir

A)	**Reservoir Capacity**			
	1	Gross capacity @ F.R.L.	:	907.88 Mm^3
		Revised	:	813.14 Mm^3
	2	Dead storage @ RL 577 Ft.	:	131.99 Mm^3
		Revised	:	67.51 Mm^3
	3	Live storage	:	775.89 Mm^3
		Revised	:	745.63 Mm^3
	4	Evaporation losses		

	a.	For 75% Reliable year	:	137.78 Mm^3
	b.	For 98% Reliable year	:	78.95 Mm^3
B)	**Submergence**			
	1	Total Area under Submergence	:	10566.81 Ha
	2	Forest	:	349.39 Ha
	3	Wasteland	:	2727.55 Ha
	4	Culturable	:	7489.87 Ha
	5	Total Villages under Submergence	:	19 Partial, 28 Full

APPENDIX -II

Main Canal Details of Dharoi Reservoir

	Canal	**Right Bank Main Canal**	**Left Bank Main Canal**
1	Length of Canal	43.5 km	29.52 km
2	Capacity (Extended Planning)		
a.	At Head	38.22 m3/s	11.32 m3/s
b.	At Tail	16.595 m3/s	5.26 m3/s
3	Type of Canal	Lined	Lined
4	Type of Lining	C.C. M-15, 7.5 cm Thick	
5	Canal Bed Width		
a.	At Head	2.13 m	4.5 m
b.	At Tail	1.52 m	3.1 m
6	Side Slope	1.5 : 1	1.5 : 1
7	Roughness Coefficient	0.02	0.02
8	Bed Gradient		
a.	Up to 13.3 km.	1 : 3000	1 : 3000
b.	13.3 to 43.50 Km.	1 : 4000	
9	Total Area Under Irrigation		
a.	Original Planning	48105 ha	12980 ha
b.	Revised Planning	71992	19480
10	No. of Villages Covered		
a.	Original Planning	123	50
b.	Revised Planning	272	88
11	Districts Covered	Mehsana, Patan, Gandhinagar	Sabarkantha

APPENDIX -III

Planned and Existing Cropping Pattern in Dharoi Right Bank Command Area

Sr. No.	Season	Name of Crop	Planned Cropping pattern	Existing Cropping pattern
			Area (ha)	Area (ha)
1	Kharif	Groundnut	3608	0
		Cotton/Tobacco	0	3347
		Castor/Raido	0	982
		Other Kharif	20204	179
		Total Kharif	**28312**	**4508**
2	Two Seasonal	Variyali	1443	0
		Vegetables	2405	0
		Cotton	3608	0
		Two Seasonal Total	**7456**	**0**
3	Rabi	Wheat	12026	6977
		Cotton/Tobacco	0	1096
		Jeeru	4811	0
		Variyali/ Vegetables	0	399
		Juwar/Bajari	0	266
		Castor/Raido	0	4668
		Mustard/Rajko	0	3165
		Other Rabi	0	4482
		Total Rabi	**16837**	**21053**
Total (RBMCA)			**52605**	**25561**

Planned and Existing Type of Crop and Area in Dharoi Left Bank Command Area

Sr. No.	Season	Name of crop	Planned crop pattern area	Present crop pattern area
			ha	ha
1	Kharif	Groundnut	1947	0
		Juwar/Bajari	3894	0
		Cotton/Tobacco	1298	787
		Pulses	1168	0
		Castor/Raido	0	142
		Other Kharif	0	13
		Total Kharif	**8372**	**942**
2	Two Seasonal	Vegetables	65	
		Cotton/Tobacco	1298	96
		Two Seasonal Total	**1363**	**0**
3	Rabi	Wheat	3829	3097
		Cotton/Tobacco	0	96
		Vegetables	65	0
		Castor/Raido	0	802
		Other Rabi	649	170
		Total Rabi	**4543**	**4165**
4	Hot Weather	Cotton/Tobacco	0	1256
Total (LBMCA)			**14278**	**6363**

APPENDIX -IV

Statistical test for trend detection

1. Mann-Kendall test

The non-parametric Mann-Kendall (MK) test is applied to detect the presence of monotonic trend in a hydroclimatological time series. The null (H_0) and alternate (H_1) hypothesis states that there is no trend and presence of monotonic trend in the time series, respectively. Consider a time series $X_t, t = 1, 2, \ldots, n$, wherein, each value is compared with all successive values of X_{t+1}, to generate a new series, and the statistic S_{MK} is calculated as (Mann, 1945; Kendall, 1975):

$$S_{MK} = \sum_{k=1}^{n-1} \sum_{j=k+1}^{n} sgn(x_j - x_k) \tag{7.1}$$

The statistic S_{MK} is approximately Gaussian when $n \geq 18$, and the mean and variance of S_{MK} is given by:

$$E(S_{MK}) = 0 \text{ and } Var(S_{MK}) = \frac{n(n-1)(2n+5) - \sum_{i=1}^{m} t_i(t_i-1)(2t_i+5)}{18} \tag{7.2}$$

where, n and m are the number of data and ties, respectively. Each tie represents a set of similar subsequent data in a time series and the data count in each of them is t. The test statistic Z_{MK}, is computed as:

$$Z_{MK} = \begin{cases} \dfrac{S_{MK} - 1}{\sqrt{Var(S_{MK})}} & ,if\ S_{MK} > 0 \\ 0 & ,if\ S_{MK} = 0 \\ \dfrac{S_{MK} + 1}{\sqrt{Var(S_{MK})}} & ,if\ S_{MK} < 0 \end{cases} \tag{7.3}$$

Hamed and Rao (1998) stated that presence of serial correlation in a time series does not falsify either the asymptotic normality or mean of the MK test statistic S_{MK}, but the variance changes. Hence, correction factor was proposed to rectify the variance of S_{MK} using only uncorrelated samples. The presence of positive or negative serial correlation shall result in increase or decrease in the variance of MK test statistic S_{MK}. Hence, the modified variance $Var\ (S_{MK})_*$ for computing the MMK test statistic (Z_{MMK}) is given by (Hamed and Rao, 1998):

$$Var\ (S_{MK})_* = CF \times Var\ (S_{MK}) \tag{7.4}$$

where, CF is the correction factor, which is given as:

$$CF = 1 + \frac{2}{n(n-1)(n-2)} \sum_{k=1}^{n-1} (n-k)\ (n-k-1) \times (n-k-2) r_k^R \tag{7.5}$$

where, r_k^R = ranks of data. The null hypothesis of this test is rejected if the value of $|Z_{MMK}| \geq 1.96$ at a 5% significance level. A positive (negative) value of Z_{MMK} would indicate presence of increasing (decreasing) trend in the time series.

2. Spearman's rho test

Spearman's rho (Lehmann, 1975) test is a rank-based non-parametric method adopted to ascertain trends in hydroclimatic data. The null (H_0) and alternate (H_1) hypothesis indicates absence of trend and existence of increasing or decreasing trend in the time series, respectively. The test statistic r_{SR} and standardized statistic t_s are defined as:

$$r_{SR} = 1 - \frac{6 \sum_{i=1}^{n} (D_i - i)^2}{n(n^2 - 1)} \tag{7.6}$$

$$t_s = r_{SR} \sqrt{\frac{n-2}{1 - r_{SR}^2}} \tag{7.7}$$

In these equations, D_i is the rank of the ith observation, i is the number in sequential order, n is the number of data points in the time series, and t_s is Student's t-distribution with $(n - 2)$ degree of freedom. The critical value of t at 5% significance level ($\alpha = 0.05$) of Student's t-distribution table is defined as t_{cr}. If $|t_s| > t_{cr}$, then null hypothesis is rejected, and a significant trend is reported in the hydrologic time series. The positive (negative) values of t_s would indicate presence of an increasing (decreasing) trend in the time series.

3. Mann-Whitney test

Mann-Whitney (MW) test is a non-parametric approach to assess the changes in two independent datasets over two temporal windows. The null hypothesis (H_0) states that the two population medians

are equal. The datasets from two temporal windows comprising of n_1 and n_2 elements, respectively are ranked from lowest to highest and the test statistic (Z_{MW}) is estimated as (Teegavarapu et al., 2013):

$$U_l = n_1 n_2 + \frac{n_i(n_i + 1)}{2} - \sum R_l \tag{7.8}$$

$$\bar{x}_u = \frac{n_1 n_2}{2} \tag{7.9}$$

$$S_u = n_1 n_2 + \sqrt{\frac{n_1 n_2 (n_1 + n_2 + 1)}{12}} \tag{7.10}$$

$$Z_{MW} = \frac{U_l - \bar{x}_u}{S_u} \tag{7.11}$$

The standard deviation (S_u), the rank (R_l) from the sample l and the mean value ($\bar{x}_u$) are used to estimate the test statistic Z_{MW}. The H_0 is rejected if $Z_{MW} \geq 1.96$ at a 5% significance level.

Appendix-V Classification of dry, normal and wet years based on Yoo, 2006

Year	Annual rainfall (mm)	Classification	Year	Annual rainfall (mm)	Classification	Year	Annual rainfall (mm)	Classification
1901	743.0	Dry	1928	1235.1	Normal	1955	1631.1	Normal
1902	1037.5	Normal	1929	1311.8	Normal	1956	1731.6	Wet
1903	1257.7	Normal	1930	1226.8	Normal	1957	1116.4	Normal
1904	790.7	Dry	1931	1491.7	Normal	1958	1328.0	Normal
1905	862.3	Dry	1932	1044.1	Normal	1959	1954.3	Wet
1906	1413.5	Normal	1933	1861.7	Wet	1960	1169.0	Normal
1907	1395.2	Normal	1934	1593.1	Normal	1961	1633.0	Normal
1908	1841.6	Wet	1935	1109.6	Normal	1962	1502.0	Normal
1909	1795.0	Wet	1936	623.0	Dry	1963	1158.1	Normal
1910	1290.8	Normal	1937	1483.8	Normal	1964	1312.6	Normal
1911	586.5	Dry	1938	1069.7	Normal	1965	815.8	Dry
1912	1239.0	Normal	1939	817.6	Dry	1966	964.1	Dry
1913	1341.4	Normal	1940	1035.2	Normal	1967	1764.4	Wet
1914	1210.6	Normal	1941	1647.0	Normal	1968	1169.7	Normal
1915	759.4	Dry	1942	1204.0	Normal	1969	935.3	Dry
1916	1531.9	Normal	1943	1547.8	Normal	1970	2106.7	Wet
1917	2556.5	Wet	1944	2415.9	Wet	1971	1377.7	Normal
1918	657.2	Dry	1945	1692.4	Wet	1972	762.6	Dry
1919	1447.5	Normal	1946	1698.3	Wet	1973	3118.0	Wet
1920	1226.9	Normal	1947	1231.4	Normal	1974	746.0	Dry
1921	1340.9	Normal	1948	836.5	Dry	1975	1676.4	Normal
1922	1459.8	Normal	1949	935.2	Dry	1976	1425.9	Normal
1923	620.5	Dry	1950	1714.7	Wet	1977	1601.5	Normal
1924	1426.6	Normal	1951	811.4	Dry	1978	1369.0	Normal
1925	899.6	Dry	1952	1483.0	Normal	1979	982.0	Dry
1926	2089.1	Wet	1953	1786.5	Wet	1980	1181.9	Normal
1927	1850.1	Wet	1954	1796.8	Wet	1981	1279.3	Normal

Year	Annual rainfall (mm)	Classification	Year	Annual rainfall (mm)	Classification
1982	1145.7	Normal	1998	1222.0	Normal
1983	1534.8	Normal	1999	670.3	Dry
1984	1316.8	Normal	2000	823.2	Dry
1985	1165.4	Normal	2001	1176.8	Normal
1986	773.9	Dry	2002	654.3	Dry
1987	456.5	Dry	2003	1372.2	Normal
1988	1354.5	Normal	2004	960.1	Dry
1989	1201.3	Normal	2005	1632.2	Normal
1990	1902.9	Wet	2006	2659.8	Wet
1991	1201.3	Normal	2007	1326.1	Normal
1992	1955.0	Wet	2008	827.4	Dry
1993	1319.3	Normal	2009	1025.1	Normal
1994	2026.4	Wet	2010	1702.0	Wet
1995	1062.7	Normal	2011	1770.4	Wet
1996	1303.6	Normal	2012	1493.4	Normal
1997	1400.1	Normal	2013	1485.1	Normal